

Cover Page



Universiteit Leiden



The handle <http://hdl.handle.net/1887/24521> holds various files of this Leiden University dissertation.

Author: Uijl, Dennis Wilhemus den

Title: Radiofrequency catheter ablation in atrial arrhythmias : insight into pre-procedural evaluation and procedural guidance

Issue Date: 2014-03-12

Radiofrequency Catheter Ablation in Atrial Arrhythmias: Insight into Pre-procedural Evaluation and Procedural Guidance

Dennis W. den Uijl



Stellingen behorende bij het proefschrift :

Radiofrequency catheter ablation in atrial arrhythmias: Insights into pre-procedural evaluation and procedural guidance

1. Comprehensive evaluation of left atrial remodeling allows identification of patients with a high likelihood to maintain sinus rhythm after radiofrequency catheter ablation of atrial fibrillation. (This thesis)
2. Left atrial size, pulmonary vein anatomy, natriuretic peptide levels, left atrial fibrosis and total atrial conduction time are predictors of atrial fibrillation recurrence after radiofrequency catheter ablation. (This thesis)
3. Integration of intracardiac echocardiography and multi-slice computed tomography combines the advantages of a real-time imaging modality and high resolution three-dimensional imaging. (This thesis)
4. **Image integration can facilitate the ablation of atrial tachycardia's in patients with congenital heart disease by visualizing the complex cardiac anatomy in its relation to the position of the ablation catheter.** (This thesis)
5. The high lifetime risk for AF underscores the important public health burden posed by AF. (Lloyd-Jones et al, Circulation. 2004 Aug 31;110(9):1042-6)
6. Catheter ablation is currently recommended in patients with symptomatic atrial fibrillation unresponsive or intolerant to at least one Class 1 or 3 antiarrhythmic drug. (Calkins et al, Europace. 2012 Apr;14(4):528-606)
7. In the last decade the number of ablation procedures performed to treat atrial fibrillation has nearly doubled, however the success rate does not seem to have improved. (Cappato et al, Circ Arrhythm Electrophysiol. 2010 Feb;3(1):32-8)
8. A careful assessment of the risks and benefits should be made for each patient considered for radiofrequency catheter ablation for atrial fibrillation. (Calkins et al, Europace. 2012 Apr;14(4):528-606)
9. I have no special talent. I am only passionately curious. (Albert Einstein, 1879-1955)
10. Time you enjoy wasting was not wasted. (John Lennon, 1940-1980)
11. The only true wisdom is in knowing you know nothing. (Socrates, 469 BC-399 BC)
12. If a problem is fixable, then there is no need to worry. If it's not fixable, then there is no help in worrying. (Dalai Lama, 1935-present)

Dennis W. den Uijl, 2014

Radiofrequency Catheter Ablation in
Atrial Arrhythmias: Insight into
Pre-procedural Evaluation and
Procedural Guidance

Dennis W. den Uijl



The studies described in this thesis were performed at the department of Cardiology of the Leiden University Medical Center, Leiden, The Netherlands

Cover design by Thierry Veltman / Dennis W. den Uijl

Lay-out by Dennis W. den Uijl

Printed by Ipskamp Drukkers

ISBN: 978-94-6259-087-8

Financial support to the costs associated with the publication of this thesis from: Bayer Healthcare Pharmaceuticals, Biosense Webster, MSD, Toshiba medical systems and ABN-AMRO is gratefully acknowledged.

© Dennis W. den Uijl 2014

All rights reserved. No part of this thesis may be reproduced, stored in a retrieval system or transmitted in any form or by any means, without prior written permission of the copyright owner.

Radiofrequency Catheter Ablation in Atrial Arrhythmias: Insight
into Pre-procedural Evaluation and Procedural Guidance

Proefschrift

ter verkrijging van
de graad van Doctor aan de Universiteit Leiden,
op gezag van Rector Magnificus prof.mr. C.J.J.M. Stolker,
volgens besluit van het College voor Promoties
te verdedigen op woensdag 12 maart 2014
klokke 16:15 uur

door

Dennis Wilhelmus den Uijl
geboren te Schiedam
in 1980

Promotiecommissie

Promotores:	Prof. Dr. Jeroen J Bax Prof. Dr. Martin J Schalijs
Co-promotor:	Dr. Victoria Delgado
Overige leden:	Prof. Dr. Katja Zeppenfeld Prof. Dr. Isabelle C van Gelder (University of Groningen) Dr. Monique R Jongbloed Dr. Serge A Trines Dr. Jerry Braun

Voor mijn ouders

'The journey is the reward' *Steve Jobs*

Table of Contents

Chapter 1	General introduction and outline of the thesis	9
Part I:	Pre-procedural evaluation of patients undergoing radiofrequency catheter ablation for atrial fibrillation	25
Chapter 2	Left atrial size as a predictor of successful radiofrequency catheter ablation for atrial fibrillation <i>Europace. 2009 Oct;11(10):1255-6</i>	27
Chapter 3	Impact of left atrial fibrosis and left atrial size on the outcome of catheter ablation for atrial fibrillation <i>Heart. 2011 Nov;97(22):1847-51</i>	33
Chapter 4	Prognostic value of total atrial conduction time estimated with tissue Doppler imaging to predict the recurrence of atrial fibrillation after radiofrequency catheter ablation <i>Europace. 2011 Nov;13(11):1533-40</i>	53
Chapter 5	Impact of coronary atherosclerosis on the efficacy of radiofrequency catheter ablation for atrial fibrillation <i>Eur Heart J Cardiovasc Imaging. 2013 Mar;14(3):247-52</i>	75
Chapter 6	Effect of pulmonary vein anatomy and left atrial dimensions on outcome of circumferential radiofrequency catheter ablation for atrial fibrillation <i>Am J Cardiol. 2011 Jan 15;107(2):243-9</i>	95

Chapter 7	Natriuretic peptide levels predict recurrence of atrial fibrillation after radiofrequency catheter ablation <i>Am Heart J. 2011 Jan;161(1):197-203</i>	115
Part II:	Imaging to facilitate ablation of complex arrhythmias	135
Chapter 8	Intracardiac echocardiography <i>Cardiovascular Catheterisation and Intervention. Informa Healthcare USA, New York</i>	137
Chapter 9	Real-time integration of intracardiac echocardiography and multi-slice computed tomography to guide radiofrequency catheter ablation for atrial fibrillation. <i>Heart Rhythm. 2008 Oct;5(10):1403-10</i>	167
Chapter 10	Real-time integration of intracardiac echocardiography to facilitate atrial tachycardia ablation in a patient with a Senning baffle <i>Circ Arrhythm Electrophysiol. 2009 Oct;2(5):e28-30</i>	191
Chapter 11	Anatomical perspective on radiofrequency ablation of AV nodal reentry tachycardia after Mustard correction for transposition of the great arteries <i>Pacing Clin Electrophysiol. 2012 Oct;35(10):e287-90</i>	199
	Samenvatting en conclusie	209
	Summary and conclusions	217
	List of publication	225
	Acknowledgements	231
	Curriculum Vitae	235

Chapter 1

General introduction and outline of the thesis



General Introduction and Outline of the Thesis

Radiofrequency catheter ablation (RFCA) has become an important treatment option in the management of supraventricular arrhythmias such as atrioventricular (nodal) re-entry tachycardia, atrial tachycardia, atrial flutter and atrial fibrillation (AF). Particularly in the management of AF the number of RFCA procedures performed is growing rapidly.¹ Three-dimensional electroanatomical mapping combined with non-invasive imaging is currently a state of the art technique to guide RFCA for complex arrhythmias such as AF ablation, providing information on anatomical landmarks and arrhythmogenic substrate with higher accuracy and with less radiation exposure than fluoroscopy or conventional catheter based mapping. Importantly, accurate characterization of the arrhythmogenic substrate and the underlying mechanisms of the arrhythmia as well as visualization of anatomical landmarks are pivotal to optimize the results of RFCA.² Comprehensive pre-procedural evaluation may help to identify the appropriate substrate as well as to identify patients with a high likelihood to benefit from a RFCA procedure.

Pre-procedural Evaluation of Patients undergoing Radiofrequency Catheter Ablation for Atrial Fibrillation

Atrial fibrillation is the most common sustained cardiac arrhythmia in the developed world, with an estimated prevalence of 1-2 %.³ Atrial fibrillation is associated with an increased risk for thromboembolic complications (e.g. stroke), congestive heart failure, hospitalisation and mortality.³⁻⁵ As a result of the global population aging, the prevalence of AF is expected to at least double in the next 50 years. Consequentially, AF poses a major problem to society in terms of medical, social and economic expenses.

Management of AF is targeted at the prevention of AF related complications (e.g. stroke, tachycardiomyopathy) and at the reduction of AF related symptoms.³ Prevention of complications is based on antithrombotic therapy, reduction of ventricular response rate and adequate treatment of concomitant cardiac disease. Although these therapies may already reduce symptoms, additional restoration of the sinus rhythm can result in further relief of symptoms. Sinus rhythm can be restored by cardioversion, antiarrhythmic medication and/or ablation therapy. Radiofrequency catheter ablation for AF is currently reserved for patients with symptomatic AF, refractory or intolerant to at least one Class 1 or 3 anti-arrhythmic drugs.²

The success of surgical treatment of AF in the early 1990s has led to an interest in the field of interventional cardiology to reproduce these results by creating a set of lesions similar to the surgical procedures using RFCA.² These approaches were based on the theoretical model by Moe et al. that a critical number of AF wavelets was needed to sustain AF.⁶ The lesions set were designed to limit the number of circulating wavelets thereby avoiding the development and maintenance of AF. In the later 90s, Haïssaguerre et al. made the landmark observation that AF could be spontaneously initiated by ectopic beats originating from the pulmonary veins and that subsequent ablation of these ectopic foci could successfully cure patients.⁷ These observations rapidly increased the increased interest in RFCA for AF and directed the attention to the pulmonary vein region. Currently, RFCA for AF is a rapidly evolving treatment modality that gains popularity.¹ A large variety of ablation strategies have evolved, however the pulmonary vein region remains the cornerstone of most RFCA procedures.^{1,2} However, with a reported success rate of 66-89 %, not all patients benefit from RFCA for AF.^{1,2} In addition, RFCA for AF is associated with a small but relevant risk for serious complications (e.g. tamponade, stroke,

atrio-esophageal fistula).¹ To improve the outcome of RFCA for AF and avoid unnecessary procedure related risks a proper patient selection is mandatory.

The current Heart Rhythm Society/European Heart Rhythm Association/European Cardiac Arrhythmia Society expert consensus statement on catheter and surgical ablation of AF, recommends careful assessment of the risks and benefits of RFCA in each patient.² Ideally, the likelihood of sinus rhythm maintenance after RFCA should be estimated based on clinical characteristics, imaging studies and biochemical results. Risk factors for AF recurrence after RFCA are non-paroxysmal AF (persistent or longstanding), sleep apnea syndrome/obesity, left atrial enlargement, increased age, hypertension, concomitant structural heart disease and a high extent of left atrial fibrosis.⁸⁻¹² However, the evidence demonstrating the accuracy of these risk factors to properly identify patients with a high probability of maintaining sinus rhythm after RFCA is limited. Therefore additional markers, for example new markers derived from imaging technique or biochemical analyses, are needed to improve the patient selection.

Echocardiography

Atrial fibrillation causes electrical and structural changes to the atria which play an important role in the perpetuation and progression of the arrhythmia.^{13,14} This process is referred to as atrial remodeling. A large extent of atrial remodeling is associated with a limited efficacy of RFCA for AF.¹¹ Therefore, pre-procedural assessment of the extent of atrial remodeling could be used to identify patients with a high risk for AF recurrence after RFCA. Measurement of left atrial size is the most common used method to estimate the extent of atrial remodeling. Left atrial size is an independent predictor of AF in the general population as well as a well-recognized risk factor for AF recurrence after RFCA.^{9,15-17} However as a selection criterion the clinical applicability of left atrial

size is limited. Recently the use of contrast-enhanced magnetic resonance imaging to visualize, localize and measure atrial fibrosis in patients with AF was demonstrated.^{18,19} However, despite the promising results, contrast-enhanced magnetic resonance imaging is not widely available in clinical practice and therefore alternative and better available methods to assess atrial remodeling are needed. In this regard, novel echocardiographic techniques provide information about atrial remodeling additional to left atrial dimensions, such as left atrial function (e.g. tissue Doppler imaging derived left atrial strain) and myocardial tissue properties (e.g. calibrated integrated backscatter derived left atrial fibrotic content and tissue Doppler imaging derived electromechanical delay [PA-TDI]).

Left atrial strain is an echocardiographic technique to assess the active contraction and relaxation of the atrial myocardium. In contrast to conventional methods to assess left atrial function (i.e. calculated from phasic volumes), left atrial strain is less dependent on loading conditions and provides information of the regional function of the myocardium. Kuppahally and coworkers demonstrated that left atrial strain and strain rate (assessed with speckle tracking echocardiography) correlated with the amount of left atrial fibrosis (assessed with contrast-enhanced magnetic resonance imaging) in patients with AF: patients with large areas of fibrosis had more impaired left atrial strain and strain rate.²⁰ In addition, these parameters have been associated with the burden of AF and with the outcomes of RFCA. In a recent study including 148 patients undergoing RFCA for AF, baseline left atrial strain was an independent determinant of favorable left atrial reverse remodeling at follow-up.²¹

Integrated backscatter is an echocardiographic technique that allows non-invasive characterization of cardiac tissue and may provide an alternative tool to estimate left atrial fibrosis and thereby atrial substrate remodeling.²²⁻²⁴

Calibrated integrated backscatter is based on the quantification of ultrasound energy reflected by scattering elements inside the myocardium. Integrated backscatter can be measured using two-dimensional echocardiographic gray-scale images and provides a global estimate of the fibrotic content of the left atrial wall.

The total atrial conduction time is determined by atrial size and conduction velocity and is thereby a marker of both electrical and structural remodeling of the atria. Echocardiographic assessment of the total atrial conduction time using tissue Doppler imaging (PA-TDI duration) may allow a more comprehensive estimation of the extent of atrial remodeling than left atrial size alone. The PA-TDI duration is measured as the time delay between the onset of the **P-wave in lead II of the surface ECG and the peak A'-wave** on the tissue Doppler tracing of the left atrial lateral wall (Figure 1).²⁵ The PA-TDI duration has been validated against P-wave duration on signal-averaged electrocardiography and has previously been used to identify patients with an atrial substrate vulnerable to develop AF.²⁶⁻²⁸

Multi-slice computed tomography

Multi-slice computed tomography (MSCT) is nowadays commonly acquired prior to RFCA for AF to plan and guide the ablation procedure.² MSCT contains information about pulmonary vein anatomy, pulmonary vein dimensions and the presence and extent of coronary artery disease. Potentially, pulmonary vein anatomy and dimensions could be of influence on the efficacy or RFCA lesion placement and the presence of coronary artery disease could have a negative impact on the efficacy of pulmonary vein isolation. Moreover, MSCT allows a more comprehensive evaluation of left atrial dimensions than two-dimensional echocardiography.²⁹ Potentially, this information could be used to improve the patient selection for RFCA for AF.

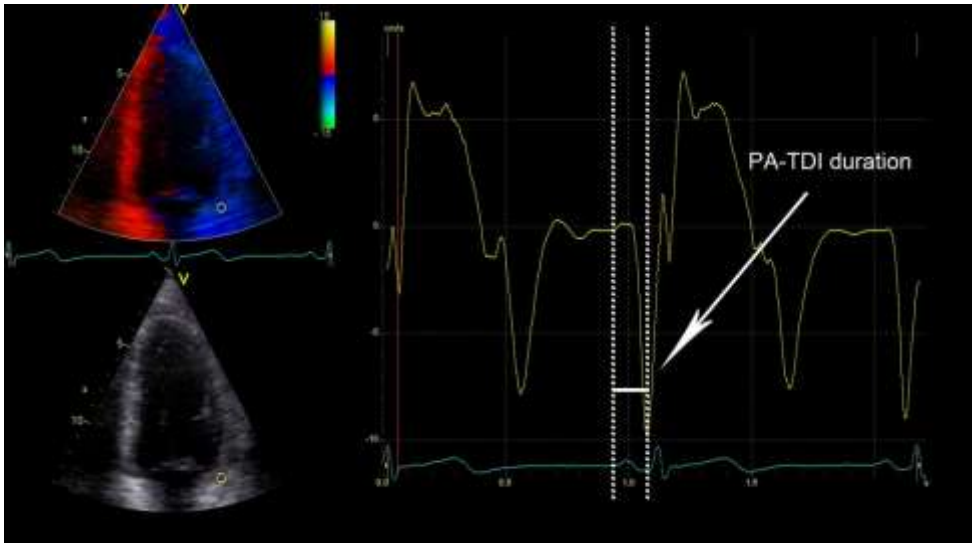


Figure 1. Measurement of the total atrial conduction time (PA-TDI duration). A fixed 9x9 pixel region of interest (yellow) was positioned in the left atrial lateral wall on a tissue Doppler recording to obtain a tracing of the mechanical activation in this area (yellow tracing). A simultaneously acquired registration of surface electrocardiogram lead II (blue tracing) was displayed underneath the tissue Doppler tracing. The PA-TDI duration (arrow) was assessed by measuring the time interval between the onset of the P-wave in lead II and the peak A'-wave on the tissue Doppler tracing.

Natriuretic peptides

Natriuretic peptides are hormones released from the atria and/or ventricles in response to volume or pressure overload and result in natriuresis.³⁰ Atrial natriuretic peptide is secreted primarily from the atria whereas B-type natriuretic peptide is primarily released from the ventricles.³⁰ It has been well recognized that in patients with AF, natriuretic peptide levels are elevated.^{31,32} However it remain unclear whether this is solely caused by the presence of AF or reflects an underlying cardiac condition.³³ Elevated natriuretic peptides have been identified as a predictor of new-onset AF in the general population and have been related to a higher risk for AF recurrence after RFCA.³⁴⁻³⁶ Potentially, natriuretic peptide levels can provide information about underlying cardiac

conditions that limit the efficacy of RFCA for AF and could therefore be a valuable addition.

Imaging to facilitate Radiofrequency Catheter Ablation of complex Atrial Arrhythmias

As RFCA procedures become more complex, the need for adequate visualization of cardiac and surrounding structures increases.² Currently, most RFCA procedures are guided by fluoroscopy, allowing real-time visualization of intracardiac catheters. However, fluoroscopy does not allow visualization of anatomical structures such as the pulmonary veins and causes radiation exposure to both patient and operator. Alternatively, electroanatomical mapping systems have been developed that allow non-fluoroscopic navigation and can create a three-dimensional reconstruction of the cardiac anatomy using point-by-point contact mapping. Similar to fluoroscopy, electroanatomical mapping does not allow visualization of all cardiac structures and surrounding anatomy.

MSCT allows detailed visualization of the cardiac anatomy and can be integrated with an electroanatomical mapping system to facilitate RFCA procedures.³⁷ By performing a segmentation and registration process, a three-dimensional shell of the cardiac anatomy can be merged with the electroanatomical map of the heart thereby combining the advantages of non-fluoroscopic navigation with the anatomical information of MSCT. However, the validity of using this approach is highly dependent on the accuracy of the registration process.^{38,39} Differences in fluid status, heart rhythm and heart rate between the time of MSCT acquisition and the RFCA procedure potentially compromise the quality of the registration process and thereby the accuracy of navigation.

Intracardiac echocardiography allows real-time visualization of important cardiac structures and can be used to guide lesion placement during RFCA.⁴⁰ In left-sided procedures (i.e. AF procedures or left atrial tachycardia), intracardiac echocardiography can be used to facilitate a safe transseptal puncture. Moreover, intracardiac echocardiography can be used to monitor and titrate energy delivery and allows for early detection of complications (e.g. thrombus formation on catheters or sheaths, pericardial effusion).^{40,41} However, intracardiac echocardiography provides two-dimensional images and lacks the 3-dimensional information that can be acquired using MSCT.

Ideally, RFCA procedures are guided by an imaging modality that provides real-time 3-dimensional visualization of the intracardiac catheters in relation to both cardiac and surrounding anatomy with low radiation exposure to patient and operator. In practice, such an imaging modality is not yet available. However, several mapping and fluoroscopy systems are being developed that allow integration of several imaging modalities.⁴²⁻⁴⁴ An integrated approach using a combination of imaging modalities (e.g. fluoroscopy, electroanatomical mapping, MSCT and/or intracardiac anatomy) allows the operator to combine the advantages of these different techniques (Figure 2). The optimal combination has not yet been established but most likely depends on the type of patient, the operators experience and the availability of each imaging technique.

Outline of the Thesis

The objectives of this thesis were (1) to study the incremental value of new diagnostic markers on the pre-procedural evaluation of patients undergoing RFCA for AF and (2) to study the role of imaging to facilitate RFCA for complex atrial arrhythmias.

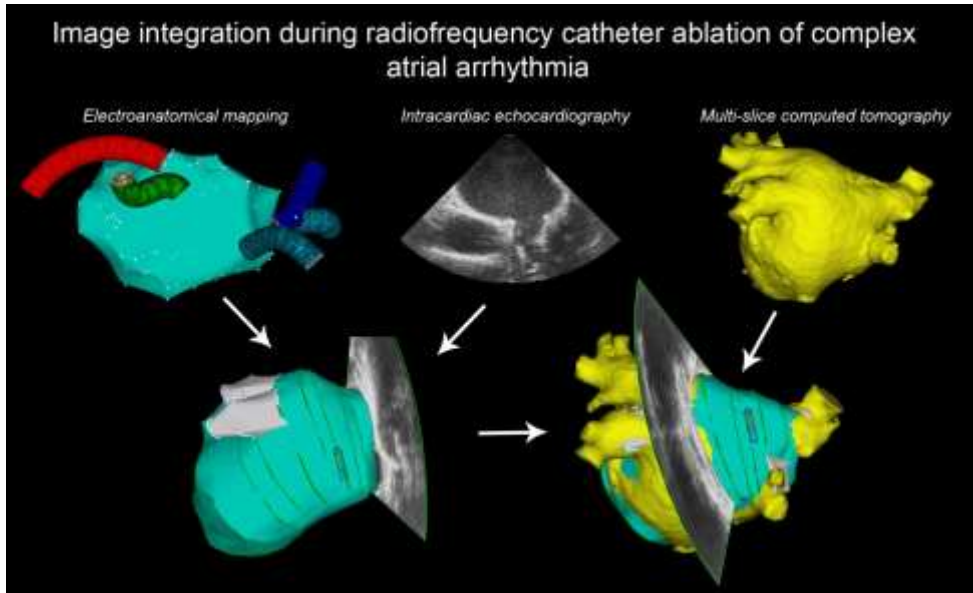


Figure 2. Example of integration of different imaging modalities to facilitate radiofrequency catheter ablation of complex atrial arrhythmia. The integration of electroanatomical mapping, intracardiac echocardiography and multi-slice computed tomography combines non-fluoroscopic navigation, real-time visualization of important cardiac structures and highly detailed three-dimensional anatomical information that can be used to guide the ablation procedure.

In part I, the impact of echocardiography, MSCT and biochemical markers on the efficacy of RFCA for AF is discussed. First, Chapter 1 reviews the limitations of left atrial size as a criterion to select patients with a high likelihood to maintain sinus rhythm after RFCA for AF. Then Chapter 2 focusses on the impact of left atrial fibrosis, assessed using echocardiography derived calibrated integrated backscatter, on the efficacy of RFCA for AF. Importantly, the interaction of left atrial size and atrial fibrosis on the efficacy of RFCA for AF is discussed. In Chapter 3 the impact of the total atrial conduction time (PA-TDI duration) on the efficacy of RFCA for AF is studied. Similar to the chapter 2, a comparison with left atrial size was made and discrepancies between left atrial size and PA-TDI duration were highlighted. In Chapter 4 the impact of

coronary artery disease on MSCT on the efficacy of RFCA for AF is discussed. Chapter 5 focusses on the impact of pulmonary vein anatomy and dimensions on the efficacy of RFCA for AF. Furthermore, this chapter evaluates the incremental value of 3-dimensional evaluation of left atrial dimensions on MSCT compared to left atrial size on echocardiography. Finally, Chapter 6 evaluates the prognostic value of atrial natriuretic peptide and B-type natriuretic peptide to predict AF recurrence after RFCA. In addition, a comprehensive echocardiographic evaluation of atrial volumes, ventricular volumes and ventricular systolic and diastolic function was performed. The prognostic impact of serum natriuretic peptide levels was studied in relation to these echocardiographic parameters.

In part II, the use of intracardiac echocardiography, MSCT and electroanatomical mapping to facilitate RFCA for complex atrial arrhythmias is discussed. Chapter 7 comprises a review of the use of intracardiac echocardiography during electrophysiological and other interventional procedures. Chapter 8 further advances on the role of integration imaging to guide RFCA for AF and Chapter 9 describes the integration of intracardiac echocardiography and electroanatomical mapping to successfully treat a patient with recurrent atrial tachycardia after a Senning operation for transposition of the great arteries. Finally, Chapter 10 describes the use of electroanatomical mapping to facilitate RFCA of an atrioventricular nodal re-entry tachycardia in a patient who previously underwent a Mustard operation for transposition of the great arteries. In addition, the anatomical situation following the Mustard operation and its implications to perform RFCA are discussed.

References

1. Cappato R, Calkins H, Chen SA, Davies W, Iesaka Y, Kalman J, Kim YH, Klein G, Natale A, Packer D, Skanes A, Ambrogi F, Biganzoli E Updated Worldwide Survey on the Methods, Efficacy, and Safety of Catheter Ablation for Human Atrial Fibrillation. *Circ Arrhythm Electrophysiol* 2010;3:32-38.
2. Calkins H, Kuck KH, Cappato R, Brugada J, Camm AJ, Chen SA, Crijns HJ, Damiano RJ, Jr., Davies DW, DiMarco J, Edgerton J, Ellenbogen K, Ezekowitz MD, Haines DE, Haissaguerre M, Hindricks G, Iesaka Y, Jackman W, Jalife J, Jais P, Kalman J, Keane D, Kim YH, Kirchhof P, Klein G, Kottkamp H, Kumagai K, Lindsay BD, Mansour M, Marchlinski FE, McCarthy PM, Mont JL, Morady F, Nademanee K, Nakagawa H, Natale A, Nattel S, Packer DL, Pappone C, Prystowsky E, Raviele A, Reddy V, Ruskin JN, Shemin RJ, Tsao HM, Wilber D 2012 HRS/EHRA/ECAS Expert Consensus Statement on Catheter and Surgical Ablation of Atrial Fibrillation: recommendations for patient selection, procedural techniques, patient management and follow-up, definitions, endpoints, and research trial design. *Europace* 2012;14:528-606.
3. Camm AJ, Kirchhof P, Lip GY, Schotten U, Savelieva I, Ernst S, Van Gelder IC, Al-Attar N, Hindricks G, Prendergast B, Heidbuchel H, Alfieri O, Angelini A, Atar D, Colonna P, De CR, De SJ, Goette A, Gorenek B, Heldal M, Hohloser SH, Kolh P, Le Heuzey JY, Ponikowski P, Rutten FH, Vahanian A, Auricchio A, Bax J, Ceconi C, Dean V, Filippatos G, Funck-Brentano C, Hobbs R, Kearney P, McDonagh T, Popescu BA, Reiner Z, Sechtem U, Sirnes PA, Tendera M, Vardas PE, Widimsky P, Vardas PE, Agladze V, Alilot E, Balabanski T, Blomstrom-Lundqvist C, Capucci A, Crijns H, Dahlöf B, Folliguet T, Glikson M, Goethals M, Gulba DC, Ho SY, Klautz RJ, Kose S, McMurray J, Perrone FP, Raatikainen P, Salvador MJ, Schalij MJ, Shpektor A, Sousa J, Stepinska J, Uuetoa H, Zamorano JL, Zupan I Guidelines for the management of atrial fibrillation: the Task Force for the Management of Atrial Fibrillation of the European Society of Cardiology (ESC). *Europace* 2010;12:1360-1420.
4. Benjamin EJ, Wolf PA, D'Agostino RB, Silbershatz H, Kannel WB, Levy D Impact of atrial fibrillation on the risk of death: the Framingham Heart Study. *Circulation* 1998;98:946-952.
5. Stewart S, Hart CL, Hole DJ, McMurray JJ A population-based study of the long-term risks associated with atrial fibrillation: 20-year follow-up of the Renfrew/Paisley study. *Am J Med* 2002;113:359-364.
6. Moe GK, Rheinboldt WC, Abildskov JA A computer model of atrial fibrillation. *Am Heart J* 1964;67:200-220.
7. Haissaguerre M, Jais P, Shah DC, Takahashi A, Hocini M, Quiniou G, Garrigue S, Le MA, Le MP, Clementy J Spontaneous initiation of atrial fibrillation by ectopic beats originating in the pulmonary veins. *N Engl J Med* 1998;339:659-666.
8. Vasamreddy CR, Lickfett L, Jayam VK, Nasir K, Bradley DJ, Eldadah Z, Dickfeld T, Berger R, Calkins H Predictors of recurrence following catheter ablation of atrial fibrillation using an irrigated-tip ablation catheter. *J Cardiovasc Electrophysiol* 2004;15:692-697.
9. Berruezo A, Tamborero D, Mont L, Benito B, Tolosana JM, Sitges M, Vidal B, Arriagada G, Mendez F, Matiello M, Molina I, Brugada J Pre-procedural predictors of atrial fibrillation recurrence after circumferential pulmonary vein ablation. *Eur Heart J* 2007;28:836-841.
10. Chen MS, Marrouche NF, Khaykin Y, Gillinov AM, Wazni O, Martin DO, Rossillo A, Verma A, Cummings J, Erciyes D, Saad E, Bhargava M, Bash D, Schweikert R, Burkhardt D, Williams-Andrews M, Perez-Lugones A, Abdul-Karim A, Saliba W, Natale A Pulmonary vein isolation for the treatment of atrial fibrillation in patients with impaired systolic function. *J Am Coll Cardiol* 2004;43:1004-1009.

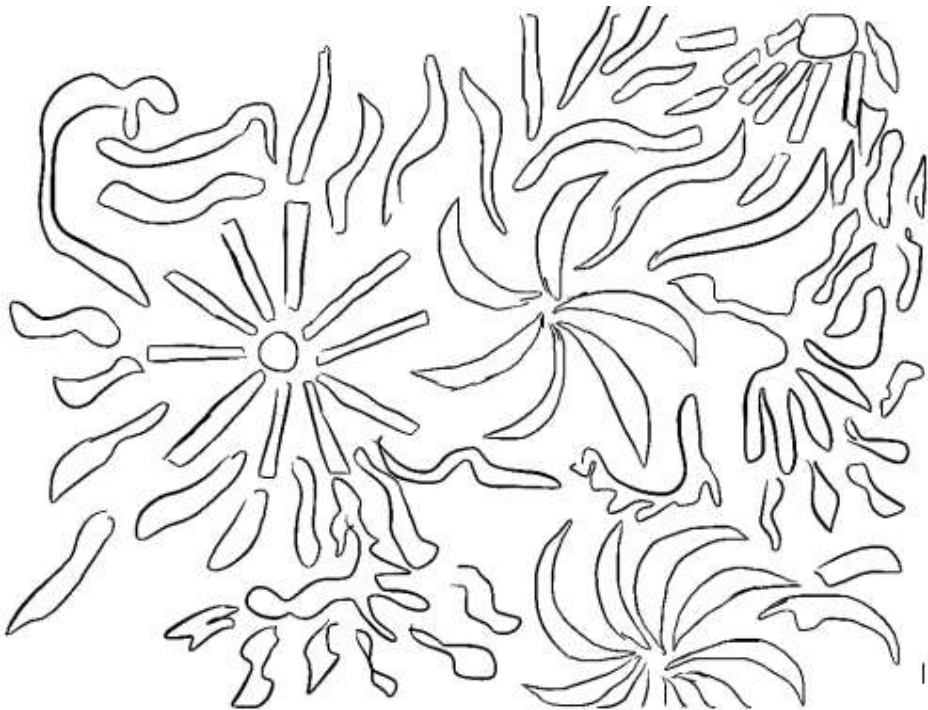
11. Verma A, Wazni OM, Marrouche NF, Martin DO, Kilicaslan F, Minor S, Schweikert RA, Saliba W, Cummings J, Burkhardt JD, Bhargava M, Belden WA, Abdul-Karim A, Natale A Pre-existent left atrial scarring in patients undergoing pulmonary vein antrum isolation: an independent predictor of procedural failure. *J Am Coll Cardiol* 2005;45:285-292.
12. Chilukuri K, Dalal D, Gadrey S, Marine JE, Macpherson E, Henrikson CA, Cheng A, Nazarian S, Sinha S, Spragg D, Berger R, Calkins H A prospective study evaluating the role of obesity and obstructive sleep apnea for outcomes after catheter ablation of atrial fibrillation. *J Cardiovasc Electrophysiol* 2010;21:521-525.
13. Wijffels MC, Kirchhof CJ, Dorland R, Allesie MA Atrial fibrillation begets atrial fibrillation. A study in awake chronically instrumented goats. *Circulation* 1995;92:1954-1968.
14. Ausma J, Litjens N, Lenders MH, Duimel H, Mast F, Wouters L, Ramaekers F, Allesie M, Borgers M Time course of atrial fibrillation-induced cellular structural remodeling in atria of the goat. *J Mol Cell Cardiol* 2001;33:2083-2094.
15. Vaziri SM, Larson MG, Benjamin EJ, Levy D Echocardiographic predictors of nonrheumatic atrial fibrillation. The Framingham Heart Study. *Circulation* 1994;89:724-730.
16. Hof I, Chilukuri K, Rbab-Zadeh A, Scherr D, Dalal D, Nazarian S, Henrikson C, Spragg D, Berger R, Marine J, Calkins H Does left atrial volume and pulmonary venous anatomy predict the outcome of catheter ablation of atrial fibrillation? *J Cardiovasc Electrophysiol* 2009;20:1005-1010.
17. Abecasis J, Dourado R, Ferreira A, Saraiva C, Cavaco D, Santos KR, Morgado FB, Adragao P, Silva A Left atrial volume calculated by multi-detector computed tomography may predict successful pulmonary vein isolation in catheter ablation of atrial fibrillation. *Europace* 2009.
18. McGann CJ, Kholmovski EG, Oakes RS, Blauer JJ, Daccarett M, Segerson N, Airey KJ, Akoum N, Fish E, Badger TJ, DiBella EV, Parker D, MacLeod RS, Marrouche NF New magnetic resonance imaging-based method for defining the extent of left atrial wall injury after the ablation of atrial fibrillation. *J Am Coll Cardiol* 2008;52:1263-1271.
19. Oakes RS, Badger TJ, Kholmovski EG, Akoum N, Burgon NS, Fish EN, Blauer JJ, Rao SN, DiBella EV, Segerson NM, Daccarett M, Windfelder J, McGann CJ, Parker D, MacLeod RS, Marrouche NF Detection and quantification of left atrial structural remodeling with delayed-enhancement magnetic resonance imaging in patients with atrial fibrillation. *Circulation* 2009;119:1758-1767.
20. Kuppahally SS, Akoum N, Burgon NS, Badger TJ, Kholmovski EG, Vijayakumar S, Rao SN, Blauer J, Fish EN, DiBella EV, MacLeod RS, McGann C, Litwin SE, Marrouche NF Left atrial strain and strain rate in patients with paroxysmal and persistent atrial fibrillation: relationship to left atrial structural remodeling detected by delayed-enhancement MRI. *Circ Cardiovasc Imaging* 2010;3:231-239.
21. Tops LF, Delgado V, Bertini M, Marsan NA, den Uijl DW, Trines SA, Zeppenfeld K, Holman E, Schalij MJ, Bax JJ Left atrial strain predicts reverse remodeling after catheter ablation for atrial fibrillation. *J Am Coll Cardiol* 2011;57:324-331.
22. Perez JE, Barzilai B, Madaras EI, Glueck RM, Saffitz JE, Johnston P, Miller JG, Sobel BE Applicability of ultrasonic tissue characterization for longitudinal assessment and differentiation of calcification and fibrosis in cardiomyopathy. *J Am Coll Cardiol* 1984;4:88-95.
23. Picano E, Pelosi G, Marzilli M, Lattanzi F, Benassi A, Landini L, L'Abbate A In vivo quantitative ultrasonic evaluation of myocardial fibrosis in humans. *Circulation* 1990;81:58-64.

24. Wang GD, Shen LH, Wang L, Li HW, Zhang YC, Chen H Relationship between integrated backscatter and atrial fibrosis in patients with and without atrial fibrillation who are undergoing coronary bypass surgery. *Clin Cardiol* 2009;32:E56-E61.
25. Merckx KL, De Vos CB, Palmans A, Habets J, Cheriex EC, Crijns HJ, Tieleman RG Atrial activation time determined by transthoracic Doppler tissue imaging can be used as an estimate of the total duration of atrial electrical activation. *J Am Soc Echocardiogr* 2005;18:940-944.
26. De Vos CB, Weijs B, Crijns HJ, Cheriex EC, Palmans A, Habets J, Prins MH, Pisters R, Nieuwlaet R, Tieleman RG Atrial tissue Doppler imaging for prediction of new-onset atrial fibrillation. *Heart* 2009;95:835-840.
27. Antoni ML, Bertini M, Atary JZ, Delgado V, ten Brinke EA, Boersma E, Holman ER, van der Wall EE, Schalij MJ, Bax JJ, van de Veire NR Predictive value of total atrial conduction time estimated with tissue Doppler imaging for the development of new-onset atrial fibrillation after acute myocardial infarction. *Am J Cardiol* 2010;106:198-203.
28. Buck S, Rienstra M, Maass AH, Nieuwland W, van Veldhuisen DJ, Van Gelder IC Cardiac resynchronization therapy in patients with heart failure and atrial fibrillation: importance of new-onset atrial fibrillation and total atrial conduction time. *Europace* 2008;10:558-565.
29. Hof I, rhab-Zadeh A, Scherr D, Chilukuri K, Dalal D, Abraham T, Lima J, Calkins H Correlation of left atrial diameter by echocardiography and left atrial volume by computed tomography. *J Cardiovasc Electrophysiol* 2009;20:159-163.
30. Levin ER, Gardner DG, Samson WK Natriuretic peptides. *N Engl J Med* 1998;339:321-328.
31. Knudsen CW, Omland T, Clopton P, Westheim A, Wu AH, Duc P, McCord J, Nowak RM, Hollander JE, Storrow AB, Abraham WT, McCullough PA, Maisel A Impact of atrial fibrillation on the diagnostic performance of B-type natriuretic peptide concentration in dyspneic patients: an analysis from the breathing not properly multinational study. *J Am Coll Cardiol* 2005;46:838-844.
32. Ellinor PT, Low AF, Patton KK, Shea MA, Macrae CA Discordant atrial natriuretic peptide and brain natriuretic peptide levels in lone atrial fibrillation. *J Am Coll Cardiol* 2005;45:82-86.
33. Yamada T, Murakami Y, Okada T, Okamoto M, Shimizu T, Toyama J, Yoshida Y, Tsuboi N, Ito T, Muto M, Kondo T, Inden Y, Hirai M, Murohara T Plasma atrial natriuretic Peptide and brain natriuretic Peptide levels after radiofrequency catheter ablation of atrial fibrillation. *Am J Cardiol* 2006;97:1741-1744.
34. Patton KK, Ellinor PT, Heckbert SR, Christenson RH, Defilippi C, Gottdiener JS, Kronmal RA N-terminal pro-B-type natriuretic peptide is a major predictor of the development of atrial fibrillation: the Cardiovascular Health Study. *Circulation* 2009;120:1768-1774.
35. Asselbergs FW, van den Berg MP, Bakker SJ, Signorovitch JE, Hillege HL, van Gilst WH, van Veldhuisen DJ N-terminal pro B-type natriuretic peptide levels predict newly detected atrial fibrillation in a population-based cohort. *Neth Heart J* 2008;16:73-78.
36. Shin DI, Deneke T, Gorr E, Anders H, Buenz K, Paesler M, Horlitz M Predicting successful pulmonary vein isolation in patients with atrial fibrillation by brain natriuretic Peptide plasma levels. *Indian Pacing Electrophysiol J* 2009;9:241-246.
37. Tops LF, Bax JJ, Zeppenfeld K, Jongbloed MR, Lamb HJ, van der Wall EE, Schalij MJ Fusion of multislice computed tomography imaging with three-dimensional electroanatomic mapping to guide radiofrequency catheter ablation procedures. *Heart Rhythm* 2005;2:1076-1081.
38. Fahmy TS, Mlcochova H, Wazni OM, Patel D, Cihak R, Kanj M, Beheiry S, Burkhardt JD, Dresing T, Hao S, Tchou P, Kautzner J, Schweikert RA, Arruda M, Saliba W, Natale A

- Intracardiac echo-guided image integration: optimizing strategies for registration. *J Cardiovasc Electrophysiol* 2007;18:276-282.
39. Zhong H, Lacomis JM, Schwartzman D On the accuracy of CartoMerge for guiding posterior left atrial ablation in man. *Heart Rhythm* 2007;4:595-602.
 40. Marrouche NF, Martin DO, Wazni O, Gillinov AM, Klein A, Bhargava M, Saad E, Bash D, Yamada H, Jaber W, Schweikert R, Tchou P, Abdul-Karim A, Saliba W, Natale A Phased-array intracardiac echocardiography monitoring during pulmonary vein isolation in patients with atrial fibrillation: impact on outcome and complications. *Circulation* 2003;107:2710-2716.
 41. Ren JF, Lin D, Marchlinski FE, Callans DJ, Patel V Esophageal imaging and strategies for avoiding injury during left atrial ablation for atrial fibrillation. *Heart Rhythm* 2006;3:1156-1161.
 42. Khaykin Y, Klemm O, Verma A First human experience with real-time integration of intracardiac echocardiography and 3D electroanatomical imaging to guide right free wall accessory pathway ablation. *Europace* 2008;10:116-117.
 43. Nolker G, Gutleben KJ, Marschang H, Ritscher G, Asbach S, Marrouche N, Brachmann J, Sinha AM Three-dimensional left atrial and esophagus reconstruction using cardiac C-arm computed tomography with image integration into fluoroscopic views for ablation of atrial fibrillation: accuracy of a novel modality in comparison with multislice computed tomography. *Heart Rhythm* 2008;5:1651-1657.
 44. Thiagalingam A, Manzke R, d'Avila A, Ho I, Locke AH, Ruskin JN, Chan RC, Reddy VY Intraprocedural volume imaging of the left atrium and pulmonary veins with rotational X-ray angiography: implications for catheter ablation of atrial fibrillation. *J Cardiovasc Electrophysiol* 2008;19:293-300.

Part 1

Pre-procedural evaluation of patients undergoing radiofrequency catheter ablation for atrial fibrillation



Chapter 2

Left atrial size as a predictor of successful radiofrequency catheter ablation for atrial fibrillation

Dennis W. den Uijl, Jeroen J. Bax

Europace. 2009 Oct;11(10):1255-6



Radiofrequency catheter ablation (RFCA) is a curative treatment option for patients with atrial fibrillation (AF). However, this treatment modality is associated with a considerable recurrence rate and a small risk for serious complications.¹ To improve the success rate and to avoid unnecessary procedure-related risks in patients with a high likelihood of AF recurrence, proper patient selection is mandatory. According to the Heart Rhythm Society/European Heart Rhythm Association/European Cardiac Arrhythmia Society expert consensus statement, considerations in the selection of patient for AF ablation should include: severity of symptoms, age, duration of AF, and left atrial (LA) diameter.² However, as an alternative to LA diameter, a more **comprehensive evaluation of the 'true' LA size may improve the identification** of patients with a high likelihood of maintaining sinus rhythm after RFCA.

Abecasis et al.³ prospectively investigated the use of LA volume assessed by multi-slice computed tomography (MSCT) as a predictor of successful ablation for AF. Ninety-nine consecutive patients undergoing circumferential pulmonary vein ablation were studied. A pre-procedural MSCT examination was performed in all patients and LA volume was measured using semi-automatic software to detect the endocardial borders. The authors demonstrated that an increase in the LA volume on MSCT was related to increased risk for AF recurrence after RFCA. Using ROC curve analysis, a cut-off value of 145 mL for LA volume was identified to provide the best predictive value for recurrent AF after RFCA.

LA enlargement is considered an important risk factor for AF. In the Framingham Heart Study, LA enlargement was found to be an independent predictor of new onset AF in the general population.⁴ Moreover, LA enlargement has been identified as a risk factor for AF recurrence after RFCA. In a group of 148 patients, Berruezo et al.⁵ demonstrated that the anterior-posterior LA diameter was an independent predictor of AF recurrence after

RFCA. This finding was confirmed by Shin et al.⁶ who demonstrated the predictive value of LA volume for AF recurrence after RFCA in a group of 68 patients. Significantly dilated atria are generally thought to be associated with a high degree of atrial remodelling which limits the efficacy of RFCA. As a consequence, many clinical trials on RFCA for AF have restricted their enrolment to patients with an LA anterior–posterior diameter of <50–55 mm. However, when using LA enlargement as a patient selection criterion, it should be noted that the LA anterior–posterior diameter is not the most accurate **representation of the ‘true’ LA size.**⁷ Owing to constraints of the thoracic cavity, LA enlargement is often asymmetric and oriented predominantly in superior–inferior and medial–lateral direction. Therefore, the application of the anterior–posterior diameter to select patients eligible for RFCA may be limited. This was demonstrated by Abecasis et al. who showed that LA volume on MSCT was related to the outcome of RFCA, whereas the LA anterior–posterior diameter on transthoracic echocardiography was not.³ The most likely explanation for this finding is that three-dimensional imaging modalities like MSCT provide a **more accurate estimation of the ‘true’ LA size than two-dimensional echocardiography** and therefore have a higher prognostic value for the outcome after RFCA.⁷ Accordingly, a similar prognostic value is expected when using other three-dimensional imaging modalities to assess the LA size such as three-dimensional echocardiography. Importantly, MSCT is associated with a considerable amount of radiation exposure which limits its applicability as a patient selection tool. Alternatively, three-dimensional echocardiography allows the accurate assessment of cardiac volumes without radiation exposure and can also be used to monitor functional improvement or reverse remodelling of the atria after RFCA.^{8,9} In contrast to MSCT, three-dimensional echocardiography does not provide information about the pulmonary vein anatomy, which is essential for safety of RFCA. Magnetic resonance imaging

provides information about the pulmonary vein anatomy and allows the accurate assessment of LA volume without radiation exposure.¹⁰ However, the use of magnetic resonance imaging is limited by its limited availability and high costs.

In conclusion, as demonstrated by Abecasis et al.,³ accurate assessment of LA volume using a three-dimensional imaging modality is essential for improvement of patient selection for RFCA of AF. Three-dimensional imaging **provides a more accurate representation of the 'true' LA size than two-dimensional imaging** and has a higher prognostic value for outcome after RFCA. The available three-dimensional imaging modalities include MSCT, magnetic resonance imaging, and three-dimensional echocardiography. Importantly, each of these imaging modalities has its own advantages and limitations. Nevertheless, all can be used to accurately assess LA size, which may significantly improve prediction of successful RFCA for AF.

References

1. Cappato R, Calkins H, Chen SA, Davies W, Iesaka Y, Kalman J, Kim YH, Klein G, Packer D, Skanes A Worldwide survey on the methods, efficacy, and safety of catheter ablation for human atrial fibrillation. *Circulation* 2005;111:1100-1105.
2. Calkins H, Brugada J, Packer DL, Cappato R, Chen SA, Crijns HJ, Damiano RJ, Jr., Davies DW, Haines DE, Haissaguerre M, Iesaka Y, Jackman W, Jais P, Kottkamp H, Kuck KH, Lindsay BD, Marchlinski FE, McCarthy PM, Mont JL, Morady F, Nademanee K, Natale A, Pappone C, Prystowsky E, Raviele A, Ruskin JN, Shemin RJ HRS/EHRA/ECAS expert consensus statement on catheter and surgical ablation of atrial fibrillation: recommendations for personnel, policy, procedures and follow-up. A report of the Heart Rhythm Society (HRS) Task Force on Catheter and Surgical Ablation of Atrial Fibrillation developed in partnership with the European Heart Rhythm Association (EHRA) and the European Cardiac Arrhythmia Society (ECAS); in collaboration with the American College of Cardiology (ACC), American Heart Association (AHA), and the Society of Thoracic Surgeons (STS). Endorsed and approved by the governing bodies of the American College of Cardiology, the American Heart Association, the European Cardiac Arrhythmia Society, the European Heart Rhythm Association, the Society of Thoracic Surgeons, and the Heart Rhythm Society. *Europace* 2007;9:335-379.
3. Abecasis J, Dourado R, Ferreira A, Saraiva C, Cavaco D, Santos KR, Morgado FB, Adragao P, Silva A Left atrial volume calculated by multi-detector computed tomography may predict successful pulmonary vein isolation in catheter ablation of atrial fibrillation. *Europace* 2009.
4. Vaziri SM, Larson MG, Benjamin EJ, Levy D Echocardiographic predictors of nonrheumatic atrial fibrillation. The Framingham Heart Study. *Circulation* 1994;89:724-730.
5. Berruezo A, Tamborero D, Mont L, Benito B, Tolosana JM, Sitges M, Vidal B, Arriagada G, Mendez F, Matiello M, Molina I, Brugada J Pre-procedural predictors of atrial fibrillation recurrence after circumferential pulmonary vein ablation. *Eur Heart J* 2007;28:836-841.
6. Shin SH, Park MY, Oh WJ, Hong SJ, Pak HN, Song WH, Lim DS, Kim YH, Shim WJ Left atrial volume is a predictor of atrial fibrillation recurrence after catheter ablation. *J Am Soc Echocardiogr* 2008;21:697-702.
7. Hof I, Rbab-Zadeh A, Scherr D, Chilukuri K, Dalal D, Abraham T, Lima J, Calkins H Correlation of left atrial diameter by echocardiography and left atrial volume by computed tomography. *J Cardiovasc Electrophysiol* 2009;20:159-163.
8. Keller AM, Gopal AS, King DL Left and right atrial volume by freehand three-dimensional echocardiography: in vivo validation using magnetic resonance imaging. *Eur J Echocardiogr* 2000;1:55-65.
9. Marsan NA, Tops LF, Holman ER, van de Veire NR, Zeppenfeld K, Boersma E, van der Wall EE, Schalij MJ, Bax JJ Comparison of left atrial volumes and function by real-time three-dimensional echocardiography in patients having catheter ablation for atrial fibrillation with persistence of sinus rhythm versus recurrent atrial fibrillation three months later. *Am J Cardiol* 2008;102:847-853.
10. Mlcochova H, Tintera J, Porod V, Pechl P, Cihak R, Kautzner J Magnetic resonance angiography of pulmonary veins: implications for catheter ablation of atrial fibrillation. *Pacing Clin Electrophysiol* 2005;28:1073-1080.

Chapter 3

Impact of left atrial fibrosis and left atrial size on the outcome of catheter ablation for atrial fibrillation

Dennis W. den Uijl, Victoria Delgado, Matteo Bertini, Laurens F. Tops, Serge A. Trines, Nico R. van de Veire, Katja Zeppenfeld, Martin J. Schalij, Jeroen J. Bax

Heart. 2011 Nov;97(22):1847-51



Abstract

Background: Left atrial (LA) dilatation is an important risk factor for recurrence of atrial fibrillation (AF) after radiofrequency catheter ablation (RFCA). However the clinical application to select patients eligible for RFCA according to LA size is limited. Additional pre-procedural assessment of LA fibrosis could improve patient selection for RFCA.

Objective: To investigate the impact of LA size and LA fibrosis on the outcome of RFCA for AF.

Methods: One-hundred-seventy consecutive patients undergoing RFCA for AF were studied. Left atrial size was assessed by measuring maximum LA volume index on echocardiography. LA wall ultrasound reflectivity was assessed by measuring echocardiography derived calibrated integrated backscatter (IBS) as a surrogate of LA fibrosis.

Results: After 12 ± 3 months follow-up, 103 patients (61%) had maintained sinus rhythm and 67 patients (39%) had recurrence of AF. Univariate Cox analyses identified LA wall ultrasound reflectivity, as well as LA size and type of AF, as predictors of AF recurrence after RFCA. Importantly, multivariate analyses showed that LA ultrasound reflectivity remained as strong predictor after correction for LA size and type of AF. Moreover, LA wall ultrasound reflectivity provided an incremental value in predicting outcome of RFCA over LA size and type of AF (increment in global Chi-square 61.6, $p < 0.001$).

Conclusion: Assessment of LA fibrosis using two-dimensional echocardiography derived calibrated IBS can be useful to predict AF recurrence after RFCA. Combined assessment of LA fibrosis and LA size improves the identification of patients with a high likelihood for a successful ablation.

Introduction

Radiofrequency catheter ablation (RFCA) is a curative treatment option for patients with symptomatic drug-refractory atrial fibrillation (AF).¹ However, RFCA is associated with a considerable recurrence rate.² To improve the outcome of RFCA proper patient selection is mandatory.

Left atrial (LA) enlargement and LA fibrosis are two of the mainstay processes involved in atrial remodeling. LA size is a well recognized risk factor for AF recurrence after RFCA.³⁻⁵ Previous studies have demonstrated that in patients with severe atrial dilatation, the risk for AF recurrence after RFCA is high.³⁻⁵ However, in patients with mild-to-moderate LA enlargement, the AF recurrence rates are still significant and, therefore, the predictive value of LA size is reduced. In addition, LA fibrosis has been related to high probability of AF recurrence after RFCA.⁶ Non-invasive evaluation of the extent of atrial remodeling by assessment of LA fibrosis additional to LA size could be used to improve patient selection for AF ablation.

Two-dimensional echocardiography derived integrated backscatter (IBS) allows non-invasive tissue characterization based on tissue ultrasound reflectivity and may provide a good surrogate of myocardial fibrosis.^{7,8} Recently, calibrated IBS has been demonstrated to provide a reliable assessment of LA fibrosis.⁹

The aim of this study was to investigate the impact of LA wall ultrasound reflectivity assessed with calibrated IBS (as a surrogate of LA fibrosis) on the outcome of RFCA for AF. In addition, the relative merits of LA size and LA wall ultrasound reflectivity to predict the outcome of RFCA were investigated.

Methods

Patient population and evaluation

One-hundred-and-seventy patients undergoing RFCA for AF were studied. Before the ablation, all patients underwent transthoracic echocardiography to assess LA size, left ventricular (LV) systolic function and to exclude valvular heart disease. In addition, IBS analysis was performed to estimate LA wall ultrasound reflectivity as a surrogate of LA fibrosis. After the ablation, all patients were evaluated at the outpatient clinic during a 12-month follow-up period. Routine electrocardiogram (ECG) recordings were acquired each visit and 24-hour Holter registrations were scheduled after 3, 6 and 12 months follow-up. All medications were continued for at least 3 months. Afterwards, anti-arrhythmic drugs were discontinued at the discretion of the physician. After a blanking period of 3 months, recurrence of AF was defined as any recording of AF on ECG or an episode longer than 30 s on 24-hour Holter monitoring.

Standard echocardiography

Two-dimensional transthoracic echocardiography was performed using a commercially available ultrasound system (Vivid 7, General Electric Vingmed, Milwaukee, WI), equipped with a 3.5-MHz transducer. All patients were imaged in left lateral decubitus position. Two-dimensional and color Doppler data were obtained in the parasternal short- and long-axis views and the apical 2- and 4-chamber views, adjusting gain settings and depth. All images were ECG-triggered and stored in cineloop format for off-line analyses (EchoPac 108.1.5, General Electric Medical Systems, Horten, Norway). Maximum LA volume was obtained from the apical 4- and 2-chamber views by disc's method and indexed to body surface area.¹⁰ Left ventricular ejection fraction was calculated

from the standard apical 2- and 4-chamber views by **Simpson's method**, according to the American Society of Echocardiography guidelines.¹⁰

Calibrated integrated backscatter

Integrated backscatter is an echocardiographic parameter based on two-dimensional gray-scale images which measures the myocardial ultrasound reflectivity and can be used to estimate myocardial fibrosis.¹¹⁻¹³ Integrated backscatter is expressed in decibels (dB) and, conventionally, cardiac structures with no fibrotic content have a low ultrasound reflectivity and are coded with negative IBS values (e.g. blood pool) whereas cardiac structures with a high content of fibrosis have a high ultrasound reflectivity and IBS values near 0 dB (e.g. pericardium). Normal myocardium has an intermediate IBS value which increases as the content of fibrosis increases.⁸ In the present study, fibrosis of the LA was evaluated by measuring calibrated IBS of the LA wall. For this purpose, two-dimensional gray-scale images were obtained from the parasternal long-axis view, with frame rates between 80 and 120 frames/s. Three cardiac cycles were stored in cine-loop format for offline analysis (EchoPAC 108.1.5, General Electric Medical Systems). A fixed 2 x 3 mm region of interest was positioned in the LA posterior wall, excluding epicardial specular reflections. In addition, the 2 x 3 mm region of interest placed at the pericardium provided the reference value of ultrasound reflectivity to estimate the calibrated IBS value of the LA. Calibrated IBS of the LA was calculated by subtracting the IBS value of the pericardium from the IBS value of the posterior LA wall. Accordingly, higher values (i.e. less negative values) of calibrated IBS correspond to a larger extent of atrial fibrosis. All IBS values were measured during the same phase of the cardiac cycle, at end-diastole.

Radiofrequency catheter ablation

The ablation was aimed at creating circular lesions around the left and right pulmonary vein ostia. All patients received intravenous heparin to maintain an activated clotting time of 300-400 s. Intracardiac echocardiography was used to exclude a cardiac thrombus and to guide the transseptal puncture. A non-fluoroscopic electroanatomical mapping system with multi-slice computed tomography integration was used to guide the ablation procedure (CARTO XP™, Cartomerge™, Biosense Webster, Diamond Bar, CA, USA). Mapping and ablation was performed using a 4-mm quadripolar open-loop irrigated mapping/ablation catheter (7Fr Navistar™, Biosense Webster). Radiofrequency current was applied at 30-35 W with a maximum temperature of 45°C and an irrigation flow of 20 ml/min until a bipolar voltage of <0.1 mV was achieved, with a maximum of 60 s per point. Pulmonary vein isolation was confirmed by recording entrance block during sinus rhythm or pacing in the coronary sinus.¹⁴

Statistical analysis

All variables were tested for a normal distribution with the Kolmogorov-Smirnov test. Continuous variables with a normal distribution are presented as mean \pm SD **and were compared with the student's t-test**. Continuous variables with a non-normal distribution are presented as median (25th-75th percentile) and statistical comparisons were performed with the Mann-Whitney U-test. Categorical variables are presented as number (percentage) and were compared with the chi-square test. Univariate and multivariate Cox proportional hazard analyses were performed to investigate the relation between calibrated IBS of the LA and risk for AF recurrence after catheter ablation. Variables with a $p < 0.05$ in the univariate analyses were included in the multivariate analysis which was performed using an '**enter**' method. The incremental value of calibrated IBS of the LA over baseline clinical and

echocardiographic characteristics to assess the risk for AF recurrence was studied by calculating the improvement in global chi-square. Finally, to test the reproducibility of the calibrated IBS measurements, 20 patients were randomly selected to evaluate the inter- and intra-observer variability. The measurements of calibrated IBS of the LA posterior wall were repeated by the same observer in a blinded-fashion and at a separate time (1 week later). To evaluate inter-observer variability, a second independent observer re-analyzed the same dataset. Intra- and inter-observer reproducibility were calculated with the Bland-Altman analysis and the intraclass correlation coefficient. **Good correlation was defined as Cronbach's $\alpha > 0.8$.** In addition, the test-retest variability of measurement of echocardiographic calibrated IBS was assessed in 20 patients. Two echocardiograms were performed within 24 hours in each patient and the data were analyzed by the same observer. All statistical analyses were performed with SPSS software (version 16.0, SPSS Inc., Chicago, IL, USA). A value of $p < 0.05$ was considered statistically significant.

Results

Patient characteristics

A total of 170 consecutive patients were included (131 men, mean age 56 ± 9 years), representing an ongoing clinical registry.¹⁵ AF was paroxysmal in 121 patients and persistent in 49 patients according to current guidelines definitions.¹⁶ Median duration of AF was 48 months (interquartile range: 24-96) and the mean number of anti-arrhythmic drugs used was 3.3 ± 1.3 per patient. No patient had previously undergone RFCA for AF. The mean LA volume index was 42.5 ± 15.4 ml/m², the mean LA diameter was 42 ± 6 mm and the mean LV ejection fraction was $58 \pm 5\%$. No significant valvular heart disease was observed in any patient. Finally, the mean calibrated IBS of the LA was $-18.0 \pm$

5.1 dB (Table 1). The intra- and inter-observer reproducibility for calibrated IBS measurements were good with small bias and tight limits of agreement (0.93 ± 1.8 dB and 0.12 ± 3.3 dB, respectively) and good intraclass correlation coefficients (0.91 and 0.82, respectively). The test-retest variability for calibrated IBS was 1.07 ± 1.9 dB with an intraclass correlation coefficient of 0.92.

Table 1. Baseline patient characteristics

Patients (n)	170
Age (years)	55.9±9.0
Male gender, n (%)	131 (77)
Body Surface Area (m ²)	2.11±0.20
Type of AF	
Paroxysmal, n (%)	121 (71)
Persistent, n (%)	49 (29)
Duration of AF (months)	48 (24-96)
Number of failed antiarrhythmic drugs (n)	3.3±1.3
Hypertension, n (%)	76 (45)
Hypercholesterolemia, n (%)	51 (30)
Coronary artery disease, n (%)	9 (5)
Beta blocker, n (%)	54 (32)
Class 1 or 3 antiarrhythmic drug, n (%)	132 (78)
ACE inhibitor/angiotensin receptor blocker, n (%)	86 (51)
Diuretic, n (%)	27 (16)
LA volume index (ml/m ²)	42.5 ±15.4
LV ejection fraction (%)	58 ± 5
Calibrated IBS LA (dB)	-18.0±5.1

AF = atrial fibrillation, ACE = angiotensin-converting enzyme, IBS = integrated backscatter, LA = left atrium, LV = left ventricular.

Outcome after radiofrequency catheter ablation

After a mean follow-up of 12 ± 3 months, 103 patients (61%) maintained sinus rhythm, whereas 67 patients (39%) had recurrence of AF. In 22 patients (13%) a repeat procedure was performed due to early recurrence of AF. In the recurrence group a higher prevalence of persistent AF was found compared to

the non-recurrence group (16 [16%] versus 33 [49%], $p < 0.001$). Moreover, in the recurrence group the mean LA volume index and LA diameter were significantly larger compared to the non-recurrence group (46.0 ± 16.9 ml/m² versus 40.2 ± 14.1 ml/m² [$p = 0.016$] and 44 ± 6 mm versus 41 ± 5 mm [$p < 0.001$], respectively). Patients with persistent AF had significantly higher values (i.e. less negative) of calibrated IBS of the LA than patients with paroxysmal AF (-16.8 ± 4.7 dB versus -18.4 ± 5.2 dB, $p = 0.049$).

To study the relation between LA size, LA calibrated IBS and outcome after RFCA, the study population was divided into 'small LA' subgroup (n=84) and 'large LA' subgroup (n=86) based on the LA volume index, using the mean value (42.5 ml/m²) as cut-off point. Similarly, the population was divided into 'low fibrosis' subgroup (n=85) and 'high fibrosis' subgroup (n=85) according to calibrated IBS value of the posterior LA wall, using the mean value (-18.0 dB) as cut-off point.

The relation between LA enlargement and calibrated IBS of the LA is shown in Figure 1. Patients in the 'small LA' group had significant lower calibrated IBS values (i.e. more negative) than patients in the 'large LA' group (-19.4 ± 5.0 dB versus -16.5 ± 4.7 dB, $p < 0.001$). Importantly, a wide range of calibrated IBS values was found among patients with a 'small LA', illustrating that a small LA may still contain a large extent of fibrosis content (Figure 1).

Patients in the 'large LA' group had a higher risk for AF recurrence after RFCA than patients in the 'small LA' group (44 [51%] versus 23 [27%], $p = 0.002$) (Figure 2, panel A). When both LA size and LA fibrosis were taken into account, patients with a 'small LA' and 'low fibrosis' (n=52) had the most favorable outcome (94% non-recurrence, $p < 0.001$ vs. others) whereas patients with a 'large LA' and 'high fibrosis' (n=53) had the worst outcome (28% non-recurrence, $p < 0.001$ vs. others). Interestingly, patients with a 'large LA' but with 'low fibrosis' (n=33) had a good prognosis compared to patients with a 'small

LA' and 'high fibrosis' (n=32) (82% non-recurrence vs. 38% non-recurrence, $p < 0.001$) (Figure 2, panel B).

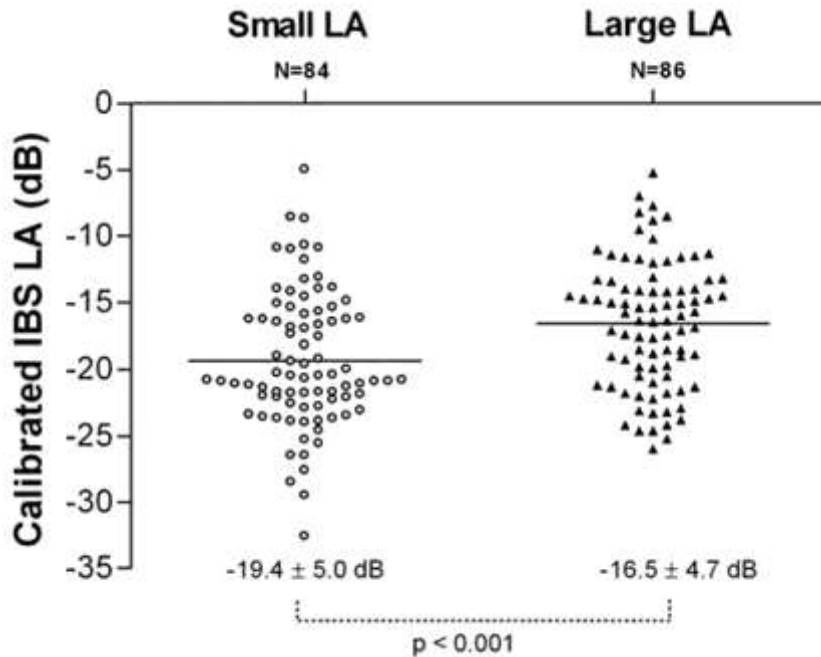


Figure 1. Relation between left atrial (LA) size and calibrated integrated backscatter (IBS) of the LA. 'Small LA' was defined as LA volume index < 42.5 ml/m² and 'large LA' was defined as LA volume index ≥ 42.5 ml/m². Importantly, in patients with "small LA", a wide scatter plot was observed indicating a significant proportion of patients with considerable amount of LA fibrosis. Similarly, the group of patients with "large LA" showed a wide range of calibrated IBS values of the LA, but with a mean value significantly higher (i.e. less negative) as compared to the group of patients with "small LA".

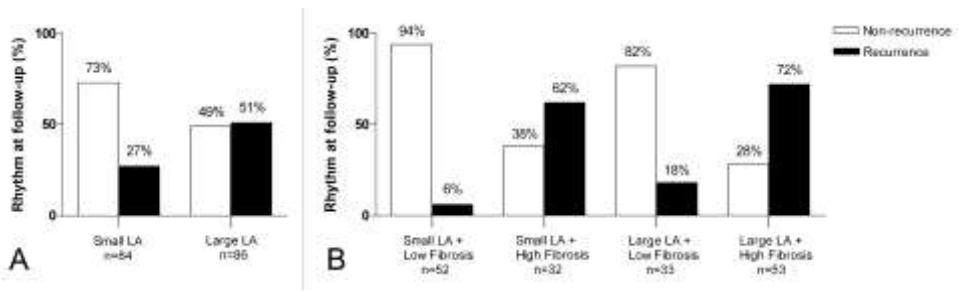


Figure 2. Outcome of radiofrequency catheter ablation (RFCA) according to left atrial (LA) size (panel A) and according to the combination of LA size and LA fibrosis. 'Small LA' was defined as LA volume index <42.5 ml/m² and 'large LA' was defined as LA volume index ≥ 42.5 ml/m². 'Low fibrosis' was defined as calibrated integrated backscatter (IBS) of the LA < -18.5 dB and 'high fibrosis' was defined as calibrated IBS of the LA ≥ -18.5 dB. In patients with "small LA" the likelihood of atrial fibrillation (AF) recurrences after RFCA was lower than patients with "large LA". However, the addition of LA fibrosis evaluation permitted a more refined stratification, with higher likelihood of AF recurrence among those patients with "high fibrosis" as compared to patients with "low fibrosis", regardless the LA size (panel B).

Finally, Figure 3 shows the relation between the occurrence of AF recurrence after RFCA and calibrated IBS and LA volume index. Patients who remained in sinus rhythm had significantly lower values of calibrated IBS (i.e. more negative) (-20.6 ± 3.7 dB vs. -13.9 ± 4.0 dB; $p < 0.001$) and smaller LA volume index (40.2 ± 14.1 ml/m² vs. 46.0 ± 16.9 ml/m², $p < 0.001$) than patients who had AF recurrences after RFCA. Interestingly, most patients with a value of calibrated IBS > -13.9 dB showed AF recurrence at follow-up. In contrast, there was a significant overlap between LA volume index values of patients who presented with AF recurrences and patients who remained in sinus rhythm and no LA volume cut-off value could be derived to differentiate these two groups of patients. Therefore, calibrated IBS may be a more accurate parameter to identify the patients who will show AF recurrences after RFCA.

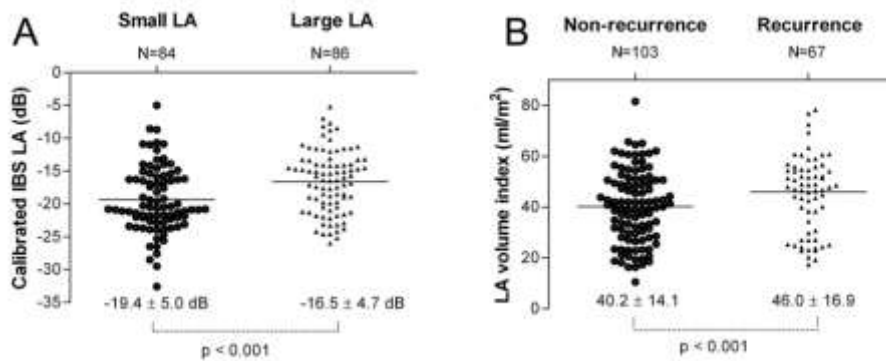


Figure 3. Calibrated integrated backscatter (IBS) of the left atrium (LA) and LA volume index in relation to outcome of radiofrequency catheter ablation. Patients who had atrial fibrillation recurrence after RFCA had significantly higher values of calibrated IBS of the LA (panel A) and LA volume index (panel B) at baseline than patients who remained in sinus rhythm.

Clinical and echocardiographic risk factors for AF recurrence

Univariate and multivariate Cox proportional hazard analyses were performed to evaluate the relation between calibrated IBS of the LA (in combination with other baseline clinical and echocardiographic variables) and the risk for AF recurrence after RFCA. Univariate analyses showed that increased calibrated IBS of the LA (i.e. less negative values) was related to a higher risk for AF recurrence after ablation, as were the presence of persistent AF and enlargement of the LA volume index (Table 2). Multivariate analysis showed that calibrated IBS of the LA was an independent predictor of AF recurrence (HR: 2.796 per 5 dB, 95% CI: 2.168-3.605, $p < 0.001$). Moreover, addition of calibrated IBS of the LA to a Cox model including LA volume index and type of AF resulted in a significant improvement in the prediction value for AF recurrence after RFCA (indicated by a significant improvement in global chi-square value: 61.6, $p < 0.001$) (Figure 4).

Table 2. Univariate Cox regression analysis of AF recurrence

	HR	95% CI	P-value
Clinical characteristics			
Age (per year)	1.005	0.977-1.033	0.74
Male gender (yes/no)	0.873	0.503-1.514	0.87
AF duration (per month)	1.008	0.959-1.059	0.76
Number of failed antiarrhythmic drugs (per drug)	1.058	0.886-1.262	0.54
Persistent AF (yes/no)	3.264	2.015-5.285	<0.001
Hypertension (yes/no)	1.063	0.658-1.717	0.80
Hypercholesterolemia (yes/no)	1.406	0.856-2.308	0.18
Coronary artery disease (yes/no)	0.217	0.030-1.564	0.13
Echocardiographic characteristics			
Calibrated IBS LA (per 5 dB)	2.670	2.119-3.363	<0.001
LA volume index (per ml/m ²)	1.023	1.006-1.039	0.007
LV ejection fraction (per %)	0.971	0.920-1.024	0.28

AF = atrial fibrillation, IBS = integrated backscatter, LA = left atrium, LV = left ventricular.

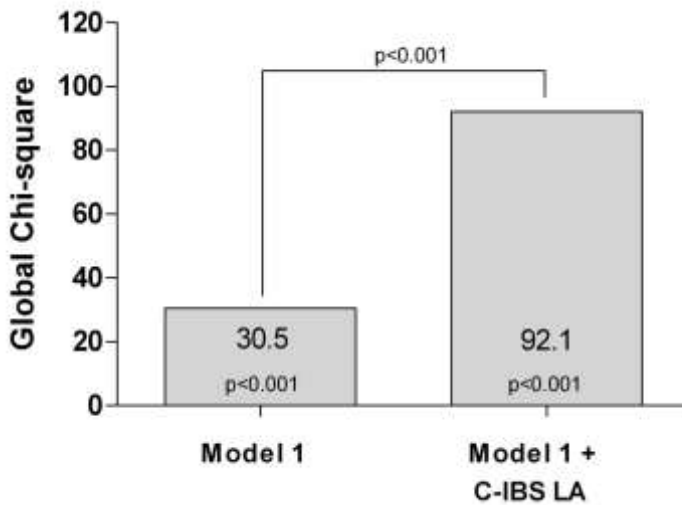


Figure 4. Incremental prognostic value of calibrated integrated backscatter (IBS) of the left atrium (LA). Bar graph illustrating the improvement in global chi-square value by the addition of calibrated IBS of the LA to a Cox regression model comprising LA volume index and type of AF (Model 1).

Discussion

The main findings of the present study were that LA enlargement was related to an increased risk for AF recurrence. More important, a high value of LA calibrated IBS as a surrogate of large extent of LA fibrosis was associated with poor outcome after RFCA. Finally, this study demonstrated that the combined assessment of LA calibrated IBS and LA size improved the identification of patients with a high likelihood for a successful ablation.

Atrial remodeling and outcome: LA size

Atrial fibrillation causes electrical and structural remodeling of the atria which play an important role in the perpetuation and progression of the arrhythmia.^{17,18} More importantly, atrial remodeling is associated with a limited efficacy of RFCA for AF.⁶ Pre-procedural evaluation of the extent of atrial remodeling can be used to improve patient selection for RFCA.

Atrial dilatation is associated with atrial remodeling.¹⁹ LA size has been shown to be an important risk factor for AF recurrence after RFCA.^{3,4} In a group of 148 patients, Berruezo et al. demonstrated that a large anterior-posterior LA diameter was related to a high risk for AF recurrence after RFCA.³ This was confirmed by Shin et al. who demonstrated that LA volume was an independent predictor of AF recurrence.⁴ However, the clinical value of LA size to select patients for RFCA may be limited. Whereas patients with severely **enlarged LA may be accurately identified as 'high risk' for AF recurrence**, patients with mild-to-moderate LA enlargement show a varying response to RFCA. Accordingly, extensive research has been performed to obtain additional parameters to better predict the outcome of RFCA for AF.

Atrial remodeling and outcome: LA fibrosis

Atrial fibrosis has been proposed as one of the processes involved in atrial remodeling.²⁰ Moreover, the presence of LA fibrosis is a risk factor for AF recurrence after RFCA.⁶ In 700 patients undergoing RFCA for AF, Verma et al. evaluated the extent of LA fibrosis by invasive voltage mapping of the left atrium. The presence of areas with low voltage in the LA (i.e. LA fibrosis) were an independent predictor AF recurrence after RFCA.⁶ However, ideally the assessment of LA fibrosis would be performed using a non-invasive and widely available imaging technique prior to the RFCA procedure. Calibrated IBS analysis allows non-invasive tissue characterization based on the quantification of ultrasound energy reflected by scattering elements inside the myocardium.^{8,11-13} Recently, assessment of LA fibrosis using calibrated IBS has been validated by Wang et al. in a group of 74 patients undergoing coronary artery bypass surgery.⁹ The authors found a good correlation between calibrated IBS value of the LA and the extent of collagen inside the LA appendage. Similarly, in the present study two-dimensional transthoracic echocardiography derived calibrated IBS was used to assess LA fibrosis. Patients with large LA size had higher values of calibrated IBS than patients with a small LA size. However, a large variation existed in the values of LA calibrated IBS in relation to LA size, and a considerable proportion of patients with a small LA had a high values of LA calibrated IBS suggesting a large amount of fibrosis. Notably, patients with small LA and high values of LA calibrated IBS had a significant percentage of AF recurrences at follow-up. Indeed, LA wall ultrasound reflectivity was a strong independent predictor of AF recurrences after RFCA and had an incremental value over LA size. Consequently, assessment of LA calibrated IBS in addition to LA size may improve the selection of patients eligible for RFCA for AF, thereby increasing the procedural success rate.

The assessment of macroscopic LA fibrosis with contrast-enhanced magnetic resonance imaging (CE-MRI) has been recently demonstrated.^{21,22} The high spatial resolution of CE-MRI permits exact localization of areas of macroscopic fibrosis within the LA wall. However, CE-MRI is not widely available and, in patients with renal dysfunction, the use of contrast may be not recommended.²³ In contrast, calibrated IBS provides a surrogate of fibrosis content of the LA wall. This analysis is performed on two-dimensional echocardiographic data and no contrast media is needed. Importantly, the present study shows that in combination with assessment of the LA size, calibrated IBS of the LA can be a valuable tool to identify patients with a high likelihood to have AF recurrence after RFCA.

Clinical implications

The present study demonstrated that pre-procedural assessment of LA fibrosis using calibrated IBS analyses can be useful to predict the outcome of RFCA for AF. LA fibrosis can be readily evaluated with this non-invasive imaging technique. Particularly in combination with measurement of LA size, pre-procedural assessment of LA fibrosis improves identification of patients with a high likelihood to maintain sinus rhythm after RFCA. Furthermore, this study extended the evidence that persistent AF is a risk factor for AF recurrence after RFCA. However, the present study also demonstrated that assessment of LA fibrosis with calibrated IBS improved patient selection compared to established risk factors as persistent AF and LA size. Consequently, an improved patient selection could result in a higher success rate of RFCA for AF. Alternatively, this information could be used to better inform patients about their likelihood to maintain sinus rhythm after RFCA.

Limitations

Left atrial fibrosis can be inhomogeneous in patients with AF.^{21,22} The inclusion **of histological data or the use of other “gold standard” techniques to estimate** LA fibrosis (e.g. electroanatomical voltage maps or late-gadolinium enhanced magnetic resonance imaging) would have strengthened our conclusions. Nevertheless, current studies have demonstrated a strong relationship between the measurement of IBS in a single area of the LA and the fibrosis content quantified by histology.⁹ In addition, calibrated IBS analyses are dependent on the settings used during image acquisition (e.g. ultrasound frequency, focus, depth, etc).

Conclusion

Assessment of LA fibrosis using two-dimensional echocardiography derived calibrated IBS can be useful to select patients for RFCA for AF. Combined assessment of LA fibrosis and LA size improves the identification of patients with a high likelihood for a successful ablation.

References

1. Pappone C, Oreto G, Rosanio S, Vicedomini G, Tocchi M, Gugliotta F, Salvati A, Dicandia C, Calabro MP, Mazzone P, Ficarra E, Di GC, Gulletta S, Nardi S, Santinelli V, Benussi S, Alfieri O Atrial electroanatomic remodeling after circumferential radiofrequency pulmonary vein ablation: efficacy of an anatomic approach in a large cohort of patients with atrial fibrillation. *Circulation* 2001;104:2539-2544.
2. Cappato R, Calkins H, Chen SA, Davies W, Iesaka Y, Kalman J, Kim YH, Klein G, Packer D, Skanes A Worldwide survey on the methods, efficacy, and safety of catheter ablation for human atrial fibrillation. *Circulation* 2005;111:1100-1105.
3. Berrueto A, Tamborero D, Mont L, Benito B, Tolosana JM, Sitges M, Vidal B, Arriagada G, Mendez F, Matiello M, Molina I, Brugada J Pre-procedural predictors of atrial fibrillation recurrence after circumferential pulmonary vein ablation. *Eur Heart J* 2007;28:836-841.
4. Shin SH, Park MY, Oh WJ, Hong SJ, Pak HN, Song WH, Lim DS, Kim YH, Shim WJ Left atrial volume is a predictor of atrial fibrillation recurrence after catheter ablation. *J Am Soc Echocardiogr* 2008;21:697-702.
5. Hof I, Chilukuri K, rbab-Zadeh A, Scherr D, Dalal D, Nazarian S, Henrikson C, Spragg D, Berger R, Marine J, Calkins H Does left atrial volume and pulmonary venous anatomy predict the outcome of catheter ablation of atrial fibrillation? *J Cardiovasc Electrophysiol* 2009;20:1005-1010.
6. Verma A, Wazni OM, Marrouche NF, Martin DO, Kilicaslan F, Minor S, Schweikert RA, Saliba W, Cummings J, Burkhardt JD, Bhargava M, Belden WA, bdul-Karim A, Natale A Pre-existent left atrial scarring in patients undergoing pulmonary vein antrum isolation: an independent predictor of procedural failure. *J Am Coll Cardiol* 2005;45:285-292.
7. Perez JE, Barzilai B, Madaras EI, Glueck RM, Saffitz JE, Johnston P, Miller JG, Sobel BE Applicability of ultrasonic tissue characterization for longitudinal assessment and differentiation of calcification and fibrosis in cardiomyopathy. *J Am Coll Cardiol* 1984;4:88-95.
8. Picano E, Pelosi G, Marzilli M, Lattanzi F, Benassi A, Landini L, L'Abbate A In vivo quantitative ultrasonic evaluation of myocardial fibrosis in humans. *Circulation* 1990;81:58-64.
9. Wang GD, Shen LH, Wang L, Li HW, Zhang YC, Chen H Relationship between integrated backscatter and atrial fibrosis in patients with and without atrial fibrillation who are undergoing coronary bypass surgery. *Clin Cardiol* 2009;32:E56-E61.
10. Lang RM, Bierig M, Devereux RB, Flachskampf FA, Foster E, Pellikka PA, Picard MH, Roman MJ, Seward J, Shanewise JS, Solomon SD, Spencer KT, Sutton MS, Stewart WJ Recommendations for chamber quantification: a report from the American Society of Echocardiography's Guidelines and Standards Committee and the Chamber Quantification Writing Group, developed in conjunction with the European Association of Echocardiography, a branch of the European Society of Cardiology. *J Am Soc Echocardiogr* 2005;18:1440-1463.
11. Yuda S, Fang ZY, Marwick TH Association of severe coronary stenosis with subclinical left ventricular dysfunction in the absence of infarction. *J Am Soc Echocardiogr* 2003;16:1163-1170.
12. Mottram PM, Haluska B, Yuda S, Leano R, Marwick TH Patients with a hypertensive response to exercise have impaired systolic function without diastolic dysfunction or left ventricular hypertrophy. *J Am Coll Cardiol* 2004;43:848-853.
13. Wong CY, O'Moore-Sullivan T, Leano R, Byrne N, Beller E, Marwick TH Alterations of left ventricular myocardial characteristics associated with obesity. *Circulation* 2004;110:3081-3087.

14. Calkins H, Brugada J, Packer DL, Cappato R, Chen SA, Crijns HJ, Damiano RJ, Jr., Davies DW, Haines DE, Haissaguerre M, Iesaka Y, Jackman W, Jais P, Kottkamp H, Kuck KH, Lindsay BD, Marchlinski FE, McCarthy PM, Mont JL, Morady F, Nademanee K, Natale A, Pappone C, Prystowsky E, Raviele A, Ruskin JN, Shemin RJ HRS/EHRA/ECAS expert Consensus Statement on catheter and surgical ablation of atrial fibrillation: recommendations for personnel, policy, procedures and follow-up. A report of the Heart Rhythm Society (HRS) Task Force on catheter and surgical ablation of atrial fibrillation. *Heart Rhythm* 2007;4:816-861.
15. Tops LF, Bax JJ, Zeppenfeld K, Jongbloed MR, van der Wall EE, Schalij MJ Effect of radiofrequency catheter ablation for atrial fibrillation on left atrial cavity size. *Am J Cardiol* 2006;97:1220-1222.
16. Fuster V, Ryden LE, Cannom DS, Crijns HJ, Curtis AB, Ellenbogen KA, Halperin JL, Le Heuzey JY, Kay GN, Lowe JE, Olsson SB, Prystowsky EN, Tamargo JL, Wann S, Smith SC, Jr., Jacobs AK, Adams CD, Anderson JL, Antman EM, Hunt SA, Nishimura R, Ornato JP, Page RL, Riegel B, Priori SG, Blanc JJ, Budaj A, Camm AJ, Dean V, Deckers JW, Despres C, Dickstein K, Lekakis J, McGregor K, Metra M, Morais J, Osterspey A, Zamorano JL ACC/AHA/ESC 2006 guidelines for the management of patients with atrial fibrillation--executive summary: a report of the American College of Cardiology/American Heart Association Task Force on Practice Guidelines and the European Society of Cardiology Committee for Practice Guidelines (Writing Committee to Revise the 2001 Guidelines for the Management of Patients With Atrial Fibrillation). *J Am Coll Cardiol* 2006;48:854-906.
17. Wijffels MC, Kirchhof CJ, Dorland R, Allesie MA Atrial fibrillation begets atrial fibrillation. A study in awake chronically instrumented goats. *Circulation* 1995;92:1954-1968.
18. Ausma J, Litjens N, Lenders MH, Duimel H, Mast F, Wouters L, Ramaekers F, Allesie M, Borgers M Time course of atrial fibrillation-induced cellular structural remodeling in atria of the goat. *J Mol Cell Cardiol* 2001;33:2083-2094.
19. Sung SH, Chang SL, Hsu TL, Yu WC, Tai CT, Lin YJ, Lo LW, Wongcharoen W, Tuan TC, Hu YF, Udyavar A, Chen SA Do the left atrial substrate properties correlate with the left atrial mechanical function? A novel insight from the electromechanical study in patients with atrial fibrillation. *J Cardiovasc Electrophysiol* 2008;19:165-171.
20. Allesie M, Ausma J, Schotten U Electrical, contractile and structural remodeling during atrial fibrillation. *Cardiovasc Res* 2002;54:230-246.
21. McGann CJ, Kholmovski EG, Oakes RS, Blauer JJ, Daccarett M, Segerson N, Airey KJ, Akoum N, Fish E, Badger TJ, DiBella EV, Parker D, MacLeod RS, Marrouche NF New magnetic resonance imaging-based method for defining the extent of left atrial wall injury after the ablation of atrial fibrillation. *J Am Coll Cardiol* 2008;52:1263-1271.
22. Oakes RS, Badger TJ, Kholmovski EG, Akoum N, Burgon NS, Fish EN, Blauer JJ, Rao SN, DiBella EV, Segerson NM, Daccarett M, Windfelder J, McGann CJ, Parker D, MacLeod RS, Marrouche NF Detection and quantification of left atrial structural remodeling with delayed-enhancement magnetic resonance imaging in patients with atrial fibrillation. *Circulation* 2009;119:1758-1767.
23. Kribben A, Witzke O, Hillen U, Barkhausen J, Daul AE, Erbel R Nephrogenic systemic fibrosis: pathogenesis, diagnosis, and therapy. *J Am Coll Cardiol* 2009;53:1621-1628.

Chapter 4

Prognostic value of total atrial conduction time estimated with tissue Doppler imaging to predict recurrence of atrial fibrillation after radiofrequency catheter ablation

Dennis W. den Uijl, Marcin Gawrysiak, Laurens F. Tops, Serge A. Trines, Katja Zeppenfeld, Martin J. Schalij, Jeroen J. Bax, Victoria Delgado.

Europace. 2011 Nov;13(11):1533-40



Abstract

Background: Total atrial activation time has been identified as an independent predictor of new-onset atrial fibrillation (AF). Echocardiographic assessment of PA-TDI duration provides an estimation of total atrial conduction time. The aim of this study was to investigate the prognostic value of total atrial conduction time to predict AF recurrence after radiofrequency catheter ablation (RFCA).

Methods: In 213 patients undergoing RFCA for symptomatic drug-refractory paroxysmal AF, the total atrial conduction time was estimated by measuring the time delay between the onset of the P-wave in lead II of the surface ECG **and the peak A'-wave** on the tissue Doppler tracing of the left atrial lateral wall (PA-TDI duration). After RFCA, all patients were evaluated on a systematic basis at the outpatient clinic.

Results: After a mean follow-up of 13 ± 3 months, 74 patients (35%) had recurrent AF whereas 139 patients (65%) maintained sinus rhythm. Left atrial maximum volume index and PA-TDI duration were identified as independent predictors of AF recurrence after RFCA. However, receiver-operator characteristics curve analyses demonstrated that PA-TDI duration had a superior accuracy to predict AF recurrence compared to left atrial maximum volume index (area under the curve 0.765 vs. 0.561, respectively).

Conclusion: Assessment of total atrial conduction time using tissue Doppler imaging can be used to predict AF recurrence after RFCA.

Introduction

Atrial fibrillation (AF) causes electrical and structural changes to the atria which play an important role in the perpetuation and progression of the arrhythmia.^{1,2} This process is referred to as atrial remodelling. A large extent of atrial remodelling is associated with a limited efficacy of radiofrequency catheter ablation (RFCA) for AF.³ Therefore, pre-procedural assessment of the extent of atrial remodelling could be used to identify patients with a high risk for AF recurrence after RFCA.

Currently, the most common used method to estimate the extent of atrial remodelling is the measurement of the left atrial (LA) size. Left atrial size is an independent predictor of new onset AF in the general population and has been identified as a predictor of AF recurrence after RFCA.⁴⁻⁷ However, the clinical applicability of LA size to identify patients with a high likelihood to maintain sinus rhythm after RFCA for AF is limited. Therefore, additional markers of atrial remodelling are needed to improve patient selection.

Total atrial conduction time has been proposed as a marker of atrial remodelling. In contrast to LA size, total atrial conduction time reflects the extent of both electrical and structural remodelling of the atria. Recently, a novel echocardiographic parameter based on tissue Doppler imaging (TDI) has been introduced to assess the total atrial conduction time: the PA-TDI duration.⁸ Potentially, this new parameter provides a more accurate assessment of the presence and extent of atrial remodelling than conventional echocardiographic parameters. The aim of this study was to investigate the prognostic value of total atrial conduction time to predict AF recurrence after RFCA.

Methods

Patient population and evaluation

The patient population consisted of a group of consecutive patients with symptomatic drug-refractory paroxysmal AF, undergoing RFCA. Atrial fibrillation was classified as paroxysmal when episodes were generally self-terminating and lasted no longer than 7 days, according to the European Society of Cardiology guidelines definitions.⁹ Prior to the procedure, all patients underwent a comprehensive transthoracic echocardiographic examination to assess LA size and function, left ventricular (LV) function, and to exclude structural heart disease. In addition, a novel echocardiographic parameter was assessed to estimate the total atrial conduction time (PA-TDI duration). The PA-TDI duration is measured using TDI during sinus rhythm. Therefore, patients who were in atrial fibrillation during echocardiography were excluded from the analysis. After the ablation, all patients were evaluated on a systematic basis at the outpatient clinic during a 12 months follow-up period. Electrocardiogram (ECG) recordings were acquired each visit and 24-hour Holter registrations were scheduled after 3, 6 and 12 months follow-up. Importantly, all patients were encouraged to immediately obtain an ECG registration when experiencing palpitations. All medications were continued for at least 3 months. Afterwards, anti-arrhythmic drugs were discontinued at the discretion of the physician. After a blanking period of 3 months, recurrence of AF was defined as any recording of AF on ECG or an episode longer than 30 s on 24-hour Holter registration.

Standard echocardiography

Two-dimensional transthoracic echocardiography was performed using a commercially available ultrasound system (Vivid 7, General Electric Vingmed, Milwaukee, WI), equipped with a 3.5-MHz transducer at a depth of 16 cm. All

patients were imaged in left lateral decubitus position. Two-dimensional and color Doppler data were obtained in the parasternal short- and long-axis views and the apical 2- and 4-chamber views. All images were ECG-triggered and stored in cine loop format for off-line analyses (EchoPac 108.1.5, General Electric Medical Systems, Horten, Norway). Left atrial volumes were obtained from the **apical views by disc's method and indexed to body surface area.**¹⁰ Left atrial volumes were measured at two phases of the cardiac cycle: LA maximum volume at the end-systolic phase (just before mitral valve opening) and LA minimum volume at the end-diastolic phase (just before mitral valve closure). The LA function was derived from the LA volumes by calculating the total LA emptying fraction according to the following formula: total LA emptying fraction = $([LA \text{ maximum volume} - LA \text{ minimum volume}] / LA \text{ maximum volume}) \times 100\%$. Left ventricular ejection fraction was calculated from the standard apical 2- and 4-**chamber views by Simpson's method**, according to the American Society of Echocardiography guidelines.¹⁰ Left ventricular diastolic function was evaluated using pulsed-wave Doppler recordings of the mitral valve inflow pattern (E-wave, A-wave, deceleration time of the E-wave) **and Doppler tissue recordings of the mitral annular motion (E'-wave)**. In addition, the diastolic function grade was classified as either normal, grade 1 (impaired relaxation), grade 2 (pseudonormalization) or grade 3 (restrictive filling pattern) as recommended by current guidelines.¹¹

Atrial tissue Doppler imaging

The PA-TDI duration is a novel echocardiographic parameter which can be used to estimate the total atrial conduction time.⁸ Color-coded TDI images of the LA were obtained from the apical 4-chamber view during end-expiration, with the sector size and depth optimized for the highest frame rates possible (>115 frames/s). The ultrasound beam was carefully aligned to keep the

incidence angle as small as possible. To assess the PA-TDI duration, a fixed 9x9 pixel region of interest was placed on the LA lateral wall just above the mitral annulus providing the tracing of the mechanical activation in that area (Figure 1). The PA-TDI duration was assessed by measuring the time interval between the onset of the P-wave in lead II of the surface ECG and the peak A'-wave on the tissue Doppler tracing (Figure 1). A long PA-TDI duration corresponds to a long total atrial conduction time.

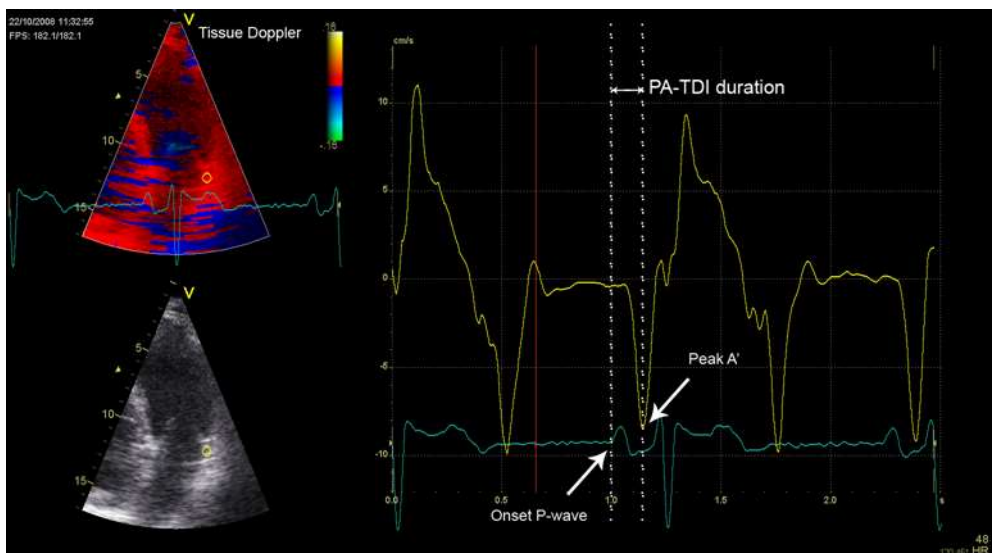


Figure 1. Measurement of the total atrial conduction time (PA-TDI duration). A fixed 9x9 pixel region of interest (yellow) was positioned in the left atrial (LA) lateral wall on a tissue Doppler recording to obtain a tracing of the mechanical activation in this area (yellow tracing). A simultaneously acquired registration of surface electrocardiogram (ECG) lead II (blue tracing) was displayed underneath the tissue Doppler tracing. The PA-TDI duration (double arrow) was assessed by measuring the time interval between the onset of the P-wave in lead II and the peak A'-wave on the tissue Doppler tracing (single arrows).

Bland-Altman analyses were performed in our laboratory to assess the inter- and intra-observer reproducibility of PA-TDI duration measurements showing minimal biases and tight limits of agreement (1.8 ± 10 ms and 1.7 ± 10 ms, respectively).¹²

Radiofrequency catheter ablation

Radiofrequency catheter ablation was aimed at creating circular lesions around the left and right pulmonary vein ostia. All patients received intravenous heparin to maintain an activated clotting time of 300-400 s. A transseptal puncture was performed to gain entrance to the LA. Intracardiac echocardiography was used to guide the transseptal puncture. A non-fluoroscopic electroanatomical mapping system with multi-slice computed tomography integration was used to guide the ablation procedure (CARTO XP™, Cartomerge™, Biosense Webster, Diamond Bar, CA, USA). Mapping and ablation were performed using a 3.5-mm quadripolar open-loop irrigated mapping/ablation catheter (7.5Fr Navistar™, Biosense Webster). Radiofrequency current was applied at 30-35 W with a maximum temperature of 45°C and an irrigation flow of 20 ml/min until a bipolar voltage of <0.1 mV was achieved, with a maximum of 60 s per point. The end-point of the procedure was pulmonary vein isolation as confirmed by recording entrance block during sinus rhythm or pacing from inside the coronary sinus.¹³

Statistical analysis

All variables were tested for a normal distribution with the Kolmogorov-Smirnov test. Continuous variables are presented as mean \pm SD and were **compared with the student's t-test**, paired or unpaired as appropriate. Categorical variables are presented as number (percentage) and were compared with the chi-square test. Univariable and multivariable Cox proportional hazard analyses were performed to investigate clinical and echocardiographic predictors of AF recurrence after RFCA. All variables mentioned in Table 1 and Table 2 were included in the univariable analyses. Variables with a p-value <0.05 in the univariate analysis were included into the

multivariate analysis. Multivariate analysis was performed using a backward stepwise conditional approach. Variables with a $p > 0.05$ were excluded from the model. The receiver-operator characteristics (ROC) curve was calculated to evaluate the performance of the strongest independent predictors of AF recurrence after RFCA obtained at multivariate analysis. All statistical analyses were performed with SPSS software (version 16.0, SPSS Inc., Chicago, IL, USA). A value of $p < 0.05$ was considered statistically significant.

Results

Patient characteristics

The present patient population was prospectively included from an ongoing clinical registry.¹⁴ Out of 323 consecutive patients undergoing RFCA for paroxysmal AF, 213 patients were in sinus rhythm during transthoracic echocardiography and comprised the patient population (165 men [77%], mean age 55 ± 11 years). Importantly, none of these patients had previously undergone RFCA for AF. The procedural end-point of PV isolation was reached in all patients and no major procedural complications occurred.

After a mean follow-up of 13 ± 3 months, 74 patients (35%) had recurrent AF and 139 patients (65%) had maintained stable sinus rhythm. Patients with AF recurrence had significantly larger LA volumes compared to patients who maintained sinus rhythm (LA maximum volume index: 42 ± 13 ml/m² versus 38 ± 11 ml/m², $p = 0.014$; LA minimum volume index: 22 ± 9 ml/m² versus 20 ± 8 ml/m², $p = 0.029$). Moreover, patients with AF recurrence more often had a history of persistent AF than patients who maintained sinus rhythm (27 [36%] versus 19 [14%], $p < 0.001$). Persistent AF was defined as AF episodes lasting longer than 7 days or requiring termination by cardioversion, according to the European Society of Cardiology guidelines definitions.⁹ More detailed comparisons of baseline characteristics and echocardiographic characteristics

between patients with AF recurrence and patients who maintained sinus rhythm are shown in Tables 1 and 2, respectively.

Table 1. Baseline characteristics

	Overall (n=213)	Non-recurrence (n=139)	Recurrence (n=74)	P-value
Clinical characteristics				
Age (years)	55 ± 11	55 ± 9	55 ± 15	0.99
Male gender, n (%)	165 (77)	108 (78)	57 (77)	0.91
Body Surface Area (m ²)	2.1 ± 0.2	2.1 ± 0.2	2.1 ± 0.2	0.18
Body Mass Index (kg/m ²)	26.5 ± 3.6	26.4 ± 3.4	26.8 ± 3.8	0.41
CHADS ₂ score ≥2, n (%)	15 (7)	13 (9)	2 (3)	0.07
Duration of atrial fibrillation (months)	67 ± 60	68 ± 56	65 ± 66	0.75
History of cardioversion, n (%)	114 (54)	68 (49)	46 (62)	0.07
History of persistent atrial fibrillation, n (%)	46 (22)	19 (14)	27 (36)	<0.001
Failed anti-arrhythmic drugs (n)	3.2 ± 1.3	3.2 ± 1.4	3.2 ± 1.2	0.92
Hypertension, n (%)	88 (41)	53 (38)	35 (47)	0.20
Diabetes, n (%)	9(4)	8 (6)	1 (1)	0.13
Medication				
• ACE-inhibitor, n (%)	48 (23)	32 (23)	16 (22)	0.82
• AT-II receptor blocker, n (%)	58 (27)	34 (24)	24 (32)	0.21
• Class IC anti-arrhythmic drug, n (%)	75 (35)	54 (39)	21 (28)	0.13
• Class III anti-arrhythmic drug, n (%)	121 (57)	77 (55)	44 (59)	0.57

ACE-inhibitor = angiotensin-converting enzyme inhibitor, AT-II = angiotensin-I

Total atrial conduction time

The mean PA-TDI duration for the overall population was 132 ± 25 ms. There was no relation between the use of class 1c or class 3 anti-arrhythmic drugs and PA-TDI duration. Patients with AF recurrence during follow-up had a significantly longer PA-TDI duration at baseline than patients who maintained sinus rhythm (146 ± 20 ms versus 124 ± 23 ms, p<0.001). Moreover, PA-TDI duration was significantly longer in patients who had been previously classified

as persistent AF (142 ± 21 ms versus 129 ± 25 ms, $p=0.002$). After 12 months follow up there was no significant change in PA-TDI duration in patients who maintained sinus rhythm (123 ± 23 ms versus 127 ± 22 ms, $p=0.054$) nor in patients with AF recurrence after RFCA (148 ± 22 ms versus 142 ± 21 ms, $p=0.16$).

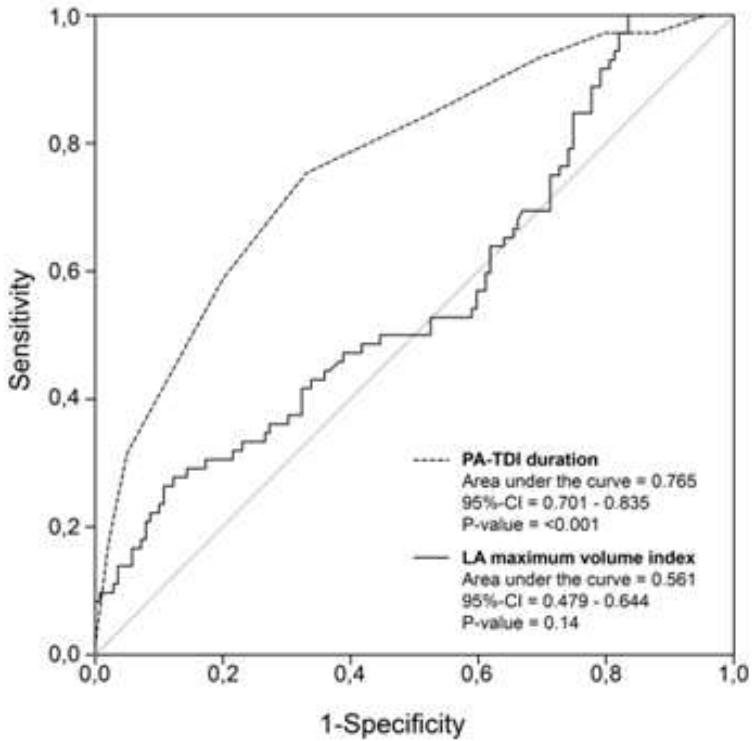


Figure 2. Receiver-operator characteristic curve analyses of the total atrial conduction time (PA-TDI duration) and left atrial (LA) maximum volume index according to the recurrence of atrial fibrillation during follow-up. CI = confidence interval.

Table 2. Echocardiographic characteristics

	Overall (n=213)	Non- recurrence (n=139)	Recurrence (n=74)	P-value
Volumes				
LA maximum volume index (ml/m ²)	39 ± 12	38 ± 11	42 ± 13	0.014
LA minimum volume index (ml/m ²)	20 ± 8	20 ± 8	22 ± 9	0.029
LA emptying fraction (%)	49 ± 12	49 ± 12	48 ± 12	0.46
LV ejection fraction (%)	59 ± 5	59 ± 5	58 ± 6	0.10
Pulsed wave Doppler:				
• E-wave (m/s)	0.63 ± 0.16	0.62 ± 0.16	0.64 ± 0.16	0.36
• A-wave (m/s)	0.54 ± 0.15	0.55 ± 0.14	0.52 ± 0.15	0.21
• E/A-ratio	1.24 ± 0.48	1.21 ± 0.46	1.31 ± 0.51	0.12
• Deceleration time (s)	212 ± 67	213 ± 68	207 ± 63	0.56
Doppler tissue imaging:				
• E'-wave (cm/s)	9.1 ± 2.4	9.0 ± 2.5	9.2 ± 2.3	0.58
• E/E'-ratio	7.3 ± 2.6	7.3 ± 2.7	7.3 ± 2.3	0.92
Diastolic function grade:				
• Normal, n (%)	168 (79)	108 (78)	60 (81)	0.57
• Gr 1: Impaired relaxation, n (%)	45 (21)	31 (22)	14 (19)	
• Gr 2: Pseudo-normalization, n (%)	0 (0)	0 (0)	0 (0)	
• Gr 3: Restrictive filling, n (%)	0 (0)	0 (0)	0 (0)	
Atrial electromechanical interval:				
• PA-TDI duration (ms)	132 ± 25	124 ± 23	146 ± 20	<0.001

Gr = grade, LA = left atrial, LV = left ventricular, PA-TDI duration = total atrial conduction time

Clinical predictors of atrial fibrillation recurrence

Univariate and multivariate Cox proportional hazard analyses were performed to identify clinical and echocardiographic predictors of AF recurrence after RFCA (Table 3). Left atrial maximum volume index (HR per ml/m²: 1.020, p=0.030) and PA-TDI duration (HR per ms: 1.035, p<0.001) were identified as independent predictors of AF recurrence. Importantly, multivariate analyses

demonstrated that there was no interaction between LA maximum volume index or PA-TDI duration and a history of AF. This illustrates that both LA maximum volume index and PA-TDI duration have a similar prognostic value in patients with and without a history of persistent AF. Therefore LA maximum volume index and PA-TDI duration can be used to predict AF recurrence in both groups of patients. To study the discriminative performance of these variables to predict AF recurrence after RFCA, ROC curve analyses were performed (Figure 2). The area under the ROC curve (index of discrimination) for LA maximum volume was 0.561 ($p=0.14$), indicating a low discriminative power. The PA-TDI duration demonstrated a higher degree of discrimination than LA maximum volume index with an area under the ROC curve of 0.765 ($p<0.001$). To illustrate the implication of this finding, an example of a patient with a relatively small LA and a long total atrial conduction time is shown in Figure 3. Despite the relatively small LA size, the prolonged total atrial conduction time indicates a high extent of atrial remodeling most likely caused by a decreased atrial conduction speed. Consequently, this patient experienced AF recurrence during follow-up, illustrating the importance of total atrial conduction time to predict AF recurrence after RFCA. To further illustrate the impact of PA-TDI duration on the risk for AF recurrence, the Kaplan Meier curve for freedom of AF after RFCA according to PA-TDI quartiles is shown in Figure 4.

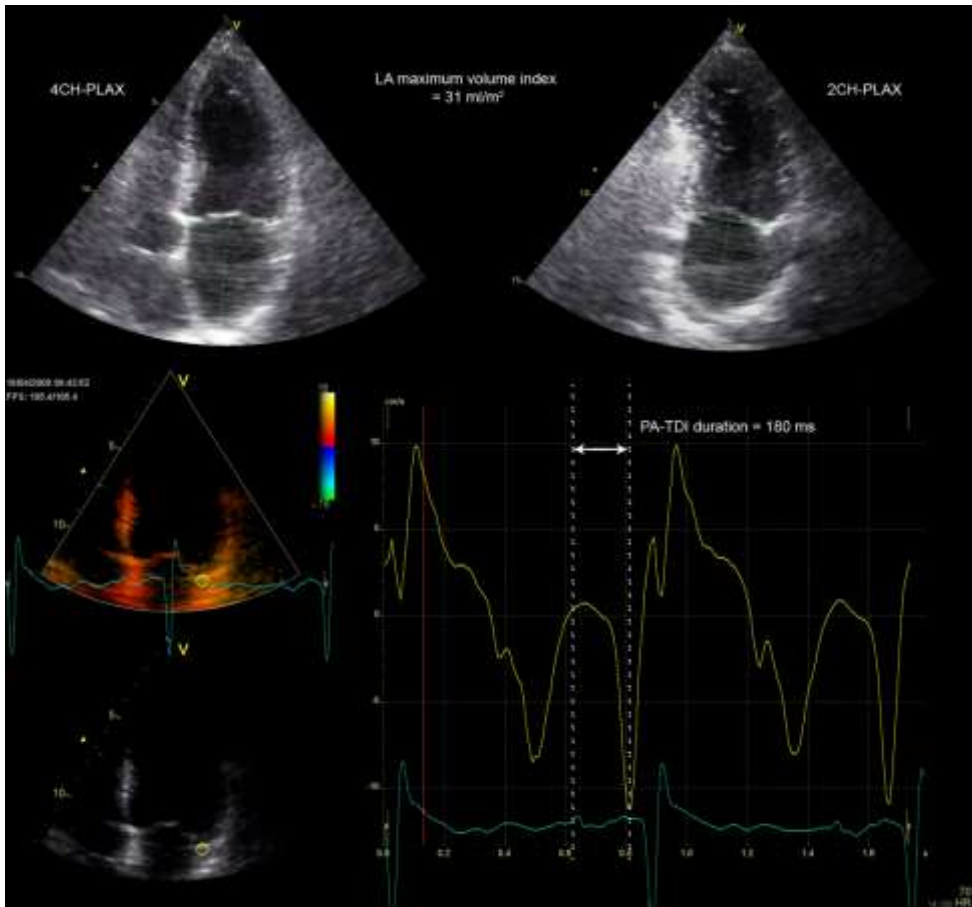


Figure 3. Example of a patient with a small left atrial (LA) size and a long total atrial conduction time (PA-TDI duration). The LA maximum volume index was obtained from the 2- and 4-chamber parasternal long-axis views (2CH-PLAX and 4CH-PLAX, respectively) and measured 31 ml/m². A tissue Doppler tracing of the LA lateral wall demonstrated a PA-TDI duration (arrow) of 180 ms. Despite the small LA size, the long PA-TDI duration indicates a large extent of atrial remodeling. This patient has experienced recurrence of atrial fibrillation during follow-up.

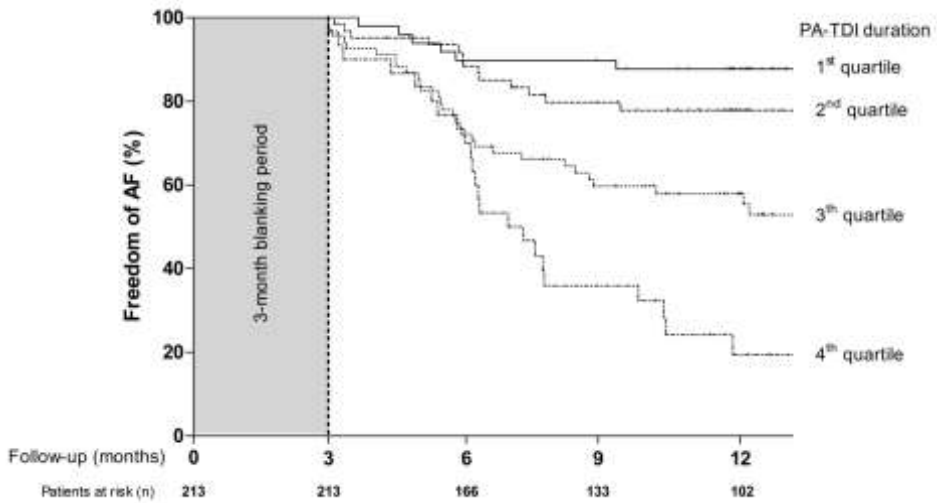


Figure 4. Kaplan Meier curve for freedom of atrial fibrillation (AF) after radiofrequency catheter ablation according to total atrial conduction time (PA-TDI duration) quartiles.

Discussion

The present study investigated the value of pre-procedural echocardiographic assessment of the total atrial conduction time using TDI to predict AF recurrence after RFCA in patients with paroxysmal AF. The main finding was that PA-TDI duration was an independent predictor of AF recurrence after RFCA. Moreover, PA-TDI duration was a stronger predictor of AF recurrence than LA maximum volume index and demonstrated a higher degree of discrimination to identify patients who will have AF recurrence after RFCA.

Conventional predictors of atrial fibrillation recurrence

Radiofrequency catheter ablation is considered a reasonable option for patients with symptomatic, drug refractory AF.¹³ However, RFCA for AF is associated with a considerable recurrence rate.¹⁵ A large number of parameters has been related to a high risk for AF recurrence after RFCA, such as age, arterial

hypertension, type of AF, LA size and impaired LV systolic function.^{5,6,16,17} Interestingly, these parameters all seem to either cause or reflect the presence and extent of atrial remodeling. A high extent of atrial remodeling is thought to limit the efficacy of RFCA for AF.

In the present study a history of persistent AF and a large LA maximum volume index were associated with a higher risk for AF recurrence. Moreover, multivariate analysis demonstrated that LA maximum volume index was an independent predictor of AF recurrence after RFCA. This is in agreement with previous studies that have identified LA size as a predictor of AF recurrence after RFCA.⁴⁻⁷ Moreover, this finding is in agreement with the assumption that significantly dilated atria are associated with a high degree of atrial remodeling that may limit the efficacy of RFCA. Nevertheless, LA size may not be the most appropriate approach to identify patients who will experience AF recurrence after RFCA, as the present study demonstrated (Figure 2). Although LA maximum volume index was independently associated with AF recurrence after RFCA, the discriminative power of this parameter was low (area under the ROC curve of 0.561 [$p=0.14$]). Therefore, additional parameters are needed to improve patient selection.

Total atrial conduction time and atrial fibrillation recurrence

In addition to atrial dilatation, slow atrial conduction velocity may be another consequence of atrial remodeling.¹⁸ Atrial enlargement and slowing of the atrial conduction velocity can result in a larger number of re-entrant wavelets inside the atria. This situation favors the development and perpetuation of AF.¹⁹ The total atrial conduction time is related to the atrial dimensions and conduction speed. Consequentially, compared to LA size, the assessment of the total atrial conduction time may provide a more comprehensive estimation of the amount of atrial remodeling since this parameter integrates LA

dimensions and electrical properties of the LA wall. Recently, Allesie et al. underlined the importance of electrical remodeling in the development of substrate for AF by demonstrating a substantially higher degree of functional reentry during longstanding AF as compared to acute AF.²⁰ Furthermore, Choi et al. demonstrated that by decreasing the total atrial conduction time with linear triple-site pacing, burst-induction of AF could be prevented in some patients with persistent AF.²¹

The PA-TDI duration is an easy, fast and reliable method to estimate the total atrial conduction time. This novel echocardiographic parameter has been validated against P-wave duration on signal-averaged electrocardiography.⁸ Accordingly, PA-TDI duration has been used to identify patients with an atrial substrate vulnerable to develop AF.²²⁻²⁴ The present study demonstrated that PA-TDI duration was an independent predictor of AF recurrence after RFCA. Importantly, PA-TDI duration was a stronger predictor of AF recurrence after RFCA than LA size and demonstrated a higher degree of discrimination (area under the ROC curve of 0.765 [$p < 0.001$]).

Clinical implications

Several risk factors for AF recurrence after RFCA have been identified. However, the ability to predict which patients will benefit from RFCA for AF based on those risk factors remains limited. Left atrial size is one of the most frequently used parameters to select patient for RFCA of AF. However, the accuracy of this parameter to predict the efficacy of RFCA for AF is suboptimal. Left atrial size reflects the amount of structural changes to the LA tissue caused by atrial remodelling. In contrast, total atrial conduction time reflect both structural changes (LA dimensions) as well as changes in the electrical properties (atrial conduction velocity) caused by atrial remodelling and provides a more comprehensive estimation of the amount of atrial remodelling. The current

study demonstrated that total atrial conduction time had a higher discriminative power than LA size and can be used to improve patient selection. If further validated, total atrial conduction time may be used during pre-procedural consultation to better inform patients about their risk for AF recurrence after RFCA. Alternatively, in patients with a prolonged total atrial conduction time, the creation of a more extensive lesion set could be considered in order to improve the outcome of the procedure. Importantly, echocardiographic assessment of the total atrial conduction time using TDI is easy, reliable, fast, widely available and can be applied in routine clinical practice.

Limitations

Some limitations of the present study should be acknowledged. First, detection of AF recurrence after RFCA was based on ECG recordings acquired on a systematic basis and/or 24-hour Holter registration. Importantly, patients were encouraged to obtain an ECG registration when experiencing palpitations in order to confirm AF as the cause of these complaints. Nevertheless, asymptomatic episodes may have been missed. Second, the present study comprised a relatively small group of patients. Therefore, the present findings need to be validated in a larger group of patients. Finally, TDI does not differentiate between active contraction or passive motion of the myocardial segments. The advent of 2-dimensional speckle tracking analysis may provide additional information by identifying active motion of the LA wall. Furthermore, total atrial conduction time can only be assessed during sinus **rhythm. Therefore it's clinical use is limited to patients with paroxysmal AF and persistent AF.**

Conclusion

An increased total atrial conduction time assessed with TDI echocardiography is an independent predictor of AF recurrence after RFCA for paroxysmal AF.

References

1. Wijffels MC, Kirchhof CJ, Dorland R, Allesie MA Atrial fibrillation begets atrial fibrillation. A study in awake chronically instrumented goats. *Circulation* 1995;92:1954-1968.
2. Ausma J, Litjens N, Lenders MH, Duimel H, Mast F, Wouters L, Ramaekers F, Allesie M, Borgers M Time course of atrial fibrillation-induced cellular structural remodeling in atria of the goat. *J Mol Cell Cardiol* 2001;33:2083-2094.
3. Verma A, Wazni OM, Marrouche NF, Martin DO, Kilicaslan F, Minor S, Schweikert RA, Saliba W, Cummings J, Burkhardt JD, Bhargava M, Belden WA, Abdul-Karim A, Natale A Pre-existent left atrial scarring in patients undergoing pulmonary vein antrum isolation: an independent predictor of procedural failure. *J Am Coll Cardiol* 2005;45:285-292.
4. Vaziri SM, Larson MG, Benjamin EJ, Levy D Echocardiographic predictors of nonrheumatic atrial fibrillation. The Framingham Heart Study. *Circulation* 1994;89:724-730.
5. Hof I, Chilukuri K, Rab-Zadeh A, Scherr D, Dalal D, Nazarian S, Henrikson C, Spragg D, Berger R, Marine J, Calkins H Does left atrial volume and pulmonary venous anatomy predict the outcome of catheter ablation of atrial fibrillation? *J Cardiovasc Electrophysiol* 2009;20:1005-1010.
6. Berrueto A, Tamborero D, Mont L, Benito B, Tolosana JM, Sitges M, Vidal B, Arriagada G, Mendez F, Matiello M, Molina I, Brugada J Pre-procedural predictors of atrial fibrillation recurrence after circumferential pulmonary vein ablation. *Eur Heart J* 2007;28:836-841.
7. Abecasis J, Dourado R, Ferreira A, Saraiva C, Cavaco D, Santos KR, Morgado FB, Adragao P, Silva A Left atrial volume calculated by multi-detector computed tomography may predict successful pulmonary vein isolation in catheter ablation of atrial fibrillation. *Europace* 2009.
8. Merckx KL, De Vos CB, Palmans A, Habets J, Cheriex EC, Crijns HJ, Tieleman RG Atrial activation time determined by transthoracic Doppler tissue imaging can be used as an estimate of the total duration of atrial electrical activation. *J Am Soc Echocardiogr* 2005;18:940-944.
9. Camm AJ, Kirchhof P, Lip GY, Schotten U, Savelieva I, Ernst S, Van Gelder IC, Al-Attar N, Hindricks G, Prendergast B, Heidbuchel H, Alfieri O, Angelini A, Atar D, Colonna P, De CR, De SJ, Goette A, Gorenek B, Heldal M, Hohloser SH, Kolh P, Le Heuzey JY, Ponikowski P, Rutten FH, Vahanian A, Auricchio A, Bax J, Ceconi C, Dean V, Filippatos G, Funck-Brentano C, Hobbs R, Kearney P, McDonagh T, Popescu BA, Reiner Z, Sechtem U, Sirnes PA, Tendera M, Vardas PE, Widimsky P, Vardas PE, Agladze V, Aliot E, Balabanski T, Blomstrom-Lundqvist C, Capucci A, Crijns H, Dahlöf B, Folliguet T, Glikson M, Goethals M, Gulba DC, Ho SY, Klautz RJ, Kose S, McMurray J, Perrone FP, Raatikainen P, Salvador MJ, Schalij MJ, Shpektor A, Sousa J, Stepinska J, Ueতো H, Zamorano JL, Zupan I Guidelines for the management of atrial fibrillation: the Task Force for the Management of Atrial Fibrillation of the European Society of Cardiology (ESC). *Europace* 2010;12:1360-1420.
10. Lang RM, Bierig M, Devereux RB, Flachskampf FA, Foster E, Pellikka PA, Picard MH, Roman MJ, Seward J, Shanewise JS, Solomon SD, Spencer KT, Sutton MS, Stewart WJ Recommendations for chamber quantification: a report from the American Society of Echocardiography's Guidelines and Standards Committee and the Chamber Quantification Writing Group, developed in conjunction with the European Association of Echocardiography, a branch of the European Society of Cardiology. *J Am Soc Echocardiogr* 2005;18:1440-1463.

11. Nagueh SF, Appleton CP, Gillebert TC, Marino PN, Oh JK, Smiseth OA, Waggoner AD, Flachskampf FA, Pellikka PA, Evangelista A Recommendations for the evaluation of left ventricular diastolic function by echocardiography. *J Am Soc Echocardiogr* 2009;22:107-133.
12. Bertini M, Borleffs CJW, Delgado V, Ng ACT, Piers SRD, Shanks M, Antoni ML, Biffi M, Boriani G, Schalij MJ, Bax JJ, Van de Veire NRL Prediction of atrial fibrillation in patients with an implantable cardioverter-defibrillator and heart failure. *European Journal of Heart Failure* 2010;12:1101-1110.
13. Calkins H, Brugada J, Packer DL, Cappato R, Chen SA, Crijns HJ, Damiano RJ, Jr., Davies DW, Haines DE, Haissaguerre M, Iesaka Y, Jackman W, Jais P, Kottkamp H, Kuck KH, Lindsay BD, Marchlinski FE, McCarthy PM, Mont JL, Morady F, Nademanee K, Natale A, Pappone C, Prystowsky E, Raviele A, Ruskin JN, Shemin RJ HRS/EHRA/ECAS expert Consensus Statement on catheter and surgical ablation of atrial fibrillation: recommendations for personnel, policy, procedures and follow-up. A report of the Heart Rhythm Society (HRS) Task Force on catheter and surgical ablation of atrial fibrillation. *Heart Rhythm* 2007;4:816-861.
14. Tops LF, Bax JJ, Zeppenfeld K, Jongbloed MR, van der Wall EE, Schalij MJ Effect of radiofrequency catheter ablation for atrial fibrillation on left atrial cavity size. *Am J Cardiol* 2006;97:1220-1222.
15. Cappato R, Calkins H, Chen SA, Davies W, Iesaka Y, Kalman J, Kim YH, Klein G, Packer D, Skanes A Worldwide survey on the methods, efficacy, and safety of catheter ablation for human atrial fibrillation. *Circulation* 2005;111:1100-1105.
16. Vasamreddy CR, Lickfett L, Jayam VK, Nasir K, Bradley DJ, Eldadah Z, Dickfeld T, Berger R, Calkins H Predictors of recurrence following catheter ablation of atrial fibrillation using an irrigated-tip ablation catheter. *J Cardiovasc Electrophysiol* 2004;15:692-697.
17. Chen MS, Marrouche NF, Khaykin Y, Gillinov AM, Wazni O, Martin DO, Rossillo A, Verma A, Cummings J, Erciyes D, Saad E, Bhargava M, Bash D, Schweikert R, Burkhardt D, Williams-Andrews M, Perez-Lugones A, Abdul-Karim A, Saliba W, Natale A Pulmonary vein isolation for the treatment of atrial fibrillation in patients with impaired systolic function. *J Am Coll Cardiol* 2004;43:1004-1009.
18. Gaspo R, Bosch RF, Talajic M, Nattel S Functional mechanisms underlying tachycardia-induced sustained atrial fibrillation in a chronic dog model. *Circulation* 1997;96:4027-4035.
19. Moe GK, Rheinboldt WC, Abildskov JA A computer model of atrial fibrillation. *Am Heart J* 1964;67:200-220.
20. Allesie MA, de Groot NM, Houben RP, Schotten U, Boersma E, Smeets JL, Crijns HJ Electropathological substrate of long-standing persistent atrial fibrillation in patients with structural heart disease: longitudinal dissociation. *Circ Arrhythm Electrophysiol* 2010;3:606-615.
21. Choi JI, Ryu K, Park E, Benser ME, Jang JK, Lee HS, Lim HE, Pak HN, Kim YH Atrial activation time and pattern of linear triple-site vs. single-site atrial pacing after cardioversion in patients with atrial fibrillation. *Europace* 2010;12:508-516.
22. De Vos CB, Weijs B, Crijns HJ, Cheriex EC, Palmans A, Habets J, Prins MH, Pisters R, Nieuwlaat R, Tieleman RG Atrial tissue Doppler imaging for prediction of new-onset atrial fibrillation. *Heart* 2009;95:835-840.
23. Antoni ML, Bertini M, Atary JZ, Delgado V, ten Brinke EA, Boersma E, Holman ER, van der Wall EE, Schalij MJ, Bax JJ, van de Veire NR Predictive value of total atrial conduction time estimated with tissue Doppler imaging for the development of new-onset atrial fibrillation after acute myocardial infarction. *Am J Cardiol* 2010;106:198-203.

24. Buck S, Rienstra M, Maass AH, Nieuwland W, van Veldhuisen DJ, Van Gelder IC Cardiac resynchronization therapy in patients with heart failure and atrial fibrillation: importance of new-onset atrial fibrillation and total atrial conduction time. *Europace* 2008;10:558-565.

Chapter 5

Impact of coronary artery disease on the efficacy of radiofrequency catheter ablation for atrial fibrillation

Dennis W. den Uijl, Mark J. Boogers, Marieke Compier, Serge A. Trines, Arthur J.H.A. Scholte, Katja Zeppenfeld, Martin J. Schalij, Jeroen J. Bax, Victoria Delgado.

Eur Heart J Cardiovasc Imaging. 2012 Jul 19



Abstract

Background: Coronary artery disease (CAD) has been associated with the development of atrial fibrillation (AF). However, little is known about the impact of CAD on the outcome treatment of AF. The aim of this study was to investigate the impact of CAD on the efficacy of radiofrequency catheter ablation (RFCA) for AF using multi-detector row computed tomography (MDCT).

Methods: In 125 consecutive patients undergoing RFCA for AF, a pre-procedural MDCT examination (coronary angiography and/or coronary calcium score) was performed to evaluate the presence and severity of CAD. Furthermore all patients underwent a comprehensive echocardiographic evaluation to measure the left atrial size and to rule out structural heart disease. After RFCA all patients were regularly evaluated at the outpatient clinic.

Results: After a mean follow-up of 12 ± 3 months, 78 patients (62%) had maintained stable sinus rhythm and 47 patients (38%) had recurrence of AF. Left atrial volume index was a significant predictor of AF recurrence after RFCA. Presence of CAD on MDCT did not influence the efficacy of RFCA for AF.

Conclusions: The presence of CAD on MDCT is not associated with a higher risk for AF recurrence after RFCA.

Introduction

Coronary artery disease (CAD) is one of the underlying mechanisms of atrial fibrillation (AF) in Western countries.¹ Coronary artery disease leads to myocardial ischemia, left ventricular dysfunction and elevated left atrial pressures that may induce ultra-structural changes within the atrial myocardium. These changes form the arrhythmogenic substrate for AF.²

Radiofrequency catheter ablation (RFCA) is a curative treatment option which is currently reserved for patients with symptomatic drug refractory AF.³ The cornerstone of most RFCA strategies is pulmonary vein isolation.³ However, in patients with a high extent of atrial remodeling, in part caused by CAD, elimination of pulmonary vein triggers may not be sufficient to cure AF. Little is known about the impact of CAD on the efficacy of RFCA for AF.²

Multi-detector computed tomography (MDCT) is frequently performed prior to RFCA for AF in order to plan and guide the ablation procedure. MDCT provides information about the number and location of pulmonary veins draining into the left atrium and also permits evaluation of CAD.^{4,5} Therefore, MDCT provides information on one of the underlying mechanisms related to AF. The aim of this study was to investigate the impact of significant and non-significant CAD on the efficacy of RFCA for AF.

Methods

Patient population and evaluation

The population comprised a cohort of consecutive patients undergoing RFCA for symptomatic drug-refractory non-valvular AF. Prior to the ablation, all patients underwent transthoracic echocardiography to assess left atrial size, left ventricular systolic function and to exclude valvular heart disease. Moreover, all patients underwent, according to the clinical protocol, an MDCT

examination in order to obtain anatomical information to guide the ablation procedure and to exclude significant CAD. After RFCA, all patients were regularly evaluated at the outpatient clinic during a 12 months follow-up period. Electrocardiogram (ECG) recordings were acquired each visit and 24-hour ECG Holter registrations were scheduled after 3, 6 and 12 months follow-up. Importantly, all patients were encouraged to immediately obtain an ECG registration when experiencing palpitations. All medications were continued for at least 3 months. Afterwards, anti-arrhythmic drugs were discontinued at the discretion of the physician. After a blanking period of 3 months, recurrence of AF was defined as any recording of AF on ECG or an episode longer than 30 s on 24-hour ECG Holter registration. All clinical, MDCT and echocardiographic data were prospectively collected in the departmental cardiology information system (EPD-Vision®) and echocardiographic database and were retrospectively analysed.

Echocardiography

Two-dimensional transthoracic echocardiography was performed using a commercially available ultrasound system (Vivid 7 and E9, General Electric Vingmed, Milwaukee, WI), equipped with a 3.5-MHz and 5S transducers. All patients were imaged in left lateral decubitus position. Two-dimensional and color Doppler data were obtained in the parasternal short- and long-axis views and the apical 2- and 4-chamber views, adjusting gain settings and depth. All images were ECG-triggered and stored in cineloop format for off-line analyses (EchoPac 111.0.00, General Electric – Vingmed). Maximum left atrial volume was obtained from the apical 4- and 2-chamber views by disc's method and indexed to body surface area.⁶ Left ventricular ejection fraction was calculated from the standard apical 2- and 4-chamber views by Simpson's method, according to the American Society of Echocardiography guidelines.⁶

Multi-detector row computed tomography

Data acquisition

MDCT scanning was performed using a Toshiba Aquilion ONE system (Toshiba Medical Systems, Otawara, Japan) with 320 detector rows, each 0.50 mm wide. One hour prior to the examination, an oral beta-adrenergic blocking agent (metoprolol 50-100 mg) was administered if the heart rate was above 65 beats per minute, unless contra-indicated. In patients with a heart rate above 65 beats per minute on arrival to the scanner an additional bolus of intravenous beta-blocking agent was administered (metoprolol 2.5-10 mg), unless contra-indicated. Before computed tomography angiography (CTA), a non-enhanced low-dose scan was performed to measure the coronary calcium score (CCS). The CCS-scan was prospectively triggered at 75% of R-R interval using a single-rotation-wide volume acquisition (slices reconstructed to 3 mm) with a gantry rotation time 350 to 500 ms, tube voltage 120 kV, and tube current 200 to 250 mA. In patients with a heart rate above 65 beats per minute the CCS-scan was prospectively triggered at 45% of R-R interval. Next, CTA scanning was performed using prospective ECG triggering, imaging the entire heart in a single volume with a maximum of 16 cm cranio-caudal coverage. Tube voltage was adapted to body mass index (<23 kg/m²: 100 kV, 23–35 kg/m²: 120 kV, >35 kg/m²: 135 kV) and tube current varied between 400–580 mA, depending on body weight. Contrast material was administered in a triple-phase protocol: first a bolus of 60 ml, followed by 30 ml of a 50:50 mixture of contrast and saline, followed by saline flush with a flow rate of 5–6 ml/s (Iomeron 400, Bracco, Milan, Italy). Automatic detection of the contrast bolus in the left ventricle was used to time the start of the scan with a threshold of +180 Hounsfield units. Scanning was performed during inspiratory breath-hold. If the heart rate was stable and <60 beats per minute the phase window was set

at 70–80% of R-R interval, if the heart rate was 60–65 beats per minute the phase window was set at 65–85% of R-R interval and if the heart rate was >65 beats per minute the phase window was set at 30–80% of the R–R interval (using multiple beats). Images were reconstructed in the end-diastolic phase (75% of R–R interval) with a slice thickness of 0.50 mm and a reconstruction interval of 0.25 mm. If motion artefacts were present, multiple phases were reconstructed to obtain maximal diagnostic image quality. Afterwards, all datasets were exported, post-processed and analysed on a dedicated workstation (Vitrea FX 1.0, Vital Images, Minnetonka, MN, USA).

Image analyses

The CCS was calculated using the Agatston method and patients were categorised as CCS=0, CCS=1-400, and CCS>400. Evaluation of the contrast-enhanced CTA datasets for the presence and severity of CAD was performed by 2 experienced investigators. All datasets were assessed as recommended by the Society of Cardiovascular Computed Tomography guidelines for the interpretation and reporting of CTA.⁷ The coronary anatomy was determined using a standardized 17-segments model according to a modified American Heart Association (AHA) classification.⁸ Each segment was scored as normal (no CAD), non-significant CAD (<50% luminal narrowing), significant CAD (>50% luminal narrowing) or uninterpretable using the axial slices with the assistance of multiplanar and curved multiplanar reconstructed images. Subsequently, vessel-based and patient-based analyses of the CTA were performed. In the vessel-based analysis, the left main was considered part of the left anterior descending coronary artery and the intermediate branch was considered part of the left circumflex coronary artery. If one segment was uninterpretable, an intention-to-diagnose strategy was applied. If more than one segment in a single vessel was uninterpretable, the vessel was considered to be of non-

diagnostic image quality. In the patient-based analysis, each CTA was classified as normal, non-significant CAD (<50% luminal narrowing) and significant CAD (>50% luminal narrowing). Similarly, if one vessel was uninterpretable, an intention-to-diagnose strategy was applied. If more than one vessel was uninterpretable, the entire examination was considered to be non-diagnostic.

Radiofrequency catheter ablation

Radiofrequency catheter ablation was aimed at pulmonary vein isolation. The procedure was performed using either a non-fluoroscopic electroanatomical mapping system with a 3.5-mm quadripolar open-loop irrigated ablation catheter and a decapolar circular mapping catheter (CARTO XP™, CARTO Merge™, 7.5Fr Navistar, LASSO, Biosense Webster, Diamond Bar, CA, USA) or a non-irrigated multi-electrode catheter with a duty-cycled, unipolar-bipolar radiofrequency generator that allows independent delivery of energy to each of the electrodes (PVAC™, GENius™, Medtronic Ablation Frontiers LLC, Carlsbad, CA, USA). All patients received intravenous heparin to maintain an activated clotting time of 300-400 s. A single or double transseptal puncture was performed to gain entrance to the left atrium. Intracardiac echocardiography was used to safely guide transseptal punctures.

Using the CARTO system, circular lesions were created around the ipsilateral left and right pulmonary vein ostia. Radiofrequency current was applied at 30-35 W with a maximum temperature of 45°C and an irrigation flow of 20 ml/min until a bipolar voltage of <0.1 mV was achieved, with a maximum of 60 s per point. Using the PVAC system, all pulmonary veins were selectively isolated. The RFCA was delivered to the antral side of the pulmonary vein ostia. Special care was taken to avoid energy application inside the pulmonary veins. Radiofrequency current was applied at a maximum power of 8 W using a 4:1 bipolar/unipolar ratio and at 10 W using a 2:1 ratio for 60 seconds per

application. Power settings were automatically adjusted in order to reach a target temperature of 60 °C. The end-point of the procedure was pulmonary vein isolation as confirmed by recording entrance block during sinus rhythm or pacing from inside the coronary sinus.

Statistical analysis

All variables were tested for a normal distribution with the Kolmogorov-Smirnov test. Continuous variables are presented as mean \pm SD and were **compared with the Student's t-test** for paired or unpaired data. Categorical variables are presented as number (percentage) and were compared with the chi-square test. The cumulative rate of AF recurrence after RFCA according to the presence or absence of significant CAD and the CCS were evaluated with the Kaplan Meier curves. Comparison of the cumulative event rates was performed using the log-rank test. Univariable Cox proportional hazard analyses were performed to investigate the impact of coronary artery disease and other clinical characteristics on the recurrence of AF after RFCA. All statistical analyses were performed with SPSS software (version 16.0, SPSS Inc., Chicago, IL, USA). A value of $p < 0.05$ was considered statistically significant.

Result

Patient characteristics

A total of 125 patients (96 men [77%], mean age 58 ± 9 years) undergoing a first RFCA procedure for drug refractory paroxysmal AF were included from an ongoing clinical registry.⁹ The mean left atrial volume index was 39.5 ± 15.5 ml/m² and AF was paroxysmal in 96 patients (77%) and persistent in 29 (23%), according to current guidelines definitions.¹⁰ In 92 patients RFCA was performed using the CARTO-system and in 33 patients the PVAC-system was

used. The procedural end point of PV isolation was reached in all patients and no major procedural complications occurred. A more detailed description of the baseline characteristics is shown in Table 1 and Table 2.

Table 1. Baseline characteristics

	Population (n=125)
Clinical characteristics	
Age (years)	58 ± 9
Male gender, n (%)	96 (77)
Body Surface Area (m ²)	2.08 ± 0.20
Duration of atrial fibrillation (months)	65 ± 53
Persistent atrial fibrillation, n (%)	29 (23)
Failed anti-arrhythmic drugs (n)	3.0 ± 1.1
Left atrial volume index (ml/m ²)	39.5 ± 15.5
Left ventricular ejection fraction (%)	58 ± 7
Medication	
Statin, n (%)	39 (31)
Angiotensin-converting enzyme inhibitor, n (%)	18 (14)
Angiotensin II receptor antagonist, n (%)	40 (32)
Class IC anti-arrhythmic drug, n (%)	47 (38)
Class III anti-arrhythmic drug, n (%)	64 (51)

Prevalence of coronary artery disease assessed with multi-detector row computed tomography

Multi-detector row computed tomography coronary angiography was performed in a total of 100 patients. In the remaining 25 patients, CTA was not attempted because of AF with a high ventricular rate unresponsive to beta-adrenergic blocking agent prior to scanning. In 5 patients the CTA examination

was considered non-diagnostic. Significant CAD (>50% luminal narrowing in at least one vessel) was present in 22 patients (23%). A more detailed description of the CTA results is shown in Table 3.

Coronary calcium score was measured in a total of 121 patients. The total CCS was 0 in 52 patients (43%), 1-400 in 56 patients (46%) and >400 in 13 patients (11%).

Table 2. Risk factors coronary artery disease

	Population n=125
Risk factors coronary artery disease	
Smoking, n (%)	41 (33)
Hypertension, n (%)	45 (36)
Hypercholesterolemia, n (%)	36 (29)
Diabetes Mellitus, n (%)	7 (6)
Family history, n (%)	38 (30)
Known coronary artery disease, n (%)	
• Percutaneous coronary intervention, n (%)	5 (4)
• Coronary bypass surgery, n (%)	1 (1)
• Acute myocardial infarction, n (%)	2 (2)

Table 3. Prevalence and extent of coronary artery disease on computed tomography angiography

	Normal	Non-significant	Significant	Non-diagnostic
Vessel-based analysis				
Right	55 (55)	34 (34)	4 (4)	7 (7)
Left anterior descending	45 (45)	41 (41)	11 (11)	3 (3)
Left circumflex	57 (57)	32 (32)	5 (5)	6 (6)
Patient-based analysis	32 (32)	41 (41)	22 (22)	5 (5)

Coronary artery disease and atrial fibrillation recurrence

After a mean follow-up of 12 ± 3 months, 47 patients (38%) had experienced AF recurrence and 78 patients (62%) had maintained stable sinus rhythm. All patients remained stable and no coronary events were recorded during the follow-up. A repeat RFCA procedure was performed in 40 patients (32%). There was no difference in AF recurrence between patients with or without significant CAD on CTA (Figure 1, panel A). Moreover, the CCS on MDCT was similar in patients with and without AF recurrence (Figure 1, panel B). Figure 2 panel A illustrates the cumulative rates of AF recurrences after RFCA in patients with significant versus non-significant CAD. At 12 months follow-up, the incidence of AF recurrence was 32% in patients with significant CAD compared with 32% in patients without significant CAD (log-rank $p=0.62$). In addition, when the patient population was divided according to the CCS, no differences were observed in the 12 month AF recurrence rate among the three groups of patients: 33%, 39% and 54% for patients with CCS 0, between 1-400 and >400 , respectively (log-rank $p=0.24$) (Figure 2 panel B). Univariable Cox proportional hazards analyses confirmed that there was no prognostic impact of significant CAD and CCS on the risk for AF recurrence after RFCA (Table 4). In contrast, left

atrial volume index was the only characteristic associated with a significantly higher risk for AF recurrence after RFCA (Table 4).

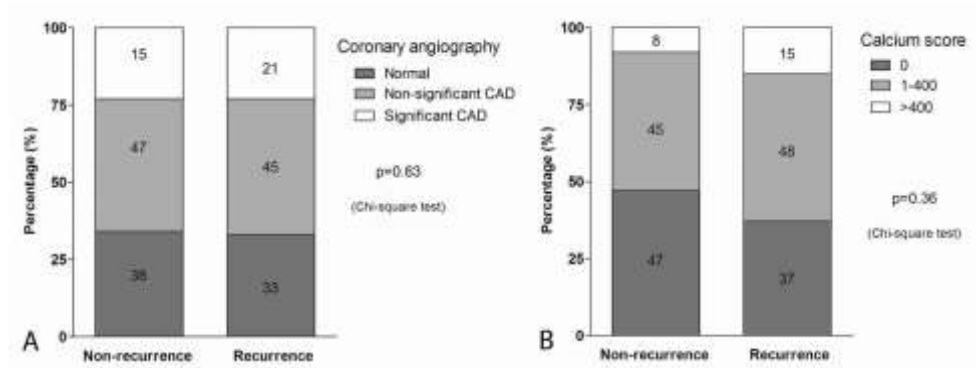


Figure 1. Panel A: Illustration of the distribution of normal findings during coronary angiography on multi-detector row computed tomography, non-significant coronary artery disease (CAD) and significant CAD among patients with recurrence of atrial fibrillation (recurrence) and patients that maintained sinus rhythm after radiofrequency catheter ablation (non-recurrence). Panel B: Illustration of the distribution of coronary calcium score on multi-detector row computed tomography divided into categories among patients with recurrence of atrial fibrillation (recurrence) and patients that maintained sinus rhythm after radiofrequency catheter ablation (non-recurrence).

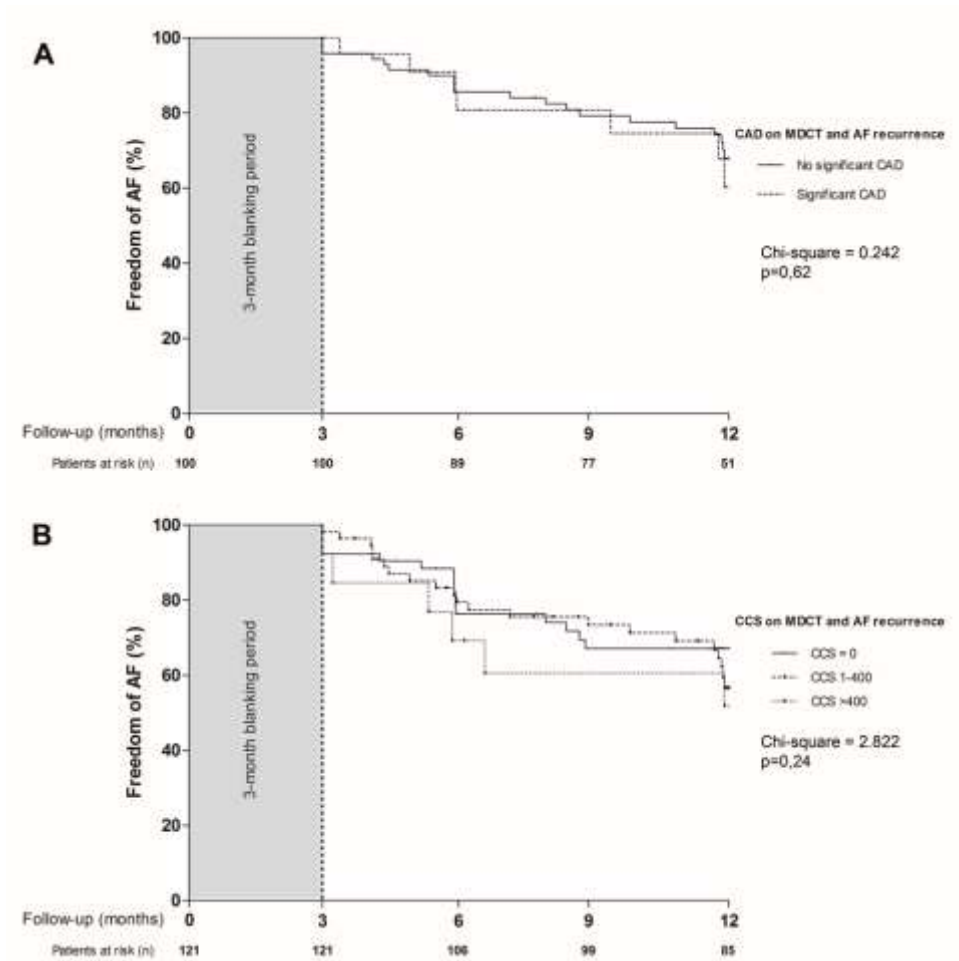


Figure 2. Kaplan Meier curve for freedom of atrial fibrillation (AF) after radiofrequency catheter ablation according to the presence or absence of significant coronary artery disease (CAD)(panel A) and coronary calcium score (CCS) divided in three categories (CCS=0, CCS 1-400 and CCS>400)(panel B).

Table 4. Cox univariable proportional hazard analyses of clinical and computed tomography characteristic to predict atrial fibrillation recurrence after catheter ablation

	HR	95% CI	P-value
Clinical characteristics			
Age (per year)	1.030	0.993-1.069	0.11
Male gender	1.381	0.641-2.973	0.41
Body Surface Area (per m ²)	1.740	0.379-7.979	0.48
Duration of atrial fibrillation (per month)	1.001	0.943-1.064	0.96
Persistent atrial fibrillation	1.735	0.919-3.275	0.09
Hypertension	1.693	0.935-3.064	0.08
Left atrial volume index (per ml/m ²)	1.017	1.003-1.032	0.018*
Left ventricular ejection fraction (per %)	1.006	0.964-1.051	0.77
Multi-detector row computed tomography			
• Significant coronary artery disease on angiography	1.238	0.527-2.903	0.62
• Coronary calcium score			
▪ > 0	1.584	0.836-2.999	0.16
▪ > 400	1.663	0.739-3.742	0.22

Discussion

The present study investigated the impact of CAD on the efficacy of RFCA for AF. The main finding was that the presence of CAD was not a determinant of RFCA outcome. Moreover, there was no relationship between the CCS and the risk for AF recurrence after RFCA.

Coronary artery disease and atrial fibrillation

Coronary artery disease has frequently been associated with the development of AF.^{1,2,5,11-13} Both conditions are commonly present in the same group of patients and many risk factors predisposing for CAD are risk factors to develop AF.^{11,12} However, it remains controversial whether there is a causal relationship between CAD and the development of AF.¹⁴ Ischemic left ventricular dysfunction can increase left atrial pressures and eventually cause left atrial wall remodeling providing the substrate for AF.² However, the Manitoba follow-up study demonstrated that the impact of symptomatic ischemic heart disease on the development of AF was independent of the presence of congestive heart failure.¹³ Importantly, these results imply that CAD can result in AF without causing left ventricular systolic dysfunction. Recently, Nishida et al. demonstrated that chronic occlusion of an atrial coronary branch in a canine model leads to increased atrial ectopy and conduction abnormalities that facilitate reentry.¹⁵ These results imply that chronic atrial ischemia or an atrial infarction can provide the triggers and substrate needed to develop AF. However, the impact of CAD on the outcome of rhythm control therapies has not been elucidated so far.

Coronary artery disease and the efficacy of radiofrequency catheter ablation

Radiofrequency catheter ablation is a curative treatment option for AF and is currently performed in an increasing number of patients.^{3,16} The cornerstone of most ablation strategies is electrical isolation of the pulmonary vein region thereby preventing the ectopic beats originating from that area to trigger AF.³ However, pulmonary vein isolation seems to be less effective in patients with a high degree of atrial disease (e.g. patients with a large left atrial volume and/or a high extent of atrial fibrosis).¹⁷⁻¹⁹ In the presence of extensive atrial disease, pulmonary vein triggers seem to be less important in the initiation and perpetuation of AF than in patients with relatively healthy atria.

Coronary artery disease can cause myocardial ischemia, resulting in an impaired relaxation of the left ventricle and leading to higher pressures in the left atrium. High left atrial pressures cause ultrastructural and electrical changes in the atrial tissue, potentially limiting the efficacy of RFCA for AF. In the present study no relationship was observed between the presence of CAD and the risk for AF recurrence after RFCA and therefore, the presence of CAD does not limit the efficacy of RFCA for AF. Most likely, in patients without symptomatic CAD, other pathophysiological factors such as age and hypertension may contribute to left atrial structural remodelling and limit the efficacy of RFCA. To our best knowledge this is the first study to investigate the impact of CAD on the efficacy of RFCA for AF.

Limitations

Some limitations of the present study should be acknowledged. First, MDCT provides anatomical information of the coronary arteries. However, MDCT does not provide information about the presence or absence of myocardial ischemia. Second, the present study included patients with symptomatic AF

but without complaints of chest pain. Therefore, the present study population comprised a low risk population for significant CAD.

Conclusion

The presence of significant or non-significant CAD on MDCT is not associated with a higher risk for AF recurrence after RFCA.

References

1. Lip GY, Beavers DG ABC of atrial fibrillation. History, epidemiology, and importance of atrial fibrillation. *BMJ* 1995;311:1361-1363.
2. Schoonderwoerd BA, Van G, I, Crijns HJ Left ventricular ischemia due to coronary stenosis as an unexpected treatable cause of paroxysmal atrial fibrillation. *J Cardiovasc Electrophysiol* 1999;10:224-228.
3. Calkins H, Brugada J, Packer DL, Cappato R, Chen SA, Crijns HJ, Damiano RJ, Jr., Davies DW, Haines DE, Haissaguerre M, Iesaka Y, Jackman W, Jais P, Kottkamp H, Kuck KH, Lindsay BD, Marchlinski FE, McCarthy PM, Mont JL, Morady F, Nademanee K, Natale A, Pappone C, Prystowsky E, Raviele A, Ruskin JN, Shemin RJ HRS/EHRA/ECAS expert Consensus Statement on catheter and surgical ablation of atrial fibrillation: recommendations for personnel, policy, procedures and follow-up. A report of the Heart Rhythm Society (HRS) Task Force on catheter and surgical ablation of atrial fibrillation. *Heart Rhythm* 2007;4:816-861.
4. den Uijl DW, Tops LF, Delgado V, Schuijff JD, Kroft LJ, de RA, Boersma E, Trines SA, Zeppenfeld K, Schalij MJ, Bax JJ Effect of pulmonary vein anatomy and left atrial dimensions on outcome of circumferential radiofrequency catheter ablation for atrial fibrillation. *Am J Cardiol* 2011;107:243-249.
5. Nucifora G, Schuijff JD, Tops LF, van Werkhoven JM, Kajander S, Jukema JW, Schreur JH, Heijnenbroek MW, Trines SA, Gaemperli O, Turta O, Kaufmann PA, Knuuti J, Schalij MJ, Bax JJ Prevalence of coronary artery disease assessed by multislice computed tomography coronary angiography in patients with paroxysmal or persistent atrial fibrillation. *Circ Cardiovasc Imaging* 2009;2:100-106.
6. Lang RM, Bierig M, Devereux RB, Flachskampf FA, Foster E, Pellikka PA, Picard MH, Roman MJ, Seward J, Shanewise JS, Solomon SD, Spencer KT, Sutton MS, Stewart WJ Recommendations for chamber quantification: a report from the American Society of Echocardiography's Guidelines and Standards Committee and the Chamber Quantification Writing Group, developed in conjunction with the European Association of Echocardiography, a branch of the European Society of Cardiology. *J Am Soc Echocardiogr* 2005;18:1440-1463.
7. Raff GL, Abidov A, Achenbach S, Berman DS, Boxt LM, Budoff MJ, Cheng V, DeFrance T, Hellinger JC, Karlsberg RP SCCT guidelines for the interpretation and reporting of coronary computed tomographic angiography. *J Cardiovasc Comput Tomogr* 2009;3:122-136.
8. Austen WG, Edwards JE, Frye RL, Gensini GG, Gott VL, Griffith LS, McGoon DC, Murphy ML, Roe BB A reporting system on patients evaluated for coronary artery disease. Report of the Ad Hoc Committee for Grading of Coronary Artery Disease, Council on Cardiovascular Surgery, American Heart Association. *Circulation* 1975;51:5-40.
9. Tops LF, Bax JJ, Zeppenfeld K, Jongbloed MR, van der Wall EE, Schalij MJ Effect of radiofrequency catheter ablation for atrial fibrillation on left atrial cavity size. *Am J Cardiol* 2006;97:1220-1222.
10. Camm AJ, Kirchhof P, Lip GY, Schotten U, Savelieva I, Ernst S, Van Gelder IC, Al-Attar N, Hindricks G, Prendergast B, Heidbuchel H, Alfieri O, Angelini A, Atar D, Colonna P, De CR, De SJ, Goette A, Gorenek B, Heldal M, Hohloser SH, Kolh P, Le Heuzey JY, Ponikowski P, Rutten FH, Vahanian A, Auricchio A, Bax J, Ceconi C, Dean V, Filippatos G, Funck-Brentano C, Hobbs R, Kearney P, McDonagh T, Popescu BA, Reiner Z, Sechtem U, Sirnes PA, Tendera M, Vardas PE, Widimsky P, Vardas PE, Agladze V, Aliot E, Balabanski T, Blomstrom-Lundqvist C, Capucci A, Crijns H, Dahlöf B, Folliguet T, Glikson M, Goethals M, Gulba DC, Ho SY, Klautz RJ, Kose S, McMurray J, Perrone FP, Raatikainen P, Salvador

- MJ, Schalij MJ, Shpektor A, Sousa J, Stepinska J, Uuetoa H, Zamorano JL, Zupan I Guidelines for the management of atrial fibrillation: the Task Force for the Management of Atrial Fibrillation of the European Society of Cardiology (ESC). *Europace* 2010;12:1360-1420.
11. Benjamin EJ, Levy D, Vaziri SM, D'Agostino RB, Belanger AJ, Wolf PA Independent risk factors for atrial fibrillation in a population-based cohort. The Framingham Heart Study. *JAMA* 1994;271:840-844.
 12. Kirchhof P, Bax J, Blomstrom-Lundquist C, Calkins H, Camm AJ, Cappato R, Cosio F, Crijns H, Diener HC, Goette A, Israel CW, Kuck KH, Lip GY, Nattel S, Page RL, Ravens U, Schotten U, Steinbeck G, Vardas P, Waldo A, Wegscheider K, Willems S, Breithardt G Early and comprehensive management of atrial fibrillation: executive summary of the proceedings from the 2nd AFNET-EHRA consensus conference 'research perspectives in AF'. *Eur Heart J* 2009;30:2969-77c.
 13. Krahn AD, Manfreda J, Tate RB, Mathewson FA, Cuddy TE The natural history of atrial fibrillation: incidence, risk factors, and prognosis in the Manitoba Follow-Up Study. *Am J Med* 1995;98:476-484.
 14. Wheeldon N Coronary heart disease and atrial fibrillation. Studies have not shown a causal relation. *BMJ* 1996;312:641-642.
 15. Nishida K, Qi XY, Wakili R, Comtois P, Chartier D, Harada M, Iwasaki YK, Romeo P, Maguy A, Dobrev D, Michael G, Talajic M, Nattel S Mechanisms of atrial tachyarrhythmias associated with coronary artery occlusion in a chronic canine model. *Circulation* 2011;123:137-146.
 16. Cappato R, Calkins H, Chen SA, Davies W, Iesaka Y, Kalman J, Kim YH, Klein G, Natale A, Packer D, Skanes A, Ambrogi F, Biganzoli E Updated Worldwide Survey on the Methods, Efficacy, and Safety of Catheter Ablation for Human Atrial Fibrillation. *Circ Arrhythm Electrophysiol* 2010;3:32-38.
 17. Berruezo A, Tamborero D, Mont L, Benito B, Tolosana JM, Sitges M, Vidal B, Arriagada G, Mendez F, Matiello M, Molina I, Brugada J Pre-procedural predictors of atrial fibrillation recurrence after circumferential pulmonary vein ablation. *Eur Heart J* 2007;28:836-841.
 18. Verma A, Wazni OM, Marrouche NF, Martin DO, Kilicaslan F, Minor S, Schweikert RA, Saliba W, Cummings J, Burkhardt JD, Bhargava M, Belden WA, Abdul-Karim A, Natale A Pre-existent left atrial scarring in patients undergoing pulmonary vein antrum isolation: an independent predictor of procedural failure. *J Am Coll Cardiol* 2005;45:285-292.
 19. den Uijl DW, Delgado V, Bertini M, Tops LF, Trines SA, van de Veire NR, Zeppenfeld K, Schalij MJ, Bax JJ Impact of left atrial fibrosis and left atrial size on the outcome of catheter ablation for atrial fibrillation. *Heart* 2011.

Chapter 6

Impact of pulmonary vein anatomy and left atrial dimensions on the outcome of circumferential radiofrequency catheter ablation for atrial fibrillation

Dennis W. den Uijl, Laurens F. Tops, Victoria Delgado, Joanne D. Schuijf, Lucia J.M. Kroft, Albert de Roos, Eric Boersma, Serge A. Trines, Katja Zeppenfeld, Martin J. Schalij, Jeroen J. Bax.

Am J Cardiol. 2011 Jan 15;107(2):243-9



Abstract

Background: Multi-slice computed tomography (MSCT) is commonly acquired prior to radiofrequency catheter ablation (RFCA) for atrial fibrillation (AF) in order to plan and guide the procedure. Importantly, MSCT allows accurate measurement of left atrial (LA) and pulmonary vein (PV) dimensions and classification of PV anatomy. The aim of this study was to investigate the impact of LA dimensions, PV dimensions and PV anatomy on the outcome of circumferential RFCA for AF.

Methods: One hundred consecutive patients undergoing RFCA for AF (paroxysmal 72%, persistent 28%) were studied. Left atrial dimensions, PV dimensions and PV anatomy were evaluated three-dimensionally on MSCT. Pulmonary vein anatomy was classified as normal or atypical based on the absence/presence of a common trunk or additional vein(s).

Results: After a mean follow up of 11.6 ± 2.8 months, 65 patients (65%) maintained sinus rhythm. Enlargement of the LA in anterior-posterior direction on MSCT was related to a higher risk for AF recurrence. No relation was found between PV dimensions and outcome of RFCA. In addition, normal right-sided PV anatomy was related to a higher risk for AF recurrence compared to atypical right-sided PV anatomy. Multivariate analysis showed that anterior-posterior LA diameter on MSCT (OR=1.083, p=0.027) and normal right-sided PV anatomy (OR=6.711, p=0.006) were independent predictors of AF recurrence after RFCA.

Conclusion: Enlargement of anterior-posterior LA diameter and presence of normal anatomy of the right PVs are independent risk factors for AF recurrence. No relation was found between PV dimensions and outcome of RFCA.

Introduction

Multi-slice computed tomography (MSCT) is nowadays commonly acquired prior to radiofrequency catheter ablation (RFCA) for atrial fibrillation (AF). Multi-slice computed tomography provides important information about the left atrial (LA) and pulmonary vein (PV) anatomy which can be used to plan and guide the RFCA procedure.¹ Moreover, MSCT allows accurate three-dimensional assessment of LA and PV dimensions.^{2,3} It has been demonstrated that LA dimensions and PV dimensions are enlarged in patients with AF.^{4,5} However, whereas LA size is a well-known risk factor for AF recurrence after RFCA,⁶⁻⁹ little is known about the prognostic importance of PV dilatation. Similarly, the impact of PV anatomy on the outcome of RFCA has not been studied extensively. Potentially, different anatomical drainage patterns could be accompanied by different tissue characteristics of the surrounding myocardium that may increase the resistance of the PV area to electrical isolation. Moreover, certain anatomical variants could pose a technical difficulty to achieve stable catheter position during ablation thereby compromising effective lesion formation. This study describes the impact of LA dimensions, PV dimensions and PV anatomy assessed by MSCT on the outcome of circumferential RFCA for AF.

Methods

Patient population and evaluation

The patient population comprised 100 consecutive patients with symptomatic drug-refractory AF, undergoing circumferential RFCA. After RFCA, all patients were evaluated on a regular basis at the outpatient clinic during a 12 months follow-up period. Routine electrocardiograms were recorded each visit and 24-hour Holter registrations were scheduled at 3, 6 and 12 months after the

ablation. Importantly, all patients were encouraged to immediately obtain an electrocardiogram when experiencing palpitations. All medications were continued for at least 3 months. Afterwards, anti-arrhythmic drugs were discontinued at the discretion of the physician. After a post-ablation blanking period of 3 months, recurrence of AF was defined as any recording of AF on electrocardiogram or an episode longer than 30 seconds on 24-hour Holter monitoring.¹⁰ After 12 months follow-up, the study population was divided into two groups: patients with maintenance of sinus rhythm (non-recurrence group) and patients who had recurrence of AF (recurrence group).

Multi-Slice Computed Tomography

Image acquisition

Prior to RFCA, all patients underwent an MSCT examination in order to guide the procedure.¹ The MSCT scan was performed with a 64-slice Toshiba Aquilion 64 system (Toshiba Medical Systems, Otawara, Japan). A bolus of 70 ml nonionic contrast material (Iomeron 400, Bracco, Milan, Italy) was infused through the antecubital vein at a rate of 5 ml/s followed by 50 ml saline solution flush. Automatic detection of the contrast bolus in the descending aorta was used to time the start of the scan. Craniocaudal scanning was performed during breath-hold, without electrocardiogram-gating. Collimation was 64 x 0.5 mm, rotation time 400 ms and the tube voltage 100 kV at 250 mA. After acquisition, the raw MSCT data were exported, post-processed and analyzed on a dedicated workstation (Vitrea 2, Vital Images, Minnetonka, Minnesota, USA).

Quantitative measurements

Pulmonary vein ostium dimensions were evaluated using a 2-dimensional viewing mode. To allow accurate assessment, multiplanar reformatting was

used to place two orthogonal planes parallel to the course of the vein (Figure 1, panel A and B). The third orthogonal plane, oriented perpendicular to the course of the vein, was then used to measure the diameter of the PV ostium in anterior-posterior and superior-inferior direction (Figure 1, panel C). The ratio between the largest and smallest diameter was calculated in order to obtain information on the oval shape of the ostium. Similarly, multiplanar reformatting was used to assess LA dimensions in 3 orthogonal directions: anterior-posterior, longitudinal and transversal direction (Figure 2). Left atrial volume was calculated using the biplane dimension-length formula: LA volume = $4/3\pi \times (\text{anterior-posterior diameter}/2) \times (\text{longitudinal diameter}/2) \times (\text{transversal diameter}/2)$.¹¹

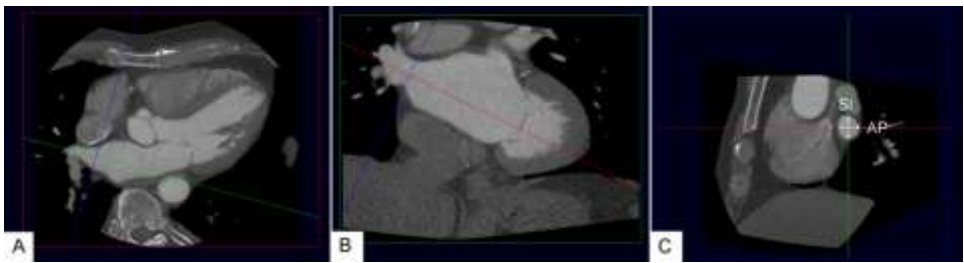


Figure 1. Assessment of pulmonary vein diameters. To assess pulmonary vein diameters, two orthogonal planes were placed parallel to the course of the vein (panel A and B). A third orthogonal plane (panel C), oriented perpendicular to the course of the vein, was then used to measure the anterior-posterior (AP) and superior-inferior (SI) pulmonary vein diameter (white arrows).

Pulmonary vein anatomy

Pulmonary vein anatomy was analyzed from an external view using a three-dimensional volume-rendered reconstruction. Pulmonary vein classification was based on the presence or absence of a common trunk and/or additional vein(s) (Figure 3). A common trunk was defined when the superior and the inferior PV joined more than 5 mm before entering in the LA. An additional vein was defined as a supranumerary vein directly entering the LA.

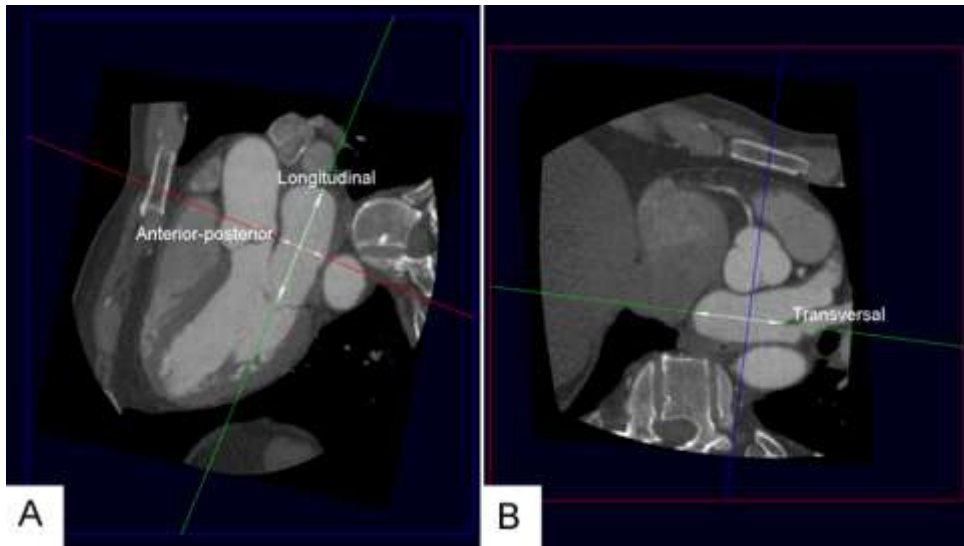


Figure 2. Assessment of left atrial dimensions. The left atrial (LA) dimensions (white arrows) were assessed in three orthogonal directions by using multiplanar reformatting. Panel A: LA dimensions in anterior-posterior (AP) (red line) and longitudinal direction (green line). Panel B: LA dimension in transversal direction (green line). Panel B is a cross-section of panel A at the level of the crosshair and parallel to the red line.

To evaluate the impact of PV anatomy on the outcome of RFCA for AF, left- and right-sided anatomy was additionally classified as normal or atypical. Atypical anatomy was defined as the presence of a common trunk or an additional PV.

Radiofrequency catheter ablation

The RFCA procedure was aimed at creating two circumferential lesions around the left- and right-sided ipsilateral PVs approximately 1 cm outside the ostia. All patients received intravenous heparin to maintain an activated clotting time of 300-400 s. Intracardiac echocardiography was used to guide the transseptal puncture. To guide the ablation, a non-fluoroscopic electroanatomical mapping system with MSCT integration was used (CARTO XP™ with Cartomerge™, Biosense Webster, Diamond Bar, California, USA). Contact

mapping and ablation was performed using a 4-mm quadripolar open-loop irrigated mapping/ablation catheter (7Fr Navistar™, Biosense Webster). A 6Fr quadripolar diagnostic catheter placed inside the right atrium served as a temporal reference. Radiofrequency current was applied at 30-35 W with a maximum temperature of 45°C and an irrigation flow of 20 ml/min until a bipolar voltage of <0.1 mV was achieved, with a maximum of 60 s per point. The end-point of the procedure was PV isolation as confirmed by recording entrance block during sinus rhythm or pacing from inside the coronary sinus.¹⁰

Statistical analysis

Statistical analyses were performed with SPSS software (version 16.0, SPSS Inc., Chicago, Illinois, USA). A p-value of <0.05 was considered statistically significant. Data are presented as mean ± SD or as number (percentage). Statistical comparisons for continuous variables were performed with the **two tailed Student's t-test**, paired or unpaired as appropriate. Statistical comparisons for categorical variables were performed with the Chi-square test. Univariate and multivariate logistic regression analyses were performed to study the impact of clinical characteristics, LA dimensions and PV dimensions and anatomy on the incidence of AF recurrence after RFCA. Variables with a p-value <0.05 in the univariate analyses were included into the multivariate analysis. **Multivariate analysis was performed using an 'enter' method.**

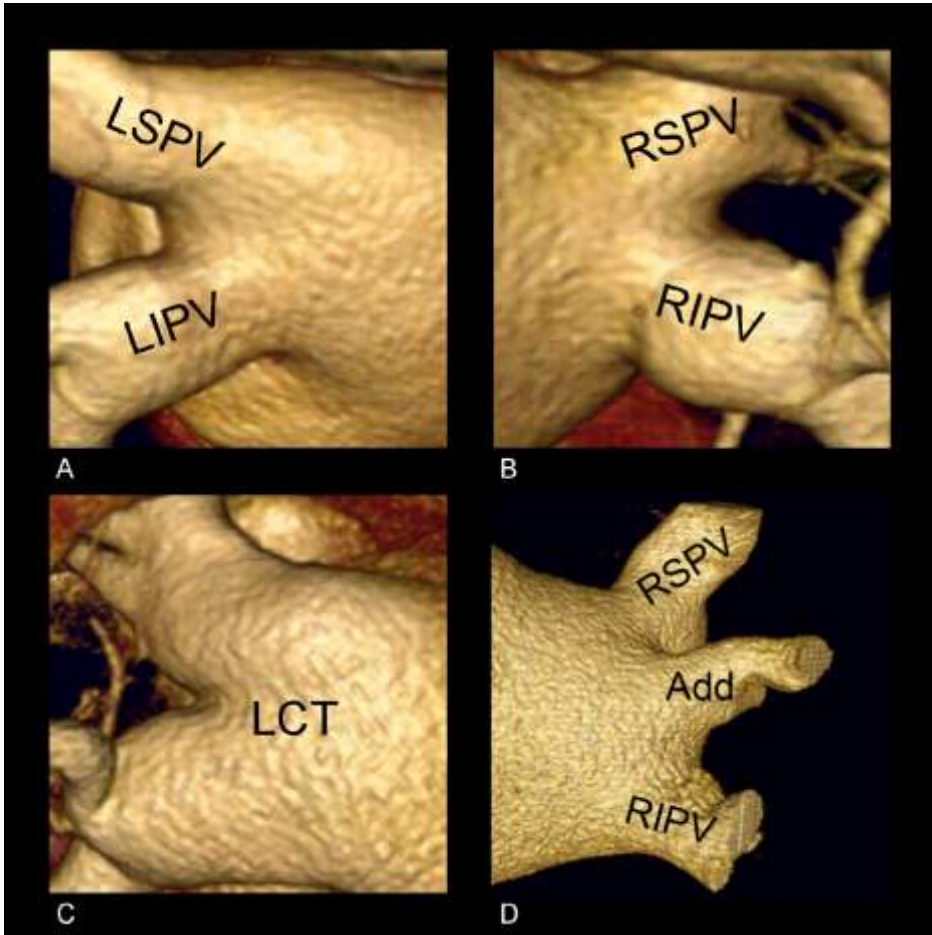


Figure 3. Classification of pulmonary vein anatomy. Panel A: Separate ostia of the left-sided pulmonary veins; Panel B: Separate ostia of the right-sided pulmonary veins; Panel C: Common trunk of the left-sided pulmonary veins (defined as a joint part of the superior and the inferior pulmonary veins of more than 5 mm, before entering the left entering); Panel D: Additional right-sided pulmonary vein (defined as a supranumerary vein directly entering the left atrium). Add = additional pulmonary vein, LIPV = left inferior pulmonary vein, LSPV = left superior pulmonary vein, RIPV = right inferior pulmonary vein, RSPV = right superior pulmonary vein.

Results

Patient characteristics

One hundred consecutive patients were included (77 men, mean age 56 ± 9 years), from an ongoing clinical registry.¹² Atrial fibrillation was paroxysmal in 72 patients and persistent in 28 patients according to the American College of Cardiology/American Heart Association/European Society of Cardiology guidelines definitions.¹³ None of the patients had previously undergone RFCA for AF. Median duration of AF was 48 months (interquartile range: 24-84) and the mean number of anti-arrhythmic drugs used was 3.1 ± 1.3 per patient. The mean anterior-posterior diameter of the LA was 43 ± 6 mm and the mean left ventricular ejection fraction was $58 \pm 8\%$ on transthoracic echocardiography (Table 1). The procedural end-point of PV isolation was achieved in all patients. In 11 patients a repeat procedure was performed due to early recurrence of AF.

After a mean follow-up of 11.6 ± 2.8 months, 65 patients (65%) had maintained sinus rhythm (non-recurrence group), whereas 35 patients (35%) had recurrence of AF (recurrence group). Anti-arrhythmic drug treatment had been discontinued in 16 patients (25%) who had maintained sinus rhythm and in 12 patients (34%) with AF recurrence ($p=0.30$). In the recurrence group a higher prevalence of persistent AF was found compared to the non-recurrence group (14 [22%] vs. 14 [40%], $p=0.049$).

Left atrial dimensions

Left atrial dimensions were measured in three orthogonal directions on MSCT: anterior-posterior, longitudinal and transversal (Figure 2). Mean anterior-posterior diameter was 41 ± 7 mm, mean longitudinal diameter was 65 ± 8 mm and mean transversal diameter was 59 ± 7 mm. Anterior-posterior LA diameter was significantly larger in the recurrence group than in the non-recurrence group (43 ± 6 mm vs. 39 ± 7 mm, $p=0.02$). Interestingly, no differences were

found between the recurrence group and non-recurrence group in longitudinal (64 ± 7 mm vs. 65 ± 9 mm, $p=0.45$) and transversal (59 ± 7 mm vs. 60 ± 7 mm, $p=0.57$) LA diameter. Mean LA volume was 82 ± 23 ml. Left atrial volume was larger in the recurrence group than in the non-recurrence group (88 ± 26 ml vs. 78 ± 21 ml, $p=0.04$).

Table 1. Baseline characteristics

Variable	Total (n = 100)
Age (years)	56.4 ± 8.6
Male/female	77/23
Body Surface Area (m ²)	2.1 ± 0.2
Type of atrial fibrillation (paroxysmal/persistent)	72/28
Duration of atrial fibrillation (months)	64 ± 60
Anti-arrhythmic drugs used per patient	3.1 ± 1.3
Hypertension	53 (53%)
Coronary artery disease	8 (8%)
Diabetes mellitus	8 (8%)
Echocardiography	
Anterior-posterior left atrial diameter (mm)	43 ± 6
Left ventricular ejection fraction (%)	58 ± 8

Pulmonary vein dimensions

Pulmonary vein ostial dimensions were assessed in anterior-posterior and superior-inferior direction on MSCT (Table 2). Pulmonary vein dimensions were larger in superior-inferior direction than in anterior-posterior direction (21.1 ± 2.3 mm vs. 16.3 ± 2.5 mm, $p<0.001$). Overall, right-sided PVs had a larger

diameter than left-sided PVs (20.0 ± 2.4 mm vs. 16.6 ± 1.6 mm, $p < 0.001$). Similarly, superior PVs had a larger diameter than inferior PVs (19.6 ± 3.8 mm vs. 17.5 ± 3.1 mm, $p < 0.001$). With regard to the shape of the PV ostium, left-sided PVs had a more pronounced oval shape than right-sided PV ostia indicated by a lower ratio between the largest and smallest PV diameter (ratio 0.65 ± 0.09 vs. 0.84 ± 0.09 , $p < 0.001$).

Table 2. Pulmonary vein measurements on multi-slice computed tomography

Variable	Anterior-posterior diameter (mm)	Superior-posterior diameter (mm)	Mean diameter (mm)	Ratio
Right superior pulmonary vein	18.8 ± 4.2	23.3 ± 4.5	21.0 ± 4.0	0.80 ± 0.11
Right inferior pulmonary vein	17.7 ± 2.9	20.3 ± 3.2	19.0 ± 2.8	0.87 ± 0.10
Left superior pulmonary vein	14.3 ± 2.6	21.1 ± 3.6	17.7 ± 2.4	0.67 ± 0.13
Left inferior pulmonary vein	12.1 ± 2.7	18.8 ± 2.5	15.4 ± 2.0	0.65 ± 0.15
Additional pulmonary vein	8.9 ± 3.1	10.1 ± 2.4	9.5 ± 2.5	0.82 ± 0.11
Left common trunk	19.5 ± 4.5	33.5 ± 4.7	26.5 ± 3.4	0.59 ± 0.15
All right pulmonary veins	18.2 ± 2.5	21.8 ± 2.8	20.0 ± 2.4	0.83 ± 0.08
All left pulmonary veins	13.2 ± 2.5	19.9 ± 2.0	16.6 ± 1.6	0.66 ± 0.11
All pulmonary veins	16.3 ± 2.5	21.1 ± 2.3	18.7 ± 2.2	0.77 ± 0.09

Pulmonary vein dimensions were not related to the recurrence of AF during follow-up: no differences were found in mean PV diameter between the recurrence and non-recurrence group (18.8 ± 2.2 mm vs. 18.6 ± 2.2 mm, $p = 0.74$). In addition, a similar oval shape of the PV ostia was found in the both groups (non-recurrence group versus recurrence group: ratio 0.77 ± 0.09 vs. 0.77 ± 0.09 , $p = 0.73$).

Pulmonary vein anatomy

Pulmonary vein anatomy was assessed based on the presence/absence of a common trunk and/or additional PV. A total of 174 left-sided PVs and 226 right-sided PVs were identified on MSCT. Separate ostia of the left superior PV and left inferior PV were present in 74 patients (74%) and a common trunk of the left PVs was present in the remaining 26 patients (26%). In addition, separate ostia of the right superior PV and right inferior PV were observed in 78 patients (78%), an additional right-sided PV in 18 patients (18%) and 2 additional right-sided veins in 4 patients (4%). Accordingly, atypical anatomy of the left-sided PVs was present in 26 patients (26%) and atypical anatomy of the right-sided PVs was observed in 22 patients (22%).

Normal anatomy of the right-sided PVs was associated with a significantly higher risk for AF recurrence compared to atypical anatomy of the right-sided PVs (unadjusted OR: 7.353, $p=0.010$). In contrast, the presence of normal or atypical anatomy of the left-sided PVs had no significant impact on the outcome of RFCA (unadjusted OR: 2.145, $p=0.14$).

Predictors of AF recurrence

Univariate logistic regression analyses were performed to study the impact of LA dimensions, PV dimensions and PV anatomy, as well as clinical risk factors (e.g. type AF, hypertension) on the outcome of RFCA for AF (Table 3). A large anterior-posterior LA diameter (unadjusted OR: 1.082, $p=0.021$) and a large LA volume (unadjusted OR: 1.019, $p=0.045$) were related to a higher risk for recurrent AF after RFCA. Similarly, patients with persistent AF had a higher risk for AF recurrence (unadjusted OR: 2.429, $p=0.049$). The presence of normal right-sided PV anatomy was related to a higher risk for AF recurrence (unadjusted OR: 7.353, $p=0.010$). Subsequent multivariate analyses demonstrated that anterior-posterior LA diameter (OR: 1.083, $p=0.027$),

persistent AF (OR: 3.004, $p=0.035$) and normal right-sided PV anatomy (OR: 6.711, $p=0.006$) were independent predictors of AF recurrence (Table 4).

Table 3. Univariate logistic regression analysis of clinical and anatomical characteristics on multi-slice computed tomography as risk factors for recurrence of atrial fibrillation after radiofrequency catheter ablation

Variable	OR	95% CI	P-value
Clinical and echocardiographic characteristics			
Age (per years)	1.027	0.978-1.079	0.28
Male gender	1.012	0.381-2.691	0.98
AF duration (per months)	1.032	0.952-1.118	0.45
Failed anti-arrhythmic drugs (per drug)	1.109	0.802-1.532	0.53
Persistent atrial fibrillation	2.429	0.989-5.963	0.049*
Hypertension	0.908	0.399-2.067	0.82
Left ventricular ejection fraction (per %)	0.971	0.920-1.026	0.30
Multi-slice computed tomography characteristics			
Normal right-sided pulmonary vein anatomy	7.353	1.603-33.333	0.010*
Normal left-sided pulmonary vein anatomy	2.146	0.771-5.988	0.14
Mean pulmonary vein diameter (per mm)	1.033	0.856-1.247	0.73
Left atrial diameter			
Anterior-posterior (per mm)	1.082	1.012-1.156	0.021*
Longitudinal (per mm)	1.021	0.967-1.078	0.45
Transversal (per mm)	1.018	0.958-1.082	0.57
Left atrial volume (per ml)	1.019	1.000-1.038	0.045*

*included in multivariate logistic regression analysis

Table 4. Multivariate logistic regression analysis of clinical and anatomical characteristics on multi-slice computed tomography as risk factors for recurrence of atrial fibrillation after radiofrequency catheter ablation

Variable	OR	95% CI	P-value
Clinical characteristics			
Persistent atrial fibrillation	3.004	1.082-8.345	0.035
Multi-slice computed tomography characteristics			
Normal right-sided pulmonary vein anatomy	6.711	1.736-26.316	0.006
Left atrial diameter			
Anterior-posterior (per mm)	1.083	1.009-1.162	0.027
Left atrial volume (per ml)	1.000	0.967-1.035	0.98

Discussion

The present study investigated the impact of LA dimensions, PV dimensions and PV anatomy on the outcome of circumferential RFCA for AF. The main findings were that enlargement of the LA in direction on MSCT was an independent predictor of AF recurrence after RFCA. In contrast, PV dimensions were not related to the outcome of RFCA. Finally, atypical anatomy of the right-sided PVs was independently associated with less recurrences of AF after RFCA.

Left atrial dimensions

Left atrial enlargement is an important risk factor for the development of AF in the general population,¹⁴ and has been identified as an independent predictor of AF recurrence after RFCA.⁶⁻⁹ Significant dilatation of the LA is thought to be a marker of a large extent of atrial remodeling which may limit the efficacy of RFCA. In the present study, assessment of LA dimensions was performed in three directions on MSCT: anterior-posterior, longitudinal and transversal. Anterior-posterior LA diameter was identified as a predictor of AF recurrence, whereas longitudinal and transversal LA diameters were not. Moreover, anterior-posterior LA diameter was a stronger predictor of AF recurrence than

LA volume. Atrial dilatation is thought to be predominantly oriented in longitudinal and transversal direction and not in anterior-posterior direction.¹¹ A potential explanation for our finding is that the dilatation of the LA in anterior-posterior direction occurs at a more advanced stage of atrial enlargement and reflects a higher extent of atrial remodeling, thereby explaining its prognostic value to predict AF recurrence after RFCA. Importantly, anterior-posterior LA diameter was an independent predictor of AF recurrence even after correction for type of AF.

Pulmonary vein dimensions and anatomy

The observations by Haissaguerre et al. that ectopic beats originating from the PVs can initiate AF, have led to an increasing interest in the PVs as target for RFCA.¹⁵ Nowadays, isolation of the PV region is the cornerstone for most ablation strategies.¹⁰ However, little is known about the impact of PV dimensions and PV anatomy on the efficacy of RFCA for AF.

Similar to LA enlargement, PV dimensions are enlarged in patients with AF.³⁻⁵ Previous series have demonstrated that superior PVs have a larger diameter compared to inferior PVs.^{3,16} This finding has been related to a higher incidence of ectopic foci initiating AF originating from the superior PVs than from the inferior PVs.^{15,16} In addition, it is suggested that PV dilatation is accompanied by different electrophysiological tissue characteristics in a way that AF is more likely to persist.⁴ However, little is known about the prognostic significance of PV dilatation in patients undergoing RFCA to predict AF recurrence.

The present study evaluated the impact of PV ostial dimensions assessed by MSCT on AF recurrence after RFCA. No differences were found in PV ostial dimensions or shape between patients with AF recurrence and patients without AF recurrence during follow-up. These results suggest that PV

dilatation has no prognostic value to predict AF recurrence after circumferential RFCA. Most likely, PV dilatation is caused by the presence of AF and can be best considered an epiphenomenon.

The relation between the anatomy of the PV region and the efficacy RFCA for AF has not been studied extensively. Several studies have shown that large variations in pulmonary venous drainage pattern into the LA exist.^{3,17-20} Potentially, certain anatomical variants could pose a technical challenge to achieve stable catheter position thereby influencing the outcome of RFCA. Moreover, different venous drainage patterns could be accompanied by different tissue characteristics of the surrounding myocardium that may increase the resistance of the PV area to electrical isolation.

In the present study, the relation between PV anatomy and AF recurrence after RFCA was studied. Pulmonary vein anatomy was analyzed on MSCT and classified according to the presence or absence of a common trunk and/or additional PV as either normal or atypical. Normal anatomy of the right-sided PVs was associated with an increased risk for AF recurrence after RFCA. After correction for anterior-posterior LA diameter and type of AF, normal right-sided PV anatomy remained as independent predictor of AF recurrence after RFCA. These findings may indicate that an atypical PV drainage pattern may be accompanied by an increased susceptibility of the surrounding myocardial tissue for electrical isolation or a lower likelihood for PV ectopy originating from the right-sided PVs. Furthermore an atypical PV drainage pattern may pose less technical difficulty to achieve stable catheter position, resulting in a more effective lesion formation and a lower risk for electrical reconnection.

Recently, Hof et al reported on the impact of PV anatomy on the efficacy of RFCA in 146 patients.⁷ Interestingly, no relation was found between PV anatomy and AF recurrence after RFCA. However, the definition of outcome

used by Hof et al included three categories (failure, improvement of AF burden and complete success),⁷ and may have precluded from obtaining statistically significant differences among the different groups. The use of this definition may also explain why type of AF, which is a commonly accepted risk factor for AF recurrence,¹⁰ was not related to AF recurrence after RFCA in their study.⁷

Limitations

Some limitations should be acknowledged. The applicability of MSCT as a pre-procedural patient selection tool is limited by the radiation exposure inherited to this technique. However, since MSCT is commonly acquired prior to RFCA to plan and guide the procedure, the present results may help determine whether additional ablation is needed in patients who are scheduled for circumferential RFCA. Furthermore, this study comprised a relatively small group of patients and present findings should be validated in a larger population.

References

1. Tops LF, Bax JJ, Zeppenfeld K, Jongbloed MR, Lamb HJ, van der Wall EE, Schalij MJ Fusion of multislice computed tomography imaging with three-dimensional electroanatomic mapping to guide radiofrequency catheter ablation procedures. *Heart Rhythm* 2005;2:1076-1081.
2. Hof I, rbab-Zadeh A, Scherr D, Chilukuri K, Dalal D, Abraham T, Lima J, Calkins H Correlation of left atrial diameter by echocardiography and left atrial volume by computed tomography. *J Cardiovasc Electrophysiol* 2009;20:159-163.
3. Jongbloed MR, Bax JJ, Lamb HJ, Dirksen MS, Zeppenfeld K, van der Wall EE, de RA, Schalij MJ Multislice computed tomography versus intracardiac echocardiography to evaluate the pulmonary veins before radiofrequency catheter ablation of atrial fibrillation: a head-to-head comparison. *J Am Coll Cardiol* 2005;45:343-350.
4. Tsao HM, Yu WC, Cheng HC, Wu MH, Tai CT, Lin WS, Ding YA, Chang MS, Chen SA Pulmonary vein dilation in patients with atrial fibrillation: detection by magnetic resonance imaging. *J Cardiovasc Electrophysiol* 2001;12:809-813.
5. Kato N, Lickfett L, Meininger G, Dickfeld T, Wu R, Juang G, Angkeow P, LaCorte J, Bluemke D, Berger R, Halperin HR, Calkins H Pulmonary vein anatomy in patients undergoing catheter ablation of atrial fibrillation: lessons learned by use of magnetic resonance imaging. *Circulation* 2003;107:2004-2010.
6. Berrueto A, Tamborero D, Mont L, Benito B, Tolosana JM, Sitges M, Vidal B, Arriagada G, Mendez F, Matiello M, Molina I, Brugada J Pre-procedural predictors of atrial fibrillation recurrence after circumferential pulmonary vein ablation. *Eur Heart J* 2007;28:836-841.
7. Hof I, Chilukuri K, rbab-Zadeh A, Scherr D, Dalal D, Nazarian S, Henrikson C, Spragg D, Berger R, Marine J, Calkins H Does left atrial volume and pulmonary venous anatomy predict the outcome of catheter ablation of atrial fibrillation? *J Cardiovasc Electrophysiol* 2009;20:1005-1010.
8. Shin SH, Park MY, Oh WJ, Hong SJ, Pak HN, Song WH, Lim DS, Kim YH, Shim WJ Left atrial volume is a predictor of atrial fibrillation recurrence after catheter ablation. *J Am Soc Echocardiogr* 2008;21:697-702.
9. Abecasis J, Dourado R, Ferreira A, Saraiva C, Cavaco D, Santos KR, Morgado FB, Adragao P, Silva A Left atrial volume calculated by multi-detector computed tomography may predict successful pulmonary vein isolation in catheter ablation of atrial fibrillation. *Europace* 2009.
10. Calkins H, Brugada J, Packer DL, Cappato R, Chen SA, Crijns HJ, Damiano RJ, Jr., Davies DW, Haines DE, Haissaguerre M, Iesaka Y, Jackman W, Jais P, Kottkamp H, Kuck KH, Lindsay BD, Marchlinski FE, McCarthy PM, Mont JL, Morady F, Nademanee K, Natale A, Pappone C, Prystowsky E, Raviele A, Ruskin JN, Shemin RJ HRS/EHRA/ECAS expert consensus statement on catheter and surgical ablation of atrial fibrillation: recommendations for personnel, policy, procedures and follow-up. A report of the Heart Rhythm Society (HRS) Task Force on Catheter and Surgical Ablation of Atrial Fibrillation developed in partnership with the European Heart Rhythm Association (EHRA) and the European Cardiac Arrhythmia Society (ECAS); in collaboration with the American College of Cardiology (ACC), American Heart Association (AHA), and the Society of Thoracic Surgeons (STS). Endorsed and approved by the governing bodies of the American College of Cardiology, the American Heart Association, the European Cardiac Arrhythmia Society, the European Heart Rhythm Association, the Society of Thoracic Surgeons, and the Heart Rhythm Society. *Europace* 2007;9:335-379.
11. Lang RM, Bierig M, Devereux RB, Flachskampf FA, Foster E, Pellikka PA, Picard MH, Roman MJ, Seward J, Shanewise JS, Solomon SD, Spencer KT, Sutton MS, Stewart WJ

- Recommendations for chamber quantification: a report from the American Society of Echocardiography's Guidelines and Standards Committee and the Chamber Quantification Writing Group, developed in conjunction with the European Association of Echocardiography, a branch of the European Society of Cardiology. *J Am Soc Echocardiogr* 2005;18:1440-1463.
12. Tops LF, Bax JJ, Zeppenfeld K, Jongbloed MR, van der Wall EE, Schalij MJ Effect of radiofrequency catheter ablation for atrial fibrillation on left atrial cavity size. *Am J Cardiol* 2006;97:1220-1222.
 13. Fuster V, Ryden LE, Cannom DS, Crijns HJ, Curtis AB, Ellenbogen KA, Halperin JL, Le Heuzey JY, Kay GN, Lowe JE, Olsson SB, Prystowsky EN, Tamargo JL, Wann S, Smith SC, Jr., Jacobs AK, Adams CD, Anderson JL, Antman EM, Halperin JL, Hunt SA, Nishimura R, Ornato JP, Page RL, Riegel B, Priori SG, Blanc JJ, Budaj A, Camm AJ, Dean V, Deckers JW, Despres C, Dickstein K, Lekakis J, McGregor K, Metra M, Morais J, Osterspey A, Tamargo JL, Zamorano JL ACC/AHA/ESC 2006 guidelines for the management of patients with atrial fibrillation: full text: a report of the American College of Cardiology/American Heart Association Task Force on practice guidelines and the European Society of Cardiology Committee for Practice Guidelines (Writing Committee to Revise the 2001 guidelines for the management of patients with atrial fibrillation) developed in collaboration with the European Heart Rhythm Association and the Heart Rhythm Society. *Europace* 2006;8:651-745.
 14. Vaziri SM, Larson MG, Benjamin EJ, Levy D Echocardiographic predictors of nonrheumatic atrial fibrillation. The Framingham Heart Study. *Circulation* 1994;89:724-730.
 15. Haissaguerre M, Jais P, Shah DC, Takahashi A, Hocini M, Quiniou G, Garrigue S, Le MA, Le MP, Clementy J Spontaneous initiation of atrial fibrillation by ectopic beats originating in the pulmonary veins. *N Engl J Med* 1998;339:659-666.
 16. Ho SY, Sanchez-Quintana D, Cabrera JA, Anderson RH Anatomy of the left atrium: implications for radiofrequency ablation of atrial fibrillation. *J Cardiovasc Electrophysiol* 1999;10:1525-1533.
 17. Mansour M, Holmvang G, Sosnovik D, Migrino R, Abbara S, Ruskin J, Keane D Assessment of pulmonary vein anatomic variability by magnetic resonance imaging: implications for catheter ablation techniques for atrial fibrillation. *J Cardiovasc Electrophysiol* 2004;15:387-393.
 18. Schwartzman D, Lacomis J, Wigginton WG Characterization of left atrium and distal pulmonary vein morphology using multidimensional computed tomography. *J Am Coll Cardiol* 2003;41:1349-1357.
 19. Marom EM, Herndon JE, Kim YH, McAdams HP Variations in pulmonary venous drainage to the left atrium: implications for radiofrequency ablation. *Radiology* 2004;230:824-829.
 20. Cronin P, Kelly AM, Gross BH, Desjardins B, Patel S, Kazerooni EA, Carlos RC Reliability of MDCT in characterizing pulmonary venous drainage, diameter and distance to first bifurcation: an interobserver study. *Acad Radiol* 2007;14:437-444.

Chapter 7

Natriuretic peptide levels predict recurrence of atrial fibrillation after radiofrequency catheter ablation

Dennis W. den Uijl, Victoria Delgado, Laurens F. Tops, Arnold C.T. Ng, Eric Boersma, Serge A. Trines, Katja Zeppenfeld, Martin J. Schalij, Arnoud van der Laarse, Jeroen J. Bax.

Am Heart J. 2011 Jan;161(1):197-203



Abstract

Background: The presence of atrial fibrillation (AF) is related to increased levels of natriuretic peptides. In addition, increased natriuretic peptide levels are predictive of the development of AF. However, the role of natriuretic peptides to predict recurrence of AF after radiofrequency catheter ablation (RFCA) is controversial.

Objective: To investigate the role of natriuretic peptides to predict AF recurrence after RFCA for AF.

Methods: In 87 patients undergoing RFCA for symptomatic drug-refractory AF, pre-procedural NT-proANP and NT-proBNP plasma levels were determined. In addition, a comprehensive clinical and echocardiographic evaluation was performed at baseline. Left atrial volumes, left ventricular volumes and function (systolic and diastolic) were assessed. During a 6 months follow-up period, AF recurrence was monitored and defined as any registration of AF on ECG or an episode of AF longer than 30 seconds on 24-hour Holter monitoring. The role of natriuretic peptide plasma levels to predict AF recurrence after RFCA was studied.

Results: During follow-up, 66 patients (76%) maintained sinus rhythm (SR), whereas 21 patients (24%) had AF recurrence. Patients with AF recurrence had higher baseline natriuretic peptide levels than patients who maintained SR (NT-proANP: 3.19 nmol/L [2.55-4.28] versus 2.52 nmol/L [1.69-3.55], $p=0.030$; NT-proBNP: 156.4 pg/mL [64.1-345.3] versus 84.6 pg/mL [43.3-142.7], $p=0.036$). However, NT-proBNP was an independent predictor of AF recurrence, whereas NT-proANP was not. Moreover, NT-proBNP had an incremental value over echocardiographic characteristics to predict AF recurrence after RFCA.

Conclusion: Baseline NT-proBNP plasma level is an independent predictor of AF recurrence after RFCA.

Introduction

Radiofrequency catheter ablation (RFCA) is considered a reasonable treatment option for patients with symptomatic, drug refractory atrial fibrillation (AF).¹ However, this treatment modality is associated with a considerable recurrence rate.² Several parameters have been related to a high risk for AF recurrence such as age, hypertension, type of AF, left atrial (LA) size and impaired left ventricular (LV) systolic function.³⁻⁶ These risk factors seem to either cause or reflect structural changes (i.e. structural remodeling) of the atria that promote the perpetuation of AF and, thereby, limit the efficacy of RFCA. Accordingly, pre-procedural evaluation of the extent of atrial remodeling could be used to identify patients with an increased risk of AF recurrence after RFCA. However, at an early stage of atrial remodeling, conventional imaging techniques (e.g. two-dimensional echocardiography to assess LA size) may not be sensitive enough to predict whether a patient will experience AF recurrence after RFCA. Therefore, more sensitive indicators of atrial remodeling are needed.

Natriuretic peptides are hormones released from the atria and/or ventricles in response to volume or pressure overload.⁷ In patients with AF, natriuretic peptide levels are elevated.⁸⁻¹⁰ Potentially, plasma levels of natriuretic peptides could provide insight into the presence of underlying cardiac conditions that cause structural changes to the LA and may limit the efficacy of RFCA.

The aim of this study was to investigate the prognostic role of natriuretic peptides to predict AF recurrence in patients with preserved LV systolic function undergoing RFCA for paroxysmal AF.

Methods

Patient population and evaluation

The study population included patients with drug-refractory symptomatic paroxysmal AF and preserved LV systolic function (ejection fraction >50%), who were referred for RFCA. Atrial fibrillation was classified as paroxysmal when episodes were generally self-terminating and lasted no longer than 7 days, according to the American College of Cardiology/American Heart Association/European Society of Cardiology guidelines definitions.¹¹ At admission, a blood sample was obtained to measure natriuretic peptide levels and a comprehensive transthoracic echocardiography examination was performed. To minimize the effect of AF on plasma natriuretic peptide levels, only patients with paroxysmal AF who were in sinus rhythm (SR) during blood sampling were studied. After ablation, all patients were evaluated on a systematic basis (1, 3 and 6 months after RFCA) at the outpatient clinic during a 6 months follow-up period. Routine electrocardiograms (ECG) were recorded each visit and 24-hour Holter registrations were scheduled after 3 and 6 months follow-up. Importantly, all patients were encouraged to obtain an ECG registration when experiencing palpitations. During follow-up, all medications were continued for at least 3 months. Afterwards, anti-arrhythmic drugs were discontinued at the discretion of the physician. After a blanking period of 3 months, recurrence of AF was defined as any recording of AF on ECG or an episode longer than 30 s on 24-hour Holter monitoring. Accordingly, the role of baseline clinical characteristics, baseline echocardiographic characteristics and baseline natriuretic peptide levels to predict AF recurrence after RFCA was studied.

Biochemical analysis

Blood samples were obtained from the antecubital vein at admission. An ECG recording was made during sampling to determine the heart rhythm. Plasma and serum samples were stored at -80°C prior to assay. Levels of amino-terminal-pro-atrial natriuretic peptide (NT-proANP) were determined using a radioimmunoassay (ELISA, Biomedica, Vienna, Austria) which has a measurement range of 0–10 nmol/L and a detection limit of 0.05 nmol/L. Inter-assay variation was 4% and intra-assay variability was 2%. Levels of amino-terminal-pro-B-type natriuretic peptide (NT-proBNP) were measured using an automated immunoassay (Elecsys, Roche, Basel, Switzerland). The reference range was 0–400 pg/mL and the intra-assay variability was 1.8% at high concentrations of NT-proBNP (800 pg/mL) and 2.7% at low concentrations (2.1 pg/mL).

Echocardiography

Two-dimensional transthoracic echocardiography was performed using a commercially available ultrasound system (Vivid 7, General Electric Vingmed, Milwaukee, WI, United States), equipped with a 3.5-MHz transducer at a depth of 16 cm. All patients were imaged in left lateral decubitus position. Two-dimensional and color Doppler data were obtained in parasternal (short- and long-axis) and apical (2- and 4-chamber images) views. All images were ECG-triggered and stored in cine loop format for offline analyses. Offline analyses were performed using EchoPac 108.1.5 (General Electric Medical Systems, Horten, Norway).

Maximum LA volume was obtained from the apical views by disc's method.¹² Left ventricular (LV) end-diastolic and end-systolic volumes were obtained from the apical views and LV ejection fraction was calculated **according to the Simpson's method.**¹² Left ventricular and atrial volumes were

indexed to body surface area. Left ventricular diastolic function was evaluated using pulsed-wave Doppler recordings of the mitral valve inflow pattern (E-wave, A-wave, deceleration time of the E-wave) and Doppler tissue recordings **of the mitral annular motion (E'-wave)**. In addition, the diastolic function grade was classified as either normal, grade 1 (impaired relaxation), grade 2 (pseudonormalization) or grade 3 (restrictive filling pattern) as recommended by current guidelines.¹³

Radiofrequency catheter ablation

The ablation was aimed at creating circular lesions around the left and right pulmonary vein ostia. All patients received intravenous heparin to maintain an activated clotting time of 300-400 s. Intracardiac echocardiography was used to exclude a cardiac thrombus and to guide the transseptal puncture. A non-fluoroscopic electroanatomical mapping system with multi-slice computed tomography integration was used to guide the ablation procedure (CARTO XP™, Cartomerge™, Biosense Webster, Diamond Bar, CA, USA). Mapping and ablation was performed using a 3.5-mm quadripolar open-loop irrigated mapping/ablation catheter (7.5Fr Navistar™, Biosense Webster). Radiofrequency current was applied at 30-35 W with a maximum temperature of 45°C and an irrigation flow of 20 ml/min until a bipolar voltage of <0.1 mV was achieved, with a maximum of 60 s per point. The end-point of the procedure was PV isolation as confirmed by recording entrance block during SR or pacing in the coronary sinus.¹

Statistical analysis

All variables were tested for a normal distribution with the Kolmogorov-Smirnov test. Normally distributed continuous variables are represented as mean \pm SD and non-normally distributed continuous variables are represented

as median (25th - 75th percentile). Categorical variables are presented as number (percentage). Statistical comparisons for continuous variables were performed **with the Student's t-test** or with the Mann-Whitney U-test as appropriate. Statistical comparisons for categorical variables were performed with the Chi-square test. Univariable and multivariable Cox proportional hazard analyses were performed to investigate the relation between natriuretic peptide levels and the risk for AF recurrence after ablation. Multivariable analyses were **performed using an 'enter' method**. Due to the limited number of events, multivariable analyses were limited to three variables. Separate models were created to correct for known clinical determinants of natriuretic peptide levels (age and gender) and to correct for the strongest univariate predictors of AF recurrence in the present population (LA volume index and LV end-systolic volume index). The incremental prognostic value of natriuretic peptides to predict AF recurrence was studied by calculating the improvement in global Chi-square after addition of NT-proANP or NT-proBNP to the model. In addition, for each Cox regression model the c-statistic was calculated. All statistical analyses were performed with SPSS software (version 16.0, SPSS Inc., Chicago, IL, USA). A value of $p < 0.05$ was considered statistically significant.

The authors are solely responsible for the design and conduct of this study, all study analyses, the drafting and editing of the paper and its final contents. No extramural funding was used to support this work.

Results

Patient characteristics

The present patient population was prospectively included from an ongoing clinical registry.¹⁴ Out of 140 consecutive patients undergoing catheter ablation for AF, 87 patients were in SR during the baseline blood test and comprised the patient population (70 men [80%], mean age 55.0 ± 9.4 years). None of the

patients previously underwent RFCA for AF. Mean duration of AF was 65 ± 60 months and the mean number of anti-arrhythmic drugs used was 3.4 ± 1.4 per patient. Mean LA volume index was 42 ± 12 ml/m² and mean LV ejection fraction was $59 \pm 6\%$ as assessed by transthoracic echocardiography. The mean pre-procedural AF burden on 24-hour Holter monitoring was $8 \pm 19\%$. None of the patients had significant valvular heart disease. The procedural end-point of PV isolation was reached in all patients. No major peri-procedural complications occurred.

Table 1. Clinical characteristics of the patient population

	All patients (n=87)	Non- recurrence (n=66)	Recurrence (n=21)	p-value*
Age (years)	55 ± 9	55 ± 9	56 ± 11	0.78
Male gender, n (%)	70 (80)	52 (79)	18 (86)	0.49
Body Surface Area (m ²)	2.1 ± 0.2	2.1 ± 0.2	2.1 ± 0.2	0.93
Duration of AF (months)	65 ± 60	62 ± 59	73 ± 64	0.48
History of cardioversion, n (%)	53 (61)	38 (58)	15 (71)	0.32
History of persistent AF, n (%)	9 (10)	6 (9)	3 (14)	0.50
Number of failed AAD	3.4 ± 1.4	3.3 ± 1.3	3.7 ± 1.4	0.27
Pre-procedural AF burden (%)	8 ± 19	8 ± 18	9 ± 20	0.68
Hypertension, n (%)	37 (43)	27 (41)	10 (48)	0.70
Medication:				
• <i>β-Blocker, n (%)</i>	21 (25)	14 (21)	7 (33)	0.27
• <i>Ca-channel blocker, n (%)</i>	16 (18)	11 (17)	5 (24)	0.46
• <i>Class IC AAD, n (%)</i>	30 (35)	24 (36)	6 (29)	0.49
• <i>Class III AAD, n (%)</i>	51 (60)	38 (58)	13 (62)	0.78
• <i>ACE inhibitor/ATII, n (%)</i>	40 (46)	28 (42)	12 (57)	0.23

AAD = Anti-arrhythmic drugs, AF = atrial fibrillation, ECV = electrocardioversion, FU = follow-up, LA = left atrium, SR = sinus rhythm. * p-value recurrence versus non-recurrence.

After a mean follow-up of 6.6 ± 3.0 months, 66 patients (76%) maintained stable SR (non-recurrence group), whereas 21 patients (24%) had recurrent AF (recurrence group). Baseline clinical and echocardiographic characteristics are reported in Tables 1 and 2, respectively. In the recurrence group significantly larger LV volumes were noted compared to the non-

recurrence group (LV end-diastolic volume index: 54 ± 9 ml/m² versus 48 ± 12 ml/m², $p=0.037$; and LV end-systolic volume index: 23 ± 4 ml/m² versus 20 ± 6 ml/m², $p=0.027$). Importantly, LV systolic function was similar in both groups (LV ejection fraction: $57 \pm 4\%$ versus $59 \pm 6\%$, $p=0.32$). Furthermore, in the recurrence group a significantly higher E-wave velocity (0.75 ± 0.23 m/s versus 0.65 ± 0.14 m/s, $p=0.021$), higher E/E'-ratio (10.1 ± 4.0 versus 8.4 ± 3.1 , $p=0.049$) and higher LA volume index (47 ± 12 ml/m² versus 41 ± 11 ml/m², $p=0.043$) were observed. However, no differences in diastolic function grade were found between both groups, with the majority of the patients showing normal LV filling pattern (Table 2).

Table 2. Echocardiographic characteristics of the patient population

	All patients (n=87)	Non- recurrence (n=66)	Recurrence (n=21)	p-value*
LA maximum volume index (ml/m ²)	42 ± 12	41 ± 11	47 ± 12	0.043
LV end-diastolic volume index (ml/m ²)	50 ± 11	48 ± 12	54 ± 9	0.037
LV end-systolic volume index (ml/m ²)	21 ± 5	20 ± 6	23 ± 4	0.027
LV ejection fraction (%)	59 ± 6	59 ± 6	57 ± 4	0.32
Pulsed wave Doppler:				
• E-wave (m/s)	0.68 ± 0.17	0.65 ± 0.14	0.75 ± 0.23	0.021
• A-wave (m/s)	0.61 ± 0.16	0.61 ± 0.17	0.61 ± 0.12	0.97
• E/A-ratio	1.14 ± 0.35	1.12 ± 0.34	1.21 ± 0.40	0.36
• Deceleration time (s)	252 ± 74	247 ± 70	267 ± 88	0.30
Doppler tissue imaging:				
• E'-wave (cm/s)	8.3 ± 2.5	8.5 ± 2.6	7.8 ± 2.1	0.30
• E/E'-ratio	8.8 ± 3.4	8.4 ± 3.1	10.1 ± 4.0	0.049
Diastolic function grade:				
• Normal, n (%)	55 (63)	43 (65)	12 (57)	0.51
• Gr 1: Impaired relaxation, n (%)	32 (37)	23 (35)	9 (43)	
• Gr 2: Pseudo-normalization, n (%)	0 (0)	0 (0)	0 (0)	
• Gr 3: Restrictive filling pattern, n (%)	0 (0)	0 (0)	0 (0)	

AF = atrial fibrillation, FU = follow-up, Gr = grade, LA = left atrium, LV = left ventricle, SR = sinus rhythm. * p-value recurrence versus non-recurrence.

Natriuretic peptides and AF recurrence after RFCA

Prior to the ablation procedure, blood samples were obtained to measure baseline NT-proANP and NT-proBNP levels. The median level of NT-proANP was 2.69 nmol/L (1.86-3.60) and the median level of NT-proBNP was 90.9 pg/mL (49.9-159.9). No relation was found between baseline NT-proANP and NT-proBNP levels and pre-procedural AF burden assessed by 24-hour Holter monitoring. Baseline NT-proANP and NT-proBNP levels were significantly higher in the recurrence group than in the non-recurrence group (NT-proANP: 3.19 nmol/L [2.55-4.28] versus 2.52 nmol/L [1.69-3.55], $p=0.030$; NT-proBNP: 156.4 pg/mL [64.1-345.3] versus 84.6 pg/mL [43.3-142.7], $p=0.036$) (Figure 1). Cox proportional hazard analyses showed that each 100 pg/mL increase in NT-proBNP level was associated with an approximately 35% increased risk for AF recurrence (unadjusted HR: 1.205, $p=0.029$) (Figure 2). In contrast, each nmol/L increase in NT-proANP level was not significantly associated with a higher risk for AF recurrence (unadjusted HR: 1.204, $p=0.055$) (Figure 2). After correction for age and gender, the prognostic value of NT-proANP to predict AF recurrence improved (HR: 1.292, $p=0.029$) but was lost after correction for LA size and LV size (HR: 1.213, $p=0.088$) (Figure 2). In contrast, NT-proBNP maintained its prognostic value to predict AF recurrence after correcting both for age and gender and for LA size and LV size (HR: 1.390, $p=0.006$; HR: 1.250, $p=0.023$, respectively) (Figure 2). Furthermore, addition of NT-proBNP to a Cox model including LA volume index and LV end-systolic volume index resulted in a significant improvement of the global Chi-square value (7.0 vs 11.7, $p=0.033$), illustrating the incremental value of NT-proBNP over LA size and LV size to predict AF recurrence after RFCA (Figure 3). In contrast, NT-proANP had no incremental value over LA volume index or LV end-systolic volume to predict AF recurrence after RFCA (global Chi-square 7.0 vs 9.9, $p=0.11$) (Figure 3). The c-statistics for each Cox model are shown in table 3.

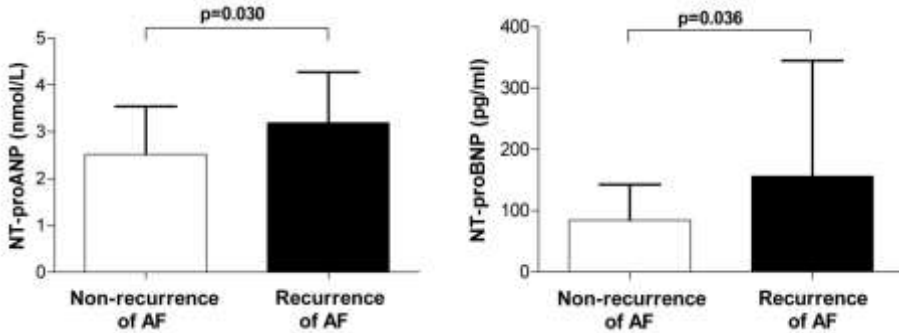


Figure 1. Baseline natriuretic peptide levels in patients with and without recurrence of atrial fibrillation (AF). Bar graphs representing median and 75th percentile of amino-terminal-pro-atrial natriuretic peptide (NT-proANP) and amino-terminal-pro-B-type natriuretic peptide (NT-proBNP) levels measured at baseline in patients with AF recurrence and in non-recurrence patients. Baseline NT-proANP and NT-proBNP levels were significantly higher in patients with recurrence of AF during follow-up compared to non-recurrence patients.

Discussion

The present study investigated the role of natriuretic peptides to predict AF recurrence after RFCA in patients without signs of structural heart disease. The main finding was that pre-procedural NT-proBNP plasma level was an independent predictor of AF recurrence after RFCA. Importantly, NT-proBNP plasma level had an incremental value over echocardiographic parameters to predict the AF recurrence after RFCA.

Conventional echocardiography and AF recurrence after RFCA

Echocardiography is an important tool to identify patients with a high risk for AF recurrence after RFCA. In particular, LA enlargement on echocardiography is a well recognized risk factor for AF recurrence after RFCA.^{4,5,15} In the present study, patients with AF recurrence had significantly larger LA than patients who maintained SR during follow-up. This finding is consistent with other studies.^{4,5,15} Most likely, a large LA size reflects a high extent of atrial remodeling, which is associated with a limited efficacy of RFCA.

Cox proportional hazard analyses of baseline natriuretic peptide levels as predictor of AF recurrence

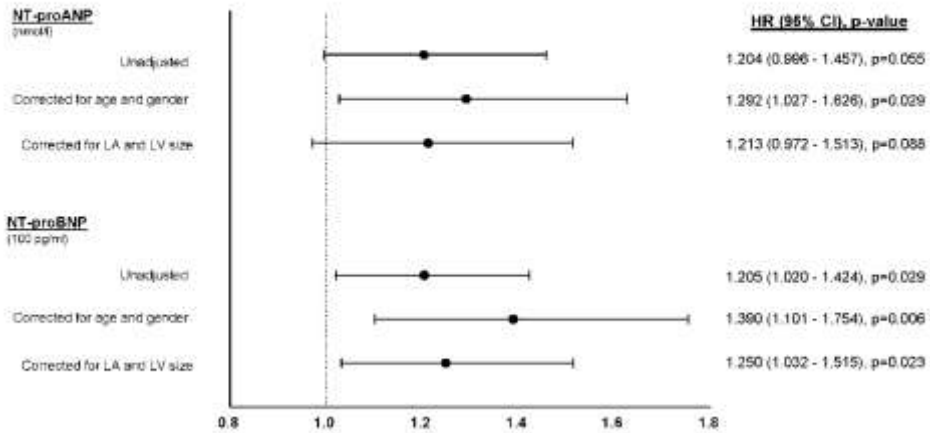


Figure 2. Cox proportional hazard analyses of baseline natriuretic peptide levels as predictor of atrial fibrillation (AF) recurrence. Hazard ratios unadjusted and corrected for age/gender and left atrial (LA) size/left ventricular (LV) size to predict AF recurrence after catheter ablation using baseline natriuretic peptide levels. Left atrial volume index and LV end-diastolic volume index were used to correct for LA and LV size, respectively. NT-proANP = amino-terminal-pro-atrial natriuretic peptide, NT-proBNP = amino-terminal-pro-B-type natriuretic peptide.

In addition to being a marker of structural LA remodeling, LA enlargement is a morphologic marker of chronic elevation in LV filling pressure (i.e. diastolic dysfunction).¹⁶ Atrial fibrillation has been associated with LV diastolic dysfunction previously.¹⁷ Elevated LV filling pressure may result in an elevated LA pressure and, consequentially, in LA dilatation. Accordingly, diastolic dysfunction may induce ultrastructural changes of the atria which facilitate re-entry and play an important role in the progression and perpetuation of AF.^{18,19} In the present study, patients with AF recurrence had a significantly larger LA size, increased E-wave velocity and an increased E/E'-ratio, compared to patients who maintained SR. However, in the present study these diastolic function parameters were within normal range. Moreover, the

majority of patients showed a normal LV filling pattern and the prevalence of diastolic dysfunction grade 1 was similar in patients with and without AF recurrence. Therefore, at an early stage of the underlying disease, conventional echocardiography may not be sensitive enough to identify patients who will develop AF recurrence after RFCA from patients who will not. The use of more sensitive markers of cardiac dysfunction may help to improve risk stratification in patients with apparent “lone” AF and without overt structural heart disease on echocardiography.

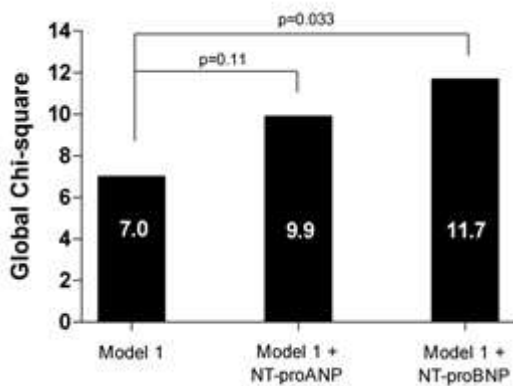


Figure 3. Incremental value of amino-terminal-pro-atrial natriuretic peptide (NT-proANP) and amino-terminal-pro-B-type natriuretic peptide (NT-proBNP) to predict atrial fibrillation (AF) recurrence after ablation. Bar graph illustrating the change in global Chi-square value by the addition of NT-proANP or NT-proBNP to a Cox proportional hazard model comprising left atrial volume index

and left ventricular end-diastolic volume index (Model 1). The addition of NT-proANP to the model did not result in significant improvement of the global Chi-square. In contrast, the addition of NT-proBNP significantly improved the global Chi-square, thereby demonstrating the incremental value of NT-proBNP to predict AF recurrence after RFCA. Natriuretic peptides and AF recurrence after RFCA

The relation between natriuretic peptide levels and AF has been well recognized.^{8-10,20,21} Previous studies have demonstrated that natriuretic peptide levels are elevated in patients with AF,⁸⁻¹⁰ and that natriuretic peptides are a predictor of new-onset AF in the general population.^{20,21} Nevertheless, the role of natriuretic peptides to identify patients with a high risk for AF recurrence after RFCA remains controversial. Although several studies have demonstrated the value of natriuretic peptides to predict AF recurrence after RFCA,^{22,23} other

studies concluded that natriuretic peptides are merely a marker of AF burden.²⁴⁻²⁶ However, most studies comprised a small number of patients and were performed without regard of the presence of AF during blood sampling. This is important because the presence of AF has a large impact on natriuretic peptide levels and can potentially limit its prognostic value.^{8,27} To minimize this potential effect in the present study, only samples acquired during SR were analyzed. After statistical correction for known determinants of natriuretic peptide levels as well as for echocardiographic risk factors for AF recurrence, NT-proBNP was found to be a strong predictor of AF recurrence after RFCA. In contrast, NT-proANP levels were only predictive for AF recurrence after correction for age and gender. These results most likely reflect the different sensitivities of the NT-proANP and NT-proBNP release mechanisms to the primary process causing AF.²⁸ Furthermore, the present study demonstrated that baseline NT-proBNP had an additional value to baseline echocardiographic parameters to predict AF recurrence after RFCA. Most likely, NT-proBNP allows detection of subtle cardiac dysfunction/conditions that limit the efficacy of RFCA for AF and may not be detected by conventional echocardiography alone.

Table 3. Cox proportional hazards models

	C-statistic	95% confidence interval
Model 1	0.719	0.601-0.836
Model 1 + NT-proANP	0.763	0.661-0.864
Model 1 + NT-proBNP	0.762	0.647-0.877

Model 1: Left atrial maximum volume index + left ventricular end-diastolic volume index. NT-proANP = amino-terminal-pro-atrial natriuretic peptide, NT-proBNP = amino-terminal-pro-B-type natriuretic peptide

Clinical implications

Pre-procedural assessment of NT-proBNP in addition to echocardiography can be used to identify patients with a high risk for AF recurrence after RFCA. In

patients with paroxysmal AF and preserved LV systolic function, NT-proBNP levels may provide insight into the presence and severity of an underlying cardiac dysfunction/condition that may not be detected by echocardiography. If further validated, this information may be used during pre-procedural consultation to better inform patients about their risk for AF recurrence after RFCA. Furthermore, in patients with high NT-proBNP levels, the creation of a more extensive lesion set could be considered in order to improve the outcome of the procedure. Finally, high NT-proBNP levels should raise the **electrophysiologist's suspicion on the presence of a** potentially treatable underlying condition. In addition, assessment of NT-proBNP is easy and tests are widely available.

Limitations

Some limitations of the present study should be acknowledged. First, detection of AF recurrence after RFCA was based on ECG recordings acquired on a regular basis and/or 24-hour Holter registration. Importantly, patients were encouraged to obtain an ECG registration when experiencing palpitations in order to confirm AF as the cause of these complaints. Nevertheless, asymptomatic episodes may have been missed. Second, to minimize the confounding effect of heart rhythm on natriuretic peptide levels, a selected population, comprising only patients with paroxysmal AF that were in SR during pre-procedural blood sampling, has been studied. Third, the present study comprised a relatively small group of patients. Therefore only a limited number of variables could be incorporated into the multivariable analyses. To create a valid risk stratification system, the present findings need to be validated in a larger group of patients including a risk reclassification analysis. Fourth, the continuation and discontinuation of anti-arrhythmic drugs during

follow-up was at the discretion of the physician and was therefore non-standardized.

Conclusion

In patients without signs of overt structural heart disease, baseline NT-proBNP plasma level obtained during SR is an independent predictor of AF recurrence after RFCA. Plasma levels of NT-proBNP may allow detection of subtle cardiac dysfunction/conditions that may not be detected by echocardiography alone.

References

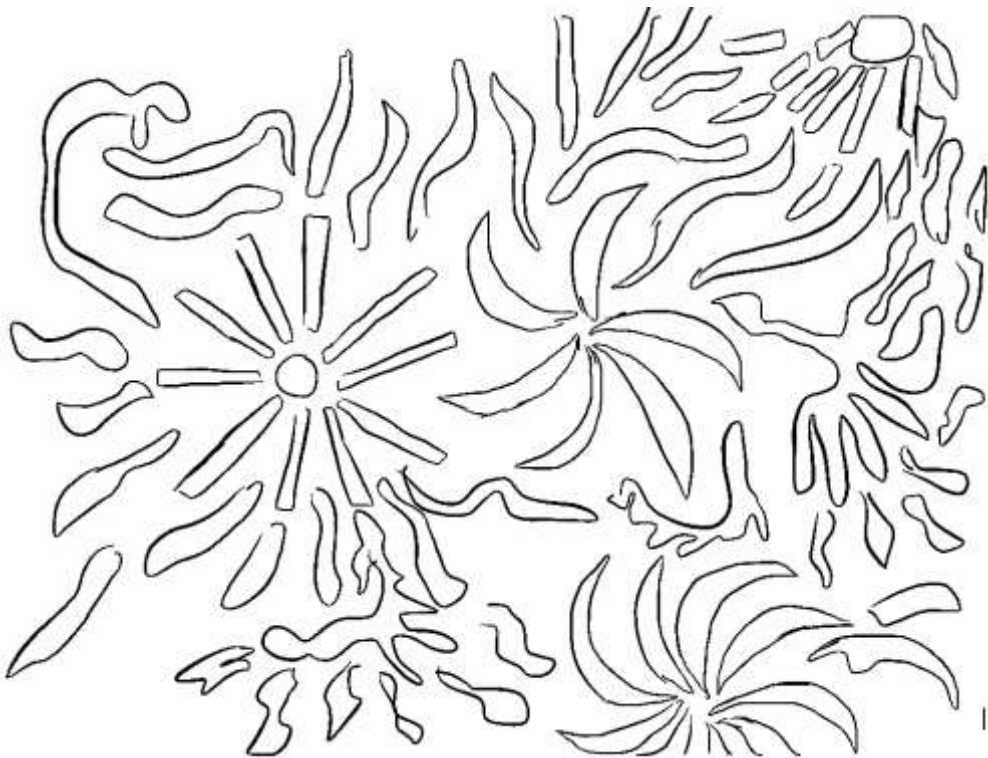
1. Calkins H, Brugada J, Packer DL, Cappato R, Chen SA, Crijns HJ, Damiano RJ, Jr., Davies DW, Haines DE, Haissaguerre M, Iesaka Y, Jackman W, Jais P, Kottkamp H, Kuck KH, Lindsay BD, Marchlinski FE, McCarthy PM, Mont JL, Morady F, Nademanee K, Natale A, Pappone C, Prystowsky E, Raviele A, Ruskin JN, Shemin RJ HRS/EHRA/ECAS expert consensus statement on catheter and surgical ablation of atrial fibrillation: recommendations for personnel, policy, procedures and follow-up. A report of the Heart Rhythm Society (HRS) Task Force on Catheter and Surgical Ablation of Atrial Fibrillation developed in partnership with the European Heart Rhythm Association (EHRA) and the European Cardiac Arrhythmia Society (ECAS); in collaboration with the American College of Cardiology (ACC), American Heart Association (AHA), and the Society of Thoracic Surgeons (STS). Endorsed and approved by the governing bodies of the American College of Cardiology, the American Heart Association, the European Cardiac Arrhythmia Society, the European Heart Rhythm Association, the Society of Thoracic Surgeons, and the Heart Rhythm Society. *Europace* 2007;9:335-379.
2. Cappato R, Calkins H, Chen SA, Davies W, Iesaka Y, Kalman J, Kim YH, Klein G, Packer D, Skanes A Worldwide survey on the methods, efficacy, and safety of catheter ablation for human atrial fibrillation. *Circulation* 2005;111:1100-1105.
3. Vasamreddy CR, Lickfett L, Jayam VK, Nasir K, Bradley DJ, Eldadah Z, Dickfeld T, Berger R, Calkins H Predictors of recurrence following catheter ablation of atrial fibrillation using an irrigated-tip ablation catheter. *J Cardiovasc Electrophysiol* 2004;15:692-697.
4. Berruezo A, Tamborero D, Mont L, Benito B, Tolosana JM, Sitges M, Vidal B, Arriagada G, Mendez F, Matiello M, Molina I, Brugada J Pre-procedural predictors of atrial fibrillation recurrence after circumferential pulmonary vein ablation. *Eur Heart J* 2007;28:836-841.
5. Hof I, Chilukuri K, Rbab-Zadeh A, Scherr D, Dalal D, Nazarian S, Henrikson C, Spragg D, Berger R, Marine J, Calkins H Does left atrial volume and pulmonary venous anatomy predict the outcome of catheter ablation of atrial fibrillation? *J Cardiovasc Electrophysiol* 2009;20:1005-1010.
6. Chen MS, Marrouche NF, Khaykin Y, Gillinov AM, Wazni O, Martin DO, Rossillo A, Verma A, Cummings J, Erciyes D, Saad E, Bhargava M, Bash D, Schweikert R, Burkhardt D, Williams-Andrews M, Perez-Lugones A, Abdul-Karim A, Saliba W, Natale A Pulmonary vein isolation for the treatment of atrial fibrillation in patients with impaired systolic function. *J Am Coll Cardiol* 2004;43:1004-1009.
7. Levin ER, Gardner DG, Samson WK Natriuretic peptides. *N Engl J Med* 1998;339:321-328.
8. Knudsen CW, Omland T, Clopton P, Westheim A, Wu AH, Duc P, McCord J, Nowak RM, Hollander JE, Storrow AB, Abraham WT, McCullough PA, Maisel A Impact of atrial fibrillation on the diagnostic performance of B-type natriuretic peptide concentration in dyspneic patients: an analysis from the breathing not properly multinational study. *J Am Coll Cardiol* 2005;46:838-844.
9. Wozakowska-Kaplon B Effect of sinus rhythm restoration on plasma brain natriuretic peptide in patients with atrial fibrillation. *Am J Cardiol* 2004;93:1555-1558.
10. Ellinor PT, Low AF, Patton KK, Shea MA, Macrae CA Discordant atrial natriuretic peptide and brain natriuretic peptide levels in lone atrial fibrillation. *J Am Coll Cardiol* 2005;45:82-86.
11. Fuster V, Ryden LE, Cannom DS, Crijns HJ, Curtis AB, Ellenbogen KA, Halperin JL, Le Heuzey JY, Kay GN, Lowe JE, Olsson SB, Prystowsky EN, Tamargo JL, Wann S, Smith SC, Jr., Jacobs AK, Adams CD, Anderson JL, Antman EM, Hunt SA, Nishimura R, Ornato JP, Page RL, Riegel B, Priori SG, Blanc JJ, Budaj A, Camm AJ, Dean V, Deckers JW, Despres C, Dickstein K, Lekakis J, McGregor K, Metra M, Morais J, Osterspey A, Zamorano JL ACC/AHA/ESC 2006 guidelines for the management of patients with atrial fibrillation--

- executive summary: a report of the American College of Cardiology/American Heart Association Task Force on Practice Guidelines and the European Society of Cardiology Committee for Practice Guidelines (Writing Committee to Revise the 2001 Guidelines for the Management of Patients With Atrial Fibrillation). *J Am Coll Cardiol* 2006;48:854-906.
12. Lang RM, Bierig M, Devereux RB, Flachskampf FA, Foster E, Pellikka PA, Picard MH, Roman MJ, Seward J, Shanewise JS, Solomon SD, Spencer KT, Sutton MS, Stewart WJ Recommendations for chamber quantification: a report from the American Society of Echocardiography's Guidelines and Standards Committee and the Chamber Quantification Writing Group, developed in conjunction with the European Association of Echocardiography, a branch of the European Society of Cardiology. *J Am Soc Echocardiogr* 2005;18:1440-1463.
 13. Nagueh SF, Appleton CP, Gillebert TC, Marino PN, Oh JK, Smiseth OA, Waggoner AD, Flachskampf FA, Pellikka PA, Evangelista A Recommendations for the evaluation of left ventricular diastolic function by echocardiography. *J Am Soc Echocardiogr* 2009;22:107-133.
 14. Tops LF, Bax JJ, Zeppenfeld K, Jongbloed MR, van der Wall EE, Schalij MJ Effect of radiofrequency catheter ablation for atrial fibrillation on left atrial cavity size. *Am J Cardiol* 2006;97:1220-1222.
 15. Shin SH, Park MY, Oh WJ, Hong SJ, Pak HN, Song WH, Lim DS, Kim YH, Shim WJ Left atrial volume is a predictor of atrial fibrillation recurrence after catheter ablation. *J Am Soc Echocardiogr* 2008;21:697-702.
 16. Lester SJ, Tajik AJ, Nishimura RA, Oh JK, Khandheria BK, Seward JB Unlocking the mysteries of diastolic function: deciphering the Rosetta Stone 10 years later. *J Am Coll Cardiol* 2008;51:679-689.
 17. Jais P, Peng JT, Shah DC, Garrigue S, Hocini M, Yamane T, Haissaguerre M, Barold SS, Roudaut R, Clementy J Left ventricular diastolic dysfunction in patients with so-called lone atrial fibrillation. *J Cardiovasc Electrophysiol* 2000;11:623-625.
 18. Li D, Shinagawa K, Pang L, Leung TK, Cardin S, Wang Z, Nattel S Effects of angiotensin-converting enzyme inhibition on the development of the atrial fibrillation substrate in dogs with ventricular tachypacing-induced congestive heart failure. *Circulation* 2001;104:2608-2614.
 19. Alessie M, Ausma J, Schotten U Electrical, contractile and structural remodeling during atrial fibrillation. *Cardiovasc Res* 2002;54:230-246.
 20. Asselbergs FW, van den Berg MP, Bakker SJ, Signorovitch JE, Hillege HL, van Gilst WH, van Veldhuisen DJ N-terminal pro B-type natriuretic peptide levels predict newly detected atrial fibrillation in a population-based cohort. *Neth Heart J* 2008;16:73-78.
 21. Patton KK, Ellinor PT, Heckbert SR, Christenson RH, Defilippi C, Gottdiener JS, Kronmal RA N-terminal pro-B-type natriuretic peptide is a major predictor of the development of atrial fibrillation: the Cardiovascular Health Study. *Circulation* 2009;120:1768-1774.
 22. Hwang HJ, Son JW, Nam BH, Joung B, Lee B, Kim JB, Lee MH, Jang Y, Chung N, Shim WH, Cho SY, Kim SS Incremental predictive value of pre-procedural N-terminal pro-B-type natriuretic peptide for short-term recurrence in atrial fibrillation ablation. *Clin Res Cardiol* 2009;98:213-218.
 23. Shin DI, Deneke T, Gorr E, Anders H, Buenz K, Paesler M, Horlitz M Predicting successful pulmonary vein isolation in patients with atrial fibrillation by brain natriuretic Peptide plasma levels. *Indian Pacing Electrophysiol J* 2009;9:241-246.
 24. Yamada T, Murakami Y, Okada T, Yoshida N, Toyama J, Yoshida Y, Tsuboi N, Inden Y, Hirai M, Murohara T Plasma brain natriuretic peptide level after radiofrequency catheter ablation of paroxysmal, persistent, and permanent atrial fibrillation. *Europace* 2007;9:770-774.

25. Date T, Yamane T, Inada K, Matsuo S, Miyanaga S, Sugimoto K, Shibayama K, Taniguchi I, Mochizuki S Plasma brain natriuretic peptide concentrations in patients undergoing pulmonary vein isolation. *Heart* 2006;92:1623-1627.
26. Sacher F, Corcuff JB, Schraub P, Le B, V, Georges A, Jones SO, Lafitte S, Bordachar P, Hocini M, Clementy J, Haissaguerre M, Bordenave L, Roudaut R, Jais P Chronic atrial fibrillation ablation impact on endocrine and mechanical cardiac functions. *Eur Heart J* 2008;29:1290-1295.
27. Rossi A, Enriquez-Sarano M, Burnett JC, Jr., Lerman A, Abel MD, Seward JB Natriuretic peptide levels in atrial fibrillation: a prospective hormonal and Doppler-echocardiographic study. *J Am Coll Cardiol* 2000;35:1256-1262.
28. Wozakowska-Kaplon B ANP and B-type peptide: Twins or kins? A different predictive value in atrial fibrillation Natriuretic peptides: Useful biomarkers in predicting the possibility of restoration and maintenance of sinus rhythm in patients with atrial fibrillation undergoing cardioversion? (IJC-D-09-01605). *Int J Cardiol* 2009.

Part II

Imaging to facilitate ablation of complex arrhythmias



Chapter 8

Intracardiac Echocardiography

Dennis W. den Uijl, Laurens F. Tops, Nico R. van de Veire, Jeroen J. Bax.

Cardiovascular Catheterisation and Intervention. *Chapter 40: Intracardiac echocardiography.*
Informa Healthcare USA, New York, NY, USA.



Introduction

In the past years intracardiac echocardiography (ICE) has emerged as a valuable imaging tool for interventional and electrophysiological procedures. Intracardiac echocardiography allows real-time visualization of important anatomical structures that cannot be visualized on fluoroscopy, and is not associated with radiation exposure to the patient and operator. This imaging modality is used to guide and monitor interventional procedures and for early detection of complications. Importantly, as an alternative to transesophageal echocardiography (TEE), ICE can be performed without general anesthesia. In this chapter, the basic principles and clinical applications of ICE will be discussed.

Anatomic considerations

Intracardiac echocardiography is generally performed from within the right atrium or the right ventricle. The images acquired with ICE should therefore be interpreted from that perspective. Depending on the position and direction of the ultrasound catheter, all large cardiac structures, including the atria, ventricles, atrioventricular and semilunar valves, coronary sinus and pericardium can be visualized with ICE. Awareness of the orientation of the scanning plane and a good understanding of the 3-dimensional (3D) cardiac anatomy are essential for a correct interpretation.

Equipment

Currently, two different ICE technologies are available. The first approach utilizes a mechanical ultrasound tipped catheter which can also be used for endovascular echocardiography. The second uses an electronic ultrasound catheter that is equipped with a phased array transducer at its tip. Both are

introduced using a retrograde femoral venous approach after the application of local anesthesia. The mechanical or rotational system uses a 9 French catheter equipped with a 9 MHz single-element transducer incorporated at its tip (Ultra ICE™, Boston Scientific, San Jose, CA). A piezoelectric crystal inside the transducer is rotated at 1800 rpm in the radial dimension and provides a 2-dimensional (2D) 360° scanning plane, oriented perpendicular to the catheter shaft. To adjust the imaging plane, the catheter can be withdrawn or advanced inside the heart. To prepare the catheter for use, the system has to be filled with 3-5 ml sterile water and connected to a dedicated ultrasound machine (iLab™ System, Galaxy® System, Galaxy2™ system or Clearview® Ultra™ system, Boston Scientific).

The electronic system uses an 8, 9 or 10 French ultrasound catheter equipped with a 64-element phased array transducer located at its tip (ACUSON Acunav™, Siemens Medical Solutions, Mountain View, CA and ViewFlex™, St. Jude Medical, West Berlin, NJ) that generates a 90° wedge shaped 2D scanning plane, oriented parallel to the catheter shaft. The high resolution transducer can be used at multiple frequencies (5-10 MHz) thereby allowing depth control and enhancement of tissue penetration to a maximum of 15 cm. The flexible catheter can be rotated around its axis, and the tip of the catheter can be deflected by manipulating the steering mechanism at the handle of the catheter. The flexibility and maneuverability of the catheter enable the operator to position it inside the right ventricle or coronary sinus. In this way, additional views can be obtained, that cannot be acquired from the right atrium. The phased array catheter is connected to a dedicated ultrasound machine (Sequoia™, Cypress™, CV70™, Siemens Medical Solutions and ViewMate®, St. Jude Medical).

Several important differences between the two ICE technologies exist. The phased array catheter allows adjustment of the ultrasound frequency,

thereby enabling depth control. Furthermore, the phased array catheter has Doppler capabilities, allowing measurement of hemodynamic and physiologic variables, and has superior flexibility compared to the rotational catheter. The advantages of rotational ICE include a 360° scanning plane instead of 90° and the considerably lower costs. In daily clinical practice, phased array ICE is the most commonly used technology in the cardiac catheterization laboratory. The focus of the present chapter will be on phased array ICE, while, mechanical intravascular ultrasound is reviewed in Chapter 28.

Fundamentals

Intracardiac echocardiography can be used to visualize nearly all cardiac structures.¹ However, unlike for transthoracic echocardiography and TEE, there are no widely accepted standard views for ICE. In the following paragraphs, a clinically oriented guide for catheter manipulation and visualization of the various cardiac structures is provided.

Intracardiac echocardiography is generally performed under conscious sedation. Using local anesthesia and a femoral vein approach, the ultrasound catheter is inserted through the inferior vena cava into the right atrium. While standing at the right side of the patient, the operator can change the orientation of the ultrasound beam by advancing or withdrawing the catheter and by rotating it around its axis. In this chapter, rotation of the ultrasound catheter away from the operator is called clockwise rotation, whereas rotation towards the operator is referred to as counter-clockwise rotation. The orientation of the ultrasound beam can also be altered by deflecting the tip of the ultrasound catheter in two orthogonal planes (anterior-posterior, left-right) through manipulation of the two steering knobs at the handle of the catheter.

Even though images acquired with ICE are quite similar to TEE, the large freedom of ultrasound beam orientation can easily cause a sense of

disorientation to the inexperienced operator. In order to gain and regain orientation, a 'home view' position is defined which can be used as the starting point for all catheter manipulations. In this chapter 'home view' position is used as the starting point from which all catheter manipulations are described. To reach this position, the ultrasound catheter is positioned in the mid-right atrium with the control knobs in a neutral position. The resulting image shows the right atrium, tricuspid valve and right ventricle (Figure 1, panel A). The operator can use these and other anatomical landmarks to maintain orientation during catheter manipulation. To further improve the operator's orientation, a marker is present on the ultrasound screen corresponding to the inferior portion of the ultrasound beam.

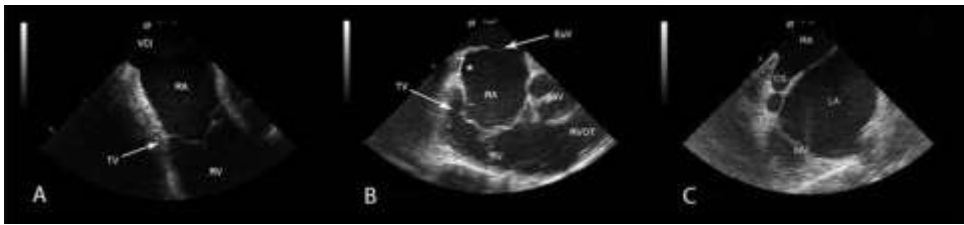


Figure 1. Panel A: 'Home view' position: right atrium (RA), right ventricle (RV), tricuspid valve (TV) and vena cava inferior (VCI). Panel B: aortic valve (AoV), cavotricuspid isthmus (*), Eustachian ridge/valve (EuV), right ventricular outflow tract (RVOT). Panel C: interatrial septum, left atrium (LA), coronary sinus (CS) and mitral valve (MV).

Right-Sided Structures

Starting from 'home view' position and slightly withdrawing the catheter into the inferior right atrium, the Eustachian ridge can be visualized (Figure 1, panel B). The tissue between the Eustachian ridge and the tricuspid valve is known as the cavotricuspid isthmus which is targeted during catheter ablation for atrial flutter. By advancing the catheter back in 'home view' position and rotating it counter-clockwise the crista terminalis and right atrial appendage are visualized. Clockwise rotation will first bring back 'home view' and will then

reveal the right ventricular outflow tract, the pulmonary artery and the ascending aorta (Figure 1, panel B).

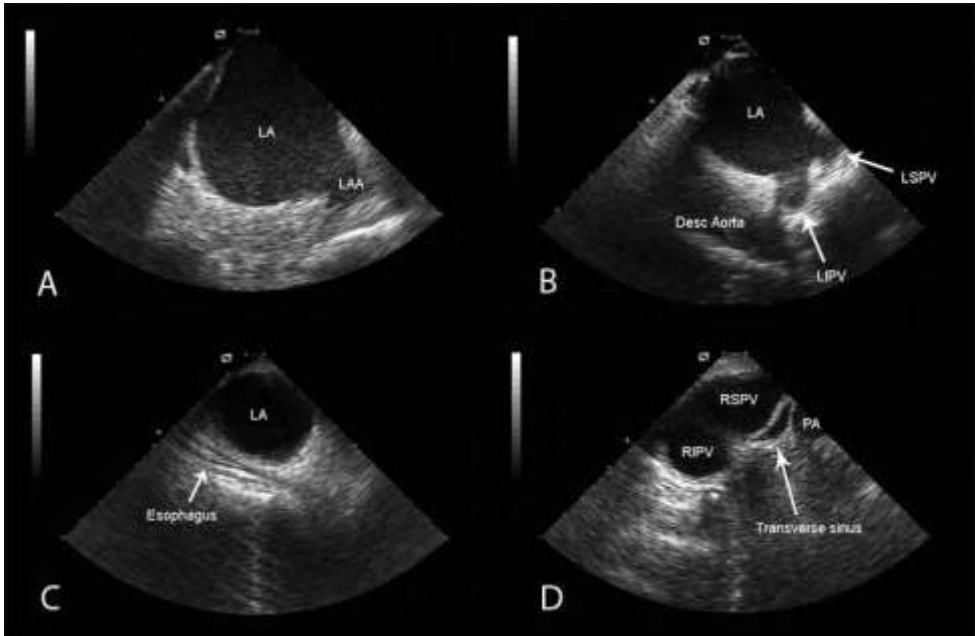


Figure 2. Panel A: Left atrium (LA) and left atrial appendage (LAA). Panel B: Descending aorta (Desc Aorta), LA, left superior pulmonary vein (LSPV) and left inferior pulmonary vein (LIPV). Panel C: Esophagus and posterior LA wall. Panel D: Pulmonary artery (PA), right inferior pulmonary vein (RIPV), right superior pulmonary vein (RSPV) and transverse sinus.

Left-Sided Structures

Clockwise rotation of the ultrasound catheter from ‘home view’ position, past the right ventricle and right ventricular outflow tract, provides a view on the left atrium, mitral valve, the interatrial septum and the coronary sinus (Figure 1, panel C). By gently deflecting the catheter tip in the left direction, the left atrial appendage can be seen (Figure 2, panel A). From this view, clockwise rotation will reveal the left-sided pulmonary veins (Figure 2, panel B). The left inferior pulmonary vein is visualized at the inferior portion of the ultrasound beam and the left superior pulmonary vein at the superior portion. In case of difficulty to

distinguish between the left superior pulmonary vein and the left atrial appendage, Doppler flow measurements can be used to differentiate between the two structures. When further rotating clockwise, the posterior left atrial wall and the esophagus can be visualized (Figure 2, panel C). Eventually, continued clockwise rotation will provide a cross-sectional view of the right-sided pulmonary veins and the right pulmonary artery (Figure 2, panel D). Similar to the left pulmonary veins, the right inferior pulmonary vein is visualized at the inferior portion of the ultrasound beam and the right superior pulmonary vein at the superior portion.

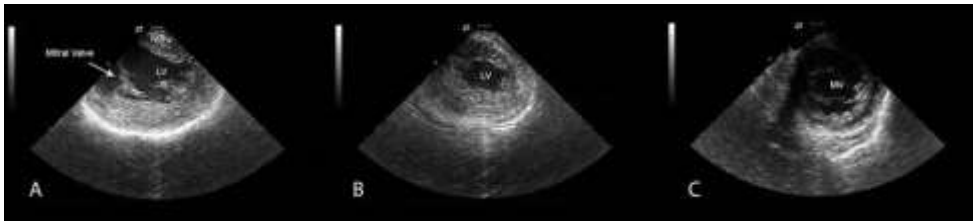


Figure 3. Panel A: Long axis view of the left ventricle (LV): interventricular septum (IVS), mitral valve (MV). Panel B: Short axis view at the apical level. Panel C: Short axis view at the basal level.

To acquire a long axis view of the left ventricle and mitral valve from 'home view', the catheter is withdrawn slightly into the inferior right atrium and the tip of the catheter is deflected in the anterior direction. By advancing the catheter through the tricuspid valve into the right ventricle and rotating the catheter clockwise, the interventricular septum and left ventricle appear (Figure 3, panel A). This long axis view can be very useful to detect pericardial effusion during interventional procedures. From the long axis view, a short axis view of the left ventricle can be acquired by deflecting the tip of the catheter in the left or right direction (Figure 3, panel B). Advancing or withdrawing the catheter will result a more apical or basal short axis views (Figure 3, panel C).

Indications and clinical applications

Intracardiac echocardiography can be used in a wide variety of diagnostic and interventional procedures. These procedures are summarized in Table 1 and will be reviewed in the following paragraphs.

Table 1. Applications of Intracardiac Echocardiography during Interventional and Electrophysiological Procedures

<ul style="list-style-type: none"> • Detection of intracardiac thrombus • Closure of atrial septal defect • Transseptal puncture • Electrophysiological procedures <ul style="list-style-type: none"> ○ Atrial fibrillation ablation ○ Complex atrial flutter ablation ○ Ventricular tachycardia ablation ○ Left ventricular lead placement in cardiac resynchronization therapy • Other interventional procedures <ul style="list-style-type: none"> ○ Biopsy of an intracardiac tumor ○ Left atrial appendage closure ○ Closure of ventricular septal defect ○ Alcohol septum ablation in hypertrophic obstructive cardiomyopathy ○ Mitral valve balloon valvuloplasty ○ Percutaneous valve procedures

Detection of Intracardiac Thrombus

Patients undergoing a left-sided interventional procedure are at a high risk for systemic embolism.^{2,3} Intracardiac echocardiography can facilitate a safe left-sided procedure by excluding intracardiac thrombus inside the left atrial appendage, left atrium and left ventricle.⁴ Furthermore, ICE can be used to assess the presence of spontaneous contrast, thereby identifying patients at a high risk for thrombus formation.⁵ Furthermore, ICE can help to detect the formation of thrombi at an early phase and allow for treatment prior to the occurrence of embolic events.^{6,7}

The efficacy of TEE to detect intracardiac thrombus has been established by the ACUTE trial (Assessment of Cardioversion Using Transesophageal Echocardiography).⁸ Even though ICE provides high quality images comparable to TEE, only few studies have compared the sensitivity of the two imaging modalities for the detection of intracardiac thrombus. The ICE-CHIP study (IntraCardiac Echocardiography guided Cardioversion to Help Interventional Procedures) was designed to address this issue.⁹ The preliminary results of the ICE-CHIP study show that ICE has a similar sensitivity for the detection of spontaneous contrast, as compared to TEE.¹⁰ In 100 patients with atrial fibrillation, spontaneous contrast of the left atrium was seen in 50% on ICE and in 55% on TEE ($p=NS$) whereas spontaneous contrast of the left atrial appendage was seen in 24% on ICE and in 34% on TEE ($p=NS$). However, the results on thrombus detection from the ICE-CHIP study are not yet available. Therefore, more studies are needed to determine the exact value of ICE for the detection of intracardiac thrombi.

Closure of Atrial Septal Defect

Percutaneous transcatheter device closure of atrial septal defect or patent foramen ovale has proven to be a safe and effective alternative to open heart surgery.^{11,12} While percutaneous closure of patent foramen ovale may be performed under fluoroscopy guidance only, closing procedures of atrial septal defect are typically guided by TEE and fluoroscopy. However, ICE does not require general anesthesia, and may provide similar images as TEE.^{13,14} It has been shown that the use of ICE during transcatheter device closure may result in a reduction of fluoroscopy time (9.5 ± 1.6 minutes vs. 6.0 ± 1.7 minutes, $p<0.0001$),¹³ procedure length (47 ± 8 minutes vs. 35 ± 6 minutes, $p<0.001$) and catheterization laboratory occupation (92 ± 18 minutes vs. 50 ± 12 minutes, $p<0.001$) compared to TEE guided interventions.¹⁵ Importantly, the high costs

of an ICE catheter may be balanced by the need for general anesthesia during TEE guided procedures.¹⁶

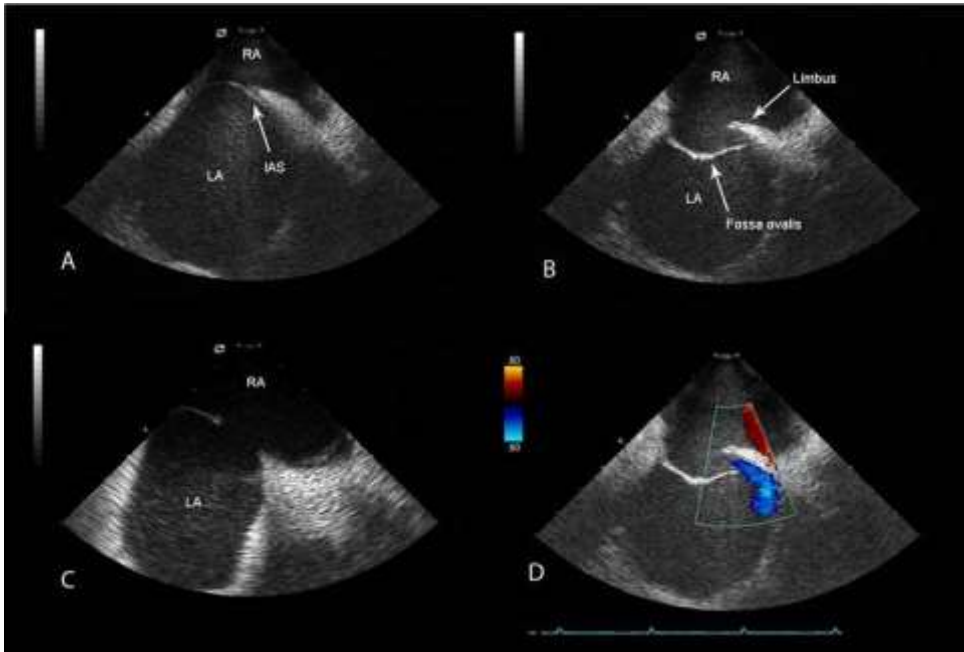


Figure 4. Panel A: Interatrial septum (IAS), left atrium (LA) and right atrium (RA). Panel B: During a Valsalva maneuver the patent foramen ovale (PFO) is revealed. Panel C: A large type II atrial septal defect (delineated by the two markers). Panel D: Doppler flow delineates the flow across PFO during a Valsalva maneuver.

To guide the placement of a transcatheter closure device, the **ultrasound catheter is positioned in the 'home view' position and is rotated clockwise to visualize the interatrial septum and fossa ovalis (Figure 4, panel A, B and C).** By using Doppler capacities, the flow between the left and right atrium can be visualized and quantified (Figure 4, panel D). A guiding wire is then placed through the atrial septal defect and inside the left atrium. Subsequently, the catheter that contains the closure device is advanced through the atrial septal defect and the left-sided portion of the occluder is deployed. After this step, the position of the device against the interatrial

septum is carefully evaluated before deploying the right-sided portion of the occluder in order to avoid malposition and the associated risk of migration of the device (Figure 5, panel A). Once the operator is convinced that the position is correct, the right-sided portion of the occluder is deployed (Figure 5, panel B). Once again the position and the stability of the device are checked and subsequently the occluder is released.

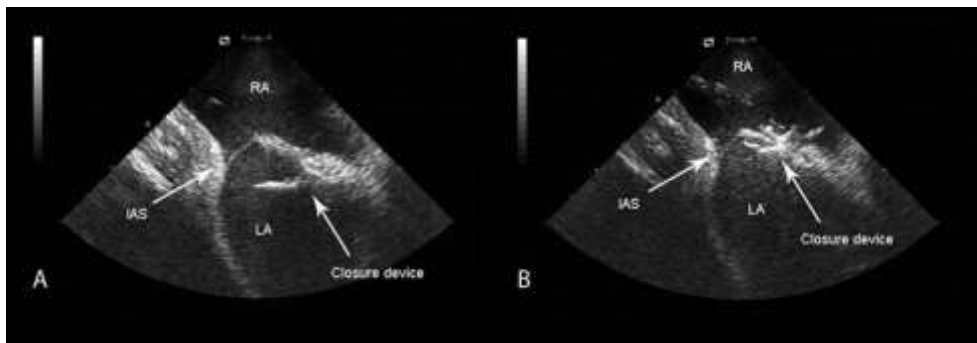


Figure 5. Panel A: A biodegradable closure device is inserted across the interatrial septum (IAS) inside the left atrium (LA). Subsequently, the left-sided occluder is deployed. (RA = right atrium). Panel B: After confirmation of the position of the device, the right-sided occluder is also deployed.

Transseptal Puncture

A transseptal puncture provides antegrade access to the left atrium and left ventricle during left-sided interventional procedures as an alternative to a retrograde approach through the aortic valve and mitral valve. However, a transseptal puncture can result in serious complications, such as aortic perforation, pericardial tamponade and perforation of the inferior vena cava.¹⁷ The fossa ovalis is considered to be the safest site to perform a transseptal puncture in order to avoid these complications. Intracardiac echocardiography allows excellent visualization of the fossa ovalis and can be used to detect a patent foramen ovale or monitor the transseptal puncture.¹⁸ At present, no

prospective studies have addressed the question whether ICE may improve the safety of transseptal punctures.

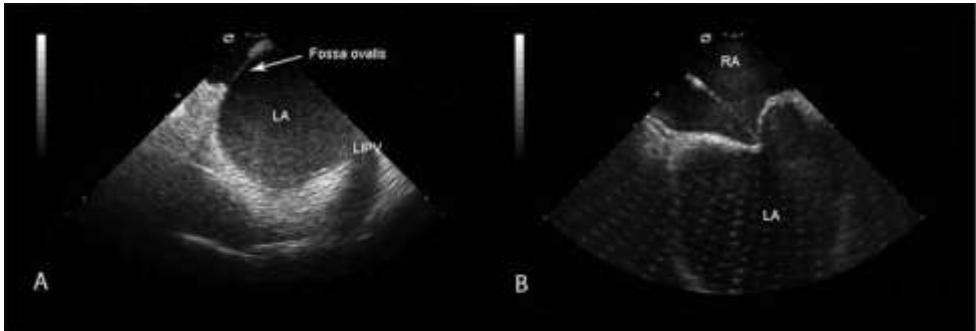


Figure 6. Panel A: Fossa ovalis, left atrium (LA), left inferior pulmonary vein (LIPV). Panel B: Tenting of the transseptal sheath against the fossa ovalis. (RA = right atrium).

To visualize the interatrial septum, the catheter is gently rotated **clockwise from 'home view' position**. The interatrial septum consists of a thicker part (limbus) and thin part (fossa ovalis) (Figure 6, panel A). To detect a patent foramen ovale, saline/contrast is injected through the femoral vein inside the right atrium and the patient is instructed to perform the Valsalva maneuver (Figure 7, panel A). In the presence of a patent foramen the contrast will cross the interatrial septum, into the left atrium (Figure 7, panel B). In the absence of a patent foramen ovale, a transseptal sheath with a concealed Brockenbrough transseptal needle is inserted through the femoral vein inside the right atrium. Using fluoroscopy and ICE, the transseptal sheath is positioned against the fossa ovalis. In case of a stable position of the sheath **against the fossa ovalis, a 'tenting' phenomenon can be seen on ICE** (Figure 6, panel B). The transseptal puncture can now be performed by pushing the needle out from the sheath, through the fossa ovalis. Successful transseptal puncture can be confirmed on ICE by injecting saline/contrast through the needle inside the left atrium.

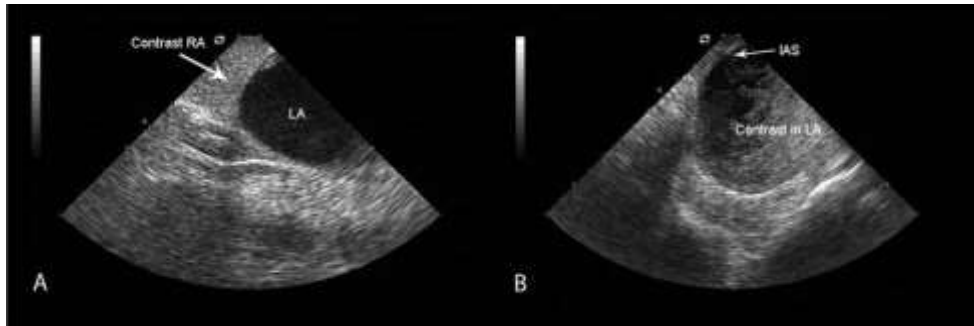


Figure 7. Panel A: Contrast inside the right atrium (RA) during Valsalva, in a patient with a closed foramen ovale. Panel B: Contrast crosses the interatrial septum (IAS) from the RA to the left atrium (LA) during Valsalva in a patient with a patent foramen ovale.

Electrophysiological Procedures

Intracardiac echocardiography has become an important imaging tool during electrophysiological procedures. In addition to thrombus detection and guidance of a transseptal puncture, ICE can be used to identify key anatomical structures to facilitate complex procedures like atrial fibrillation ablation and atrial flutter ablation.¹⁹⁻²¹ Intracardiac echocardiography can visualize the exact location of the mapping catheter and confirm stable contact of the catheter against the myocardium. Moreover, ICE can be used to visualize morphological changes in the myocardium, such as increased echo density, wall thickening and crater formation as a sign of effective lesion formation,²² and the development of micro bubbles as a sign of tissue heating and potential char formation.^{23,24} In the following paragraphs, the specific role of ICE in various electrophysiological procedures will be reviewed.

Atrial fibrillation ablation

Radiofrequency catheter ablation targeting the pulmonary veins is a potential curative treatment option for patients with drug-refractory atrial fibrillation.^{25,26} However, it is associated with long procedure times and a small risk for severe

complications, including pulmonary vein stenosis, systemic embolism, cardiac tamponade and esophagus injury.² Intracardiac echocardiography can facilitate these complex procedures by visualization of the pulmonary veins and monitoring of the location of the ablation catheter, and may help in avoiding complications by visualization of the esophagus and other important surrounding structures.^{19,23,27}

Several studies have shown that pulmonary vein anatomy is highly variable.²⁸⁻³⁰ Application of radiofrequency current inside a pulmonary vein ostium may cause pulmonary vein stenosis and pulmonary hypertension.³¹ Accurate visualization of the pulmonary vein region is therefore of utmost importance to safely and effectively perform catheter ablation. A head-to-head comparison between ICE and multi-slice computed tomography (MSCT) demonstrated that ICE enables accurate assessment of pulmonary vein anatomy and mean ostial diameters (ICE 1.51 ± 0.22 mm vs. MSCT 1.45 ± 0.29 mm, $p=NS$). However, less additional pulmonary veins were detected using ICE, as compared with MSCT (ICE 2 (8%) vs. MSCT 5 (21%)).²⁹ This was confirmed by Jongbloed et al who detected less additional pulmonary veins with ICE, as compared with MSCT (ICE 7 (17%) vs. MSCT 13 (32%)).³⁰ In addition, an underestimation of the ostial diameter on ICE compared to the ostial diameter in superior-inferior direction on MSCT was noted (14.9 ± 4.0 mm vs. 18.4 ± 3.4 mm, $p<0.01$).³⁰ This finding suggests the need for 3D imaging to accurately visualize the shape and dimensions of the pulmonary vein ostia. Nevertheless, in a group of 259 patients, Marrouche et al demonstrated that anatomical guidance of radiofrequency catheter ablation with ICE is both safe and effective.²³ Importantly, the use of ICE in addition to a circular catheter resulted in an improved outcome compared to a circular catheter alone.²³

The esophagus and left atrial posterior wall are very closely related. With the use of ICE, Ren and colleagues demonstrated that the mean distance

between the left atrial posterior wall and the esophagus was 5.8 ± 1.2 mm (range 3.2-10.1 mm) and that the left atrial posterior wall and the esophagus were contiguous over a mean length of 36.0 ± 7.7 mm (range 18-59 mm).²⁷ As a consequence, the temperature inside the esophagus may increase significantly during left atrial ablation.³² Heating of the esophagus can result in esophageal injury varying from transient erythematous changes to tissue necrosis and the development of an atrioesophageal fistula.^{27,33,34} While monitoring the relation between the esophagus and the ablation catheter with ICE, the ablation power and duration can be adjusted in order to reduce esophageal damage.²⁷ Monitoring lesion development and the occurrence of micro bubbles as an indication of an increased esophageal temperature, allows the operator to perform additional energy titration, thereby further minimizing the risk of esophageal damage.^{27,32}

As an alternative to anatomical guidance with ICE, image integration with MSCT or magnetic resonance imaging integration is commonly used to guide radiofrequency catheter ablation for AF.³⁵ A 3D image of the left atrium can be integrated with an electroanatomical map by performing a semi-automatic registration process. However, the validity of this technique is largely dependent on the quality of the registration.³⁶⁻³⁸ An inaccurate registration process can result in a large shift of landmark points up to of 5-10 mm, thereby compromising the safety and efficiency of lesion placement.^{36,37} Adjunctive real-time imaging with ICE can be used to confirm the accuracy of the registration process in order to ensure an accurate delivery of radiofrequency energy.³⁷

Recently, an electroanatomical mapping system (CARTO Sound, Biosense Webster, Diamond Bar, CA) has been released that allows the integration of ICE and electroanatomical mapping.³⁹ By integrating ICE and electroanatomical mapping, an accurate 3D anatomical shell of the left atrium

and pulmonary veins can be acquired without performing a registration process.⁴⁰ A modified phased array ultrasound catheter with an imbedded navigation sensor at its tip (Soundstar, Biosense Webster) is positioned inside the right atrium. The mapping system can detect the position and direction of the ICE catheter, thereby enabling the projection of the scanning plane inside its 3D environment. By gently rotating the ultrasound catheter, ECG-gated images of the left atrium and pulmonary veins are acquired. On each image, the endocardial borders (contours) are traced manually and are thereafter assigned to a designated map (Figure 8, panel A). Separate maps are created for the left atrial body and each of the pulmonary veins. All contours within a map are used to create a 3D shell of the structure (Figure 8, panel B). By combining all maps, the 3D geometry of the whole left atrium and pulmonary veins is visualized, which can be merged with a MSCT image in order to facilitate the ablation procedure (Figure 8, panel C).

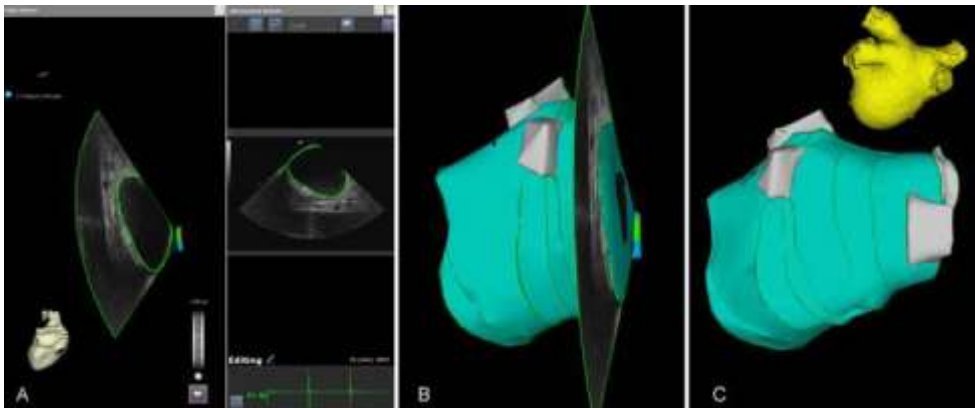


Figure 8. Panel A: After acquisition of an ECG-gated ultrasound image, the endocardial contours (green) of the left atrium (LA) and pulmonary veins are manually traced and are thereafter assigned to a corresponding map. Panel B: By systematically collecting images of the whole LA and marking the endocardial borders, a registered three-dimensional (3D) reconstruction of the LA anatomy is created. Panel C: The acquired 3D geometry can be used to guide radiofrequency catheter ablation for atrial fibrillation.

Complex atrial flutter ablation

A common atrial flutter is an organized tachycardia with a reentry circuit inside the right atrium and a protected isthmus between the tricuspid valve and the inferior vena cava (cavo-tricuspid isthmus).²⁰ Ablation of a common flutter is performed by creating a linear line of block across the cavo-tricuspid isthmus.⁴¹ Even though it is considered unnecessary to use special imaging or mapping during a standard procedure, during complex cases ICE may be used to facilitate the procedure.²¹ Intracardiac echocardiography can identify the cavo-tricuspid isthmus and other anatomical structures that can act as electrical barriers during atrial flutter, like the crista terminalis and Eustachian ridge.²⁰ Ablation of an atrial flutter can be complicated by complex anatomy, for example in patients previously operated for congenital heart disease. Particularly in these patients, ICE can facilitate the ablation procedure by visualizing important anatomical structures and guiding catheter placement.⁴²

Ventricular tachycardia ablation

Ablation of ventricular tachycardia is usually limited to inducible and tolerated arrhythmias.^{43,44} Techniques to identify the arrhythmogenic substrate without inducing the tachycardia are being developed in order to treat patients who do not meet these criteria. Intracardiac echocardiography allows identification of akinetic and dyskinetic (aneurysmatic) myocardial segments in patients with ischemic ventricular tachycardia, thereby visualizing the exact location and extent of the substrate.^{45,46} Furthermore, ICE can be used to visualize small aneurysms of the right ventricle in patients with (suspected) arrhythmogenic right ventricular dysplasia, thereby detecting the arrhythmogenic substrate in these patients.⁴⁶

Recently, the feasibility of the integration of ICE and electroanatomical mapping to guide ischemic ventricular tachycardia ablation was

demonstrated.⁴⁷ By creating a 3D geometry of the left ventricle and marking the akinetic and dyskinetic segments as seen on ICE, the ischemic substrate could be mapped and the ablation procedure could be performed successfully.

Left ventricular lead placement in cardiac resynchronization therapy

Cardiac resynchronization therapy (CRT) has a beneficial effect on clinical symptoms, exercise capacity and left ventricular systolic function in selected patients with drug-refractory heart failure.⁴⁸⁻⁵⁰ Moreover, CRT is associated with an increased survival and a reduction in the number of re-hospitalizations for heart failure, as compared to optimal medical treatment.⁴⁸ However, implantation of a CRT device — usually performed under fluoroscopic and angiographic guidance — can be challenging due to venous anatomy, resulting in a failure to place the left ventricular pacing lead in up to 8% of the patients.⁴⁸⁻⁵⁰ A number of case studies report on the use of ICE to visualize the coronary sinus in order to guide left ventricular lead placement.^{51,52} However, at present no prospective studies have reported a beneficial effect of ICE guidance on the success rate for left ventricular lead placement.

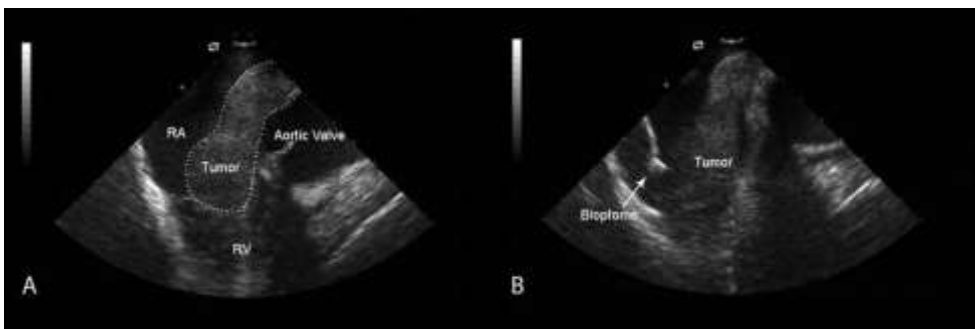


Figure 9. Panel A: An intracardiac mass originating from the superior vena cava is extending into the right atrium (RA) and tricuspid valve. (RV = right ventricle). Panel B: Intracardiac echocardiography is used to monitor and guide the biopsy by visualizing both tumor and biopptome.

Other Interventional Procedures

Biopsy of intracardiac mass. Intracardiac echocardiography can be used to visualize the origin and extent of an intracardiac mass (Figure 9, panel A). Therefore, ICE may be used to guide biopsies (Figure 9, panel B) and to monitor associated complications such as perforation or bleeding as suggested by few preliminary reports.^{53,54}

Left atrial appendage closure. Implantation of a left atrial appendage occlusion device has been advocated as a strategy to reduce the risk for systemic embolism in patients with atrial fibrillation and contraindications for anticoagulation and the procedure is typically guided by TEE. Recently, in a small group of patients the feasibility of ICE guidance as an alternative to TEE was reported.⁵⁵ Intracardiac echocardiography provided similar visualization of the left atrial appendage and similar assessment of the left atrial appendage orifice diameter compared to TEE (ICE 22.6 ± 3.4 mm vs. TEE 19.5 ± 1.5 mm, $p=NS$). Importantly, the degree of accuracy with respect to exclusion of a thrombus inside the left atrial appendage, the exact positioning of the delivery sheath and the verification of the location and stability of the occlusion device using ICE were comparable to TEE.

Ventricular septal defect closure. Intracardiac echocardiography can be used to guide transcatheter closure of a perimembranous ventricular septal defect.⁵⁶ This imaging modality allows identification and visualization of the defect and monitoring the placement of a guiding wire through the defect and the deployment of the left-sided occluder. Subsequently, ICE is used to confirm the correct position of the left-sided occluder against the interventricular septum before the deployment of the right-sided occluder. After deployment of the second occluder, ICE can be used to assess any residual shunt and valvular

regurgitation that may have resulted from the procedure. In 12 patients, Cao et al documented that ICE may be used as a safe and effective alternative for TEE to guide closure of a ventricular septal defect.⁵⁶

Alcohol ablation in hypertrophic obstructive cardiomyopathy. Alcohol septal ablation is an effective treatment to reduce the intraventricular gradient in patients with hypertrophic obstructive cardiomyopathy.⁵⁷ However, the efficacy and safety of the procedure is dependent on the identification of the correct septal artery. In order to identify this branch, echocontrast is commonly injected into a septal artery at the time of coronary angiography and transthoracic echocardiography is used to detect the extent and localization of the corresponding myocardial territory. Intracardiac echocardiography allows high quality visualization of the entire interventricular septum and may be a useful tool to guide alcohol septal ablation.⁵⁸ In 9 patients, Pedone et al demonstrated that the use of ICE to guide the procedure was feasible.⁵⁹ However, more studies are needed to define the role of ICE in alcohol septal ablation in patients with hypertrophic obstructive cardiomyopathy.

Mitral valve balloon valvuloplasty. Percutaneous balloon valvuloplasty is an accepted alternative to surgical commissurotomy in selected patients with symptomatic mitral stenosis. In this setting, ICE can be used to exclude thrombus formation at the level of the left atrium, assess the morphology and function of the mitral valve, guide the transseptal puncture, monitor the positioning of the balloon and assess any residual valvular gradient or postprocedural mitral regurgitation.⁶⁰ In addition it may allow an early detection of complications such as cardiac tamponade.

Percutaneous valve procedures. Intracardiac echocardiography may provide online anatomical information useful to guide percutaneous valve repair or replacement.^{61,62} Accordingly, this imaging modality may be used to determine the appropriate size and site of deployment of the percutaneous valve as well as to monitor the anatomical and functional result of the procedure.⁶² Studies are needed to define the role of ICE during percutaneous valve procedures.

Intrapericardial use of intracardiac echocardiography. Positioning the ICE catheter inside the pericardium has the potential to provide valuable information during complex ablation procedures. Recently, the safety and feasibility of this approach was demonstrated in both experimental and clinical setting.^{63,64} In 10 patients, endocardial structures could be visualized in great detail from various angles.⁶⁴ The ability to visualize cardiac anatomy from different angles could benefit catheter navigation. However, this invasive approach is limited to patients undergoing epicardial access for catheter ablation.^{63,64}

Limitations

Although phased array ICE enables adjustment of the ultrasound frequency, tissue penetration remains a limiting factor in visualizing cardiac anatomy. The use of a lower ultrasound frequency would result in a higher degree of tissue penetration allowing visualization of structures further away from the transducer, but at the cost of a lower image resolution. In addition, the costs of phased array ICE are relatively high as compared to TEE and these expensive catheters are for single use only. However, the costs of ICE are somewhat balanced by the need for general anesthesia and an echocardiographer during TEE. Moreover, intracardiac echocardiography provides 2D monoplane images.

This limitation can be partially overcome by the flexibility of the catheter enabling to visualize the same structure from another angle. Nevertheless, operators who are used to multiplane TEE may still have difficulty obtaining the same views. Finally, there are no widely accepted standard views for ICE, in contrast to TEE and transthoracic echocardiography. This may be difficult, in particular for the inexperienced operator. Standard manipulation of the **ultrasound catheter starting from 'home view' position as well as recognition of landmark structures** may be helpful.

Special issues

Intracardiac echocardiography is an invasive imaging modality and its use is usually confined to patients undergoing a percutaneous interventional procedure. In general, the contraindications for ICE are similar to other right-sided cardiac catheterization procedures using a transfemoral access. In pediatric patients, the use of ICE is limited by the respective diameters of the femoral vein and the ultrasound catheter.

Conclusions

Intracardiac echocardiography is a valuable imaging tool for a wide variety of interventional and electrophysiological procedures. This imaging modality allows real-time visualization of anatomical structures, catheters and devices thereby enabling the monitoring and guidance of complex procedures like catheter ablation for atrial fibrillation and placement of a transcatheter closure device for atrial or ventricular septal defects. Since it provides images of quality comparable to TEE, ICE may be used — in the hands of an experienced operator — as an alternative to TEE during closure of an atrial septal defect or ventricular septal defect and during percutaneous occlusion of the left atrial appendage.

In addition, ICE is a potentially safe alternative for TEE to detect an intracardiac thrombus.

References

1. Packer DL, Stevens CL, Curley MG, Bruce CJ, Miller FA, Khandheria BK, Oh JK, Sinak LJ, Seward JB Intracardiac phased-array imaging: methods and initial clinical experience with high resolution, under blood visualization: initial experience with intracardiac phased-array ultrasound. *J Am Coll Cardiol* 2002;39:509-516.
2. Cappato R, Calkins H, Chen SA, Davies W, Iesaka Y, Kalman J, Kim YH, Klein G, Packer D, Skanes A Worldwide survey on the methods, efficacy, and safety of catheter ablation for human atrial fibrillation. *Circulation* 2005;111:1100-1105.
3. Thakur RK, Klein GJ, Yee R, Zardini M Embolic complications after radiofrequency catheter ablation. *Am J Cardiol* 1994;74:278-279.
4. Jongbloed MR, Bax JJ, van der Wall EE, Schalij MJ Thrombus in the left atrial appendage detected by intracardiac echocardiography. *Int J Cardiovasc Imaging* 2004;20:113-116.
5. Ren JF, Marchlinski FE, Callans DJ, Gerstenfeld EP, Dixit S, Lin D, Nayak HM, Hsia HH Increased intensity of anticoagulation may reduce risk of thrombus during atrial fibrillation ablation procedures in patients with spontaneous echo contrast. *J Cardiovasc Electrophysiol* 2005;16:474-477.
6. Ren JF, Marchlinski FE, Callans DJ Left atrial thrombus associated with ablation for atrial fibrillation: identification with intracardiac echocardiography. *J Am Coll Cardiol* 2004;43:1861-1867.
7. Keane D, Mansour M, Singh J Detection by intracardiac echocardiography of early formation of left atrial thrombus during pulmonary vein isolation. *Europace* 2004;6:109-110.
8. Klein AL, Grimm RA, Murray RD, pperson-Hansen C, Asinger RW, Black IW, Davidoff R, Erbel R, Halperin JL, Orsinelli DA, Porter TR, Stoddard MF Use of transesophageal echocardiography to guide cardioversion in patients with atrial fibrillation. *N Engl J Med* 2001;344:1411-1420.
9. Rao HB, Saksena S, Mitruka R Intra-cardiac echocardiography guided cardioversion to help interventional procedures (ICE-CHIP) study: study design and methods. *J Interv Card Electrophysiol* 2005;13 Suppl 1:31-36.
10. Nagarakanti R, Saksena S, Sra J, Jordaens L Cardiac arrhythmias. *J Am Coll Cardiol* 2005;45:A91-A128.
11. Du ZD, Hijazi ZM, Kleinman CS, Silverman NH, Larntz K Comparison between transcatheter and surgical closure of secundum atrial septal defect in children and adults: results of a multicenter nonrandomized trial. *J Am Coll Cardiol* 2002;39:1836-1844.
12. Jones TK, Latson LA, Zahn E, Fleishman CE, Jacobson J, Vincent R, Kanter K Results of the U.S. multicenter pivotal study of the HELEX septal occluder for percutaneous closure of secundum atrial septal defects. *J Am Coll Cardiol* 2007;49:2215-2221.
13. Bartel T, Konorza T, Arjumand J, Ebradlidze T, Eggebrecht H, Caspari G, Neudorf U, Erbel R Intracardiac echocardiography is superior to conventional monitoring for guiding device closure of interatrial communications. *Circulation* 2003;107:795-797.
14. Mullen MJ, Dias BF, Walker F, Siu SC, Benson LN, McLaughlin PR Intracardiac echocardiography guided device closure of atrial septal defects. *J Am Coll Cardiol* 2003;41:285-292.
15. Bocalandro F, Muench A, Salloum J, Awadalla H, Carter C, Barasch E, Smalling RW Interatrial defect sizing by intracardiac and transesophageal echocardiography compared with fluoroscopic measurements in patients undergoing percutaneous transcatheter closure. *Catheter Cardiovasc Interv* 2004;62:415-420.

16. Alboliras ET, Hijazi ZM Comparison of costs of intracardiac echocardiography and transesophageal echocardiography in monitoring percutaneous device closure of atrial septal defect in children and adults. *Am J Cardiol* 2004;94:690-692.
17. Lundqvist C, Olsson SB, Varnauskas E Transseptal left heart catheterization: a review of 278 studies. *Clin Cardiol* 1986;9:21-26.
18. Epstein LM, Smith T, TenHoff H Nonfluoroscopic transseptal catheterization: safety and efficacy of intracardiac echocardiographic guidance. *J Cardiovasc Electrophysiol* 1998;9:625-630.
19. Verma A, Marrouche NF, Natale A Pulmonary vein antrum isolation: intracardiac echocardiography-guided technique. *J Cardiovasc Electrophysiol* 2004;15:1335-1340.
20. Olgin JE, Kalman JM, Fitzpatrick AP, Lesh MD Role of right atrial endocardial structures as barriers to conduction during human type I atrial flutter. Activation and entrainment mapping guided by intracardiac echocardiography. *Circulation* 1995;92:1839-1848.
21. Morton JB, Sanders P, Davidson NC, Sparks PB, Vohra JK, Kalman JM Phased-array intracardiac echocardiography for defining cavotricuspid isthmus anatomy during radiofrequency ablation of typical atrial flutter. *J Cardiovasc Electrophysiol* 2003;14:591-597.
22. Ren JF, Marchlinski FE Utility of intracardiac echocardiography in left heart ablation for tachyarrhythmias. *Echocardiography* 2007;24:533-540.
23. Marrouche NF, Martin DO, Wazni O, Gillinov AM, Klein A, Bhargava M, Saad E, Bash D, Yamada H, Jaber W, Schweikert R, Tchou P, Abdul-Karim A, Saliba W, Natale A Phased-array intracardiac echocardiography monitoring during pulmonary vein isolation in patients with atrial fibrillation: impact on outcome and complications. *Circulation* 2003;107:2710-2716.
24. Wazni OM, Rossillo A, Marrouche NF, Saad EB, Martin DO, Bhargava M, Bash D, Beheiry S, Wexman M, Potenza D, Pisano E, Fanelli R, Bonso A, Themistoclakis S, Erciyes D, Saliba WI, Schweikert RA, Brachmann J, Raviele A, Natale A Embolic events and char formation during pulmonary vein isolation in patients with atrial fibrillation: impact of different anticoagulation regimens and importance of intracardiac echo imaging. *J Cardiovasc Electrophysiol* 2005;16:576-581.
25. Pappone C, Rosanio S, Oreto G, Tocchi M, Gugliotta F, Vicedomini G, Salvati A, Dicandia C, Mazzone P, Santinelli V, Gulletta S, Chierchia S Circumferential radiofrequency ablation of pulmonary vein ostia: A new anatomic approach for curing atrial fibrillation. *Circulation* 2000;102:2619-2628.
26. Haissaguerre M, Jais P, Shah DC, Takahashi A, Hocini M, Quiniou G, Garrigue S, Le MA, Le MP, Clementy J Spontaneous initiation of atrial fibrillation by ectopic beats originating in the pulmonary veins. *N Engl J Med* 1998;339:659-666.
27. Ren JF, Lin D, Marchlinski FE, Callans DJ, Patel V Esophageal imaging and strategies for avoiding injury during left atrial ablation for atrial fibrillation. *Heart Rhythm* 2006;3:1156-1161.
28. Marom EM, Herndon JE, Kim YH, McAdams HP Variations in pulmonary venous drainage to the left atrium: implications for radiofrequency ablation. *Radiology* 2004;230:824-829.
29. Wood MA, Wittkamp M, Henry D, Martin R, Nixon JV, Shepard RK, Ellenbogen KA A comparison of pulmonary vein ostial anatomy by computerized tomography, echocardiography, and venography in patients with atrial fibrillation having radiofrequency catheter ablation. *Am J Cardiol* 2004;93:49-53.
30. Jongbloed MR, Bax JJ, Lamb HJ, Dirksen MS, Zeppenfeld K, van der Wall EE, de RA, Schalij MJ Multislice computed tomography versus intracardiac echocardiography to

- evaluate the pulmonary veins before radiofrequency catheter ablation of atrial fibrillation: a head-to-head comparison. *J Am Coll Cardiol* 2005;45:343-350.
31. Robbins IM, Colvin EV, Doyle TP, Kemp WE, Loyd JE, McMahon WS, Kay GN Pulmonary vein stenosis after catheter ablation of atrial fibrillation. *Circulation* 1998;98:1769-1775.
 32. Cummings JE, Schweikert RA, Saliba WI, Burkhardt JD, Brachmann J, Gunther J, Schibgilla V, Verma A, Dery M, Drago JL, Kilicaslan F, Natale A Assessment of temperature, proximity, and course of the esophagus during radiofrequency ablation within the left atrium. *Circulation* 2005;112:459-464.
 33. Pappone C, Oral H, Santinelli V, Vicedomini G, Lang CC, Manguso F, Torracca L, Benussi S, Alfieri O, Hong R, Lau W, Hirata K, Shikuma N, Hall B, Morady F Atrio-esophageal fistula as a complication of percutaneous transcatheter ablation of atrial fibrillation. *Circulation* 2004;109:2724-2726.
 34. Marrouche NF, Guenther J, Segerson NM, Daccarett M, Rittger H, Marschang H, Schibgilla V, Schmidt M, Ritscher G, Noelker G, Brachmann J Randomized comparison between open irrigation technology and intracardiac-echo-guided energy delivery for pulmonary vein antrum isolation: procedural parameters, outcomes, and the effect on esophageal injury. *J Cardiovasc Electrophysiol* 2007;18:583-588.
 35. Tops LF, Bax JJ, Zeppenfeld K, Jongbloed MR, Lamb HJ, van der Wall EE, Schalij MJ Fusion of multislice computed tomography imaging with three-dimensional electroanatomic mapping to guide radiofrequency catheter ablation procedures. *Heart Rhythm* 2005;2:1076-1081.
 36. Fahmy TS, Mlcochova H, Wazni OM, Patel D, Cihak R, Kanj M, Beheiry S, Burkhardt JD, Dresing T, Hao S, Tchou P, Kautzner J, Schweikert RA, Arruda M, Saliba W, Natale A Intracardiac echo-guided image integration: optimizing strategies for registration. *J Cardiovasc Electrophysiol* 2007;18:276-282.
 37. Daccarett M, Segerson NM, Gunther J, Nolker G, Gutleben K, Brachmann J, Marrouche NF Blinded correlation study of three-dimensional electro-anatomical image integration and phased array intra-cardiac echocardiography for left atrial mapping. *Europace* 2007;9:923-926.
 38. Zhong H, Lacomis JM, Schwartzman D On the accuracy of CartoMerge for guiding posterior left atrial ablation in man. *Heart Rhythm* 2007;4:595-602.
 39. Khaykin Y, Klemm O, Verma A First human experience with real-time integration of intracardiac echocardiography and 3D electroanatomical imaging to guide right free wall accessory pathway ablation. *Europace* 2008;10:116-117.
 40. den Uijl DW, Tops LF, Tolosana JM, Schuijff JD, Trines SA, Zeppenfeld K, Bax JJ, Schalij MJ Real-time integration of intracardiac echocardiography and multislice computed tomography to guide radiofrequency catheter ablation for atrial fibrillation. *Heart Rhythm* 2008;5:1403-1410.
 41. Nakagawa H, Lazzara R, Khastgir T, Beckman KJ, McClelland JH, Imai S, Pitha JV, Becker AE, Arruda M, Gonzalez MD, Widman LE, Rome M, Neuhauser J, Wang X, Calame JD, Goudeau MD, Jackman WM Role of the tricuspid annulus and the eustachian valve/ridge on atrial flutter. Relevance to catheter ablation of the septal isthmus and a new technique for rapid identification of ablation success. *Circulation* 1996;94:407-424.
 42. Kedia A, Hsu PY, Holmes J, Burnham D, West G, Kusumoto FM Use of intracardiac echocardiography in guiding radiofrequency catheter ablation of atrial tachycardia in a patient after the senning operation. *Pacing Clin Electrophysiol* 2003;26:2178-2180.
 43. Callans DJ, Zado E, Sarter BH, Schwartzman D, Gottlieb CD, Marchlinski FE Efficacy of radiofrequency catheter ablation for ventricular tachycardia in healed myocardial infarction. *Am J Cardiol* 1998;82:429-432.

44. Morady F, Harvey M, Kalbfleisch SJ, el-Atassi R, Calkins H, Langberg JJ Radiofrequency catheter ablation of ventricular tachycardia in patients with coronary artery disease. *Circulation* 1993;87:363-372.
45. Callans DJ, Ren JF, Michele J, Marchlinski FE, Dillon SM Electroanatomic left ventricular mapping in the porcine model of healed anterior myocardial infarction. Correlation with intracardiac echocardiography and pathological analysis. *Circulation* 1999;100:1744-1750.
46. Jongbloed MR, Bax JJ, van der Burg AE, van der Wall EE, Schalij MJ Radiofrequency catheter ablation of ventricular tachycardia guided by intracardiac echocardiography. *Eur J Echocardiogr* 2004;5:34-40.
47. Khaykin Y, Skanes A, Whaley B, Hill C, Beardsall M, Seabrook C, Wulffhart Z, Oosthuizen R, Gula L, Verma A Real-time integration of 2D intracardiac echocardiography and 3D electroanatomical mapping to guide ventricular tachycardia ablation. *Heart Rhythm* 2008;5:1396-1402.
48. Cleland JG, Daubert JC, Erdmann E, Freemantle N, Gras D, Kappenberger L, Tavazzi L The effect of cardiac resynchronization on morbidity and mortality in heart failure. *N Engl J Med* 2005;352:1539-1549.
49. Abraham WT, Fisher WG, Smith AL, Delurgio DB, Leon AR, Loh E, Kocovic DZ, Packer M, Clavell AL, Hayes DL, Ellestad M, Trupp RJ, Underwood J, Pickering F, Truex C, McAtee P, Messenger J Cardiac resynchronization in chronic heart failure. *N Engl J Med* 2002;346:1845-1853.
50. Cazeau S, Leclercq C, Lavergne T, Walker S, Varma C, Linde C, Garrigue S, Kappenberger L, Haywood GA, Santini M, Bailleul C, Daubert JC Effects of multisite biventricular pacing in patients with heart failure and intraventricular conduction delay. *N Engl J Med* 2001;344:873-880.
51. Shalaby AA Utilization of intracardiac echocardiography to access the coronary sinus for left ventricular lead placement. *Pacing Clin Electrophysiol* 2005;28:493-497.
52. Scholten MF, Szili-Torok T, Thornton AS, Roelandt JRTC, Jordaens LJ Visualization of a coronary sinus valve using intracardiac echocardiography. *Eur J Echocardiogr* 2004;5:93-96.
53. Segar DS, Bourdillon PD, Elsner G, Kesler K, Feigenbaum H Intracardiac echocardiography-guided biopsy of intracardiac masses. *J Am Soc Echocardiogr* 1995;8:927-929.
54. Mitchell AR, Timperley J, Hudsmith L, Neubauer S, Bashir Y Intracardiac echocardiography to guide myocardial biopsy of a primary cardiac tumour. *Eur J Echocardiogr* 2007;8:505-506.
55. Ho IC, Neuzil P, Mraz T, Beldova Z, Gross D, Formanek P, Taborsky M, Niederle P, Ruskin JN, Reddy VY Use of intracardiac echocardiography to guide implantation of a left atrial appendage occlusion device (PLAATO). *Heart Rhythm* 2007;4:567-571.
56. Cao QL, Zabal C, Koenig P, Sandhu S, Hijazi ZM Initial clinical experience with intracardiac echocardiography in guiding transcatheter closure of perimembranous ventricular septal defects: feasibility and comparison with transesophageal echocardiography. *Catheter Cardiovasc Interv* 2005;66:258-267.
57. Sorajja P, Valeti U, Nishimura RA, Ommen SR, Rihal CS, Gersh BJ, Hodge DO, Schaff HV, Holmes DR, Jr. Outcome of alcohol septal ablation for obstructive hypertrophic cardiomyopathy. *Circulation* 2008;118:131-139.
58. Alfonso F, Martin D, Fernandez-Vazquez F Intracardiac echocardiography guidance for alcohol septal ablation in hypertrophic obstructive cardiomyopathy. *J Invasive Cardiol* 2007;19:E134-E136.

59. Pedone C, Vijayakumar M, Ligthart JM, Valgimigli M, Biagini E, De JN, Serruys PW, Ten Cate FJ Intracardiac echocardiography guidance during percutaneous transluminal septal myocardial ablation in patients with obstructive hypertrophic cardiomyopathy. *Int J Cardiovasc Intervent* 2005;7:134-137.
60. Green NE, Hansgen AR, Carroll JD Initial clinical experience with intracardiac echocardiography in guiding balloon mitral valvuloplasty: technique, safety, utility, and limitations. *Catheter Cardiovasc Interv* 2004;63:385-394.
61. Naqvi TZ, Zabatany D, Molloy MD, Logan J, Buchbinder M Intracardiac echocardiography for percutaneous mitral valve repair in a swine model. *J Am Soc Echocardiogr* 2006;19:147-153.
62. Chessa M, Butera G, Carminati M Intracardiac echocardiography during percutaneous pulmonary valve replacement. *Eur Heart J* 2008;In press.
63. Rodrigues AC, d'Avila A, Houghtaling C, Ruskin JN, Picard M, Reddy VY Intrapericardial echocardiography: a novel catheter-based approach to cardiac imaging. *J Am Soc Echocardiogr* 2004;17:269-274.
64. Horowitz BN, Vaseghi M, Mahajan A, Cesario DA, Buch E, Valderrabano M, Boyle NG, Ellenbogen KA, Shivkumar K Percutaneous intrapericardial echocardiography during catheter ablation: a feasibility study. *Heart Rhythm* 2006;3:1275-1282.

Chapter 9

Real-time integration of intracardiac echocardiography and multi-slice computed tomography to guide radiofrequency catheter ablation for atrial fibrillation

Dennis W. den Uijl, Laurens F. Tops, José M. Tolosana, Joanne D. Schuijf, Serge A. Trines, Katja Zeppenfeld, Jeroen J. Bax, Martin J. Schalij.

Heart Rhythm. 2008 Oct;5(10):1403-10



Abstract

Background: Multi-slice computed tomography (MSCT) integration is commonly used to guide radiofrequency catheter ablation (RFCA) for atrial fibrillation (AF). MSCT provides detailed anatomical information but lacks the ability to provide real-time anatomy during RFCA. Intracardiac echocardiography (ICE) allows real-time visualization of cardiac structures.

Objective: The purpose of this study was to investigate the feasibility of three-dimensional (3D) anatomical mapping of the left atrium (LA) with ICE and integrating the 3D map with MSCT to facilitate RFCA for AF.

Methods: In seventeen patients undergoing RFCA for AF, 3D mapping of the LA was performed with ICE using a new mapping system (CARTOSOUND™, Biosense Webster) which allows tracking of a new ICE probe. On each ICE image endocardial contours were traced and used to generate a 3D map of the LA and pulmonary veins (PVs). A preprocedural acquired MSCT image of the LA was then integrated with the 3D map. Additionally, PV assessment with ICE was compared with MSCT.

Results: Accurate 3D mapping could be performed in all patients with a mean number of 31.1 ± 8.5 contours. Integration with MSCT resulted in a mean distance between MSCT and ICE contours of 2.2 ± 0.3 mm for the LA and PVs together and of 1.7 ± 0.2 mm around the PV ostia specifically. Agreement in assessment of PV anatomy and diameters between ICE and MSCT was excellent.

Conclusion: 3D ICE mapping of the LA is feasible. The 3D map created with ICE can be merged with MSCT to facilitate RFCA for AF.

Introduction

Ectopic beats originating from the pulmonary veins (PVs) can initiate atrial fibrillation (AF) ¹. Radiofrequency catheter ablation (RFCA) is considered a reasonable option in the treatment of patients with AF, when at least one anti-arrhythmic drug has failed ². Ablation strategies targeting the PVs are the cornerstone of these RFCA procedures ². To plan and guide these ablation procedures, non-invasive three-dimensional (3D) imaging modalities like magnetic resonance imaging and multi-slice computed tomography (MSCT) are available to visualize the left atrium (LA) and PVs ^{3,4}. Electrophysiological navigation systems allowing the integration of MSCT with electroanatomical maps, combine accurate real-time navigation with detailed anatomical information thereby facilitating the ablation procedure ⁵ and reducing fluoroscopy time and procedural duration ⁶.

However, a limiting factor of using MSCT to guide the ablation procedure is the time interval between image acquisition and the ablation procedure which may result in differences in heart rhythm, heart rate and fluid status potentially causing an inaccurate registration process. Because the quality of the registration process determines the accuracy of navigating ⁷, this could result in less accurate lesion placement during RFCA. Recently, a new electroanatomical mapping system has been released that allows integration of 3D mapping and real-time intracardiac echocardiography (ICE). Using this system, a registered 3D shell of the LA and PV anatomy can be generated from two-dimensional (2D) ICE images.

The aim of this study was to investigate the feasibility of creating a 3D map of the LA and PVs with ICE and integrating this map with a MSCT surface image in order to facilitate RFCA for AF. In addition, a direct comparison between this new ICE technique and MSCT for the assessment of PV anatomy was performed.

Methods

Study population and protocol

The study population comprised 17 consecutive patients with symptomatic drug refractory AF, who underwent RFCA in our institution. In all patients a MSCT was acquired two days before the ablation. Prior to the procedure, the raw MSCT data was loaded into an electroanatomical mapping system (CARTO XP™, Biosense Webster, Diamond Bar, California) equipped with a newly developed image integration module (CARTOSOUND™, Biosense Webster). During the ablation procedure 3D maps of the LA and PVs were created using an ICE catheter with an imbedded CARTO navigation sensor (10Fr Soundstar™, Biosense Webster) allowing the mapping system to detect its position and generate a registered 3D shell from the recorded two-dimensional (2D) images. After completion of the mapping procedure a registration process was performed to integrate the MSCT image with the 3D map made with ICE. Thereafter the merged MSCT image and 3D maps were used to guide the RFCA procedure.

Multi-Slice Computed Tomography

In all patients MSCT data were acquired two days before the ablation procedure. The MSCT examination was performed with a 64-slice Toshiba Aquilion 64 system (Toshiba Medical Systems, Otawara, Japan) (7 patients) or a 320-slice Toshiba Aquilion One system (Toshiba Medical Systems) (10 patients). Craniocaudal scanning was performed during breath holding. For the Aquilion 64 system collimation was 64 x 0.5 mm, rotation time 400 ms and tube voltage between 100 and 135 kV at 250 to 400 mA. For the Aquilion One system collimation was 320 x 0.5 mm, rotation time 350 ms and tube voltage 120 kV at 400 to 500 mA. In all patients nonionic contrast material (Iomeron 400, Bracco, Milan, Italy; 105 ml for Aquilion 64 and 50 ml for Aquilion One scanning) was

infused through the antecubital vein at a rate of 5 ml/s followed by 50 ml saline solution flush. Automatic detection of the contrast bolus was used to time the start of the scan. Before the ablation procedure, all MSCT data were analyzed on a dedicated workstation (Vitrea 2; Vital Images, Minnetonka, Minnesota).

Image processing and segmentation

Prior to the ablation procedure, the raw MSCT data were loaded into the image integration module of the mapping system (CartoMerge™, Biosense Webster) and a segmentation process was performed. The segmentation process consisted of three phases as described previously⁵. The first step was to delineate the borders of interest on the MSCT (LA and PVs) by manually setting the threshold intensity range. A 3D volume was subsequently created of all structures within the set threshold range. The second step was to segment this 3D volume into different structures by placing markers in the middle of the different areas. An algorithm was used to automatically depict the different structures based on the placement of the markers and the border of the 3D volume. Finally, the segmented surface images were exported to the mapping system.

Anatomical mapping with intracardiac echocardiography

During the catheter ablation procedure, a 3D anatomical map was created with ICE images. A new mapping system was used, equipped with a new image integration module that allows the integration of ICE and 3D mapping (CARTOSOUND™). This system is able to detect the position and direction of a specifically designed ICE catheter with an imbedded CARTO navigation sensor located at its tip (Soundstar™). By positioning the ICE catheter inside the right atrium, ECG gated images of the LA and PVs were acquired. To provide ECG gating, either a quadripolar electrophysiological catheter placed inside the

right atrium or the body surface ECG was used as a reference signal in patients with sinus rhythm or AF, respectively. In order to correct for respiratory phase, all ICE images were acquired during expiratory breath hold.

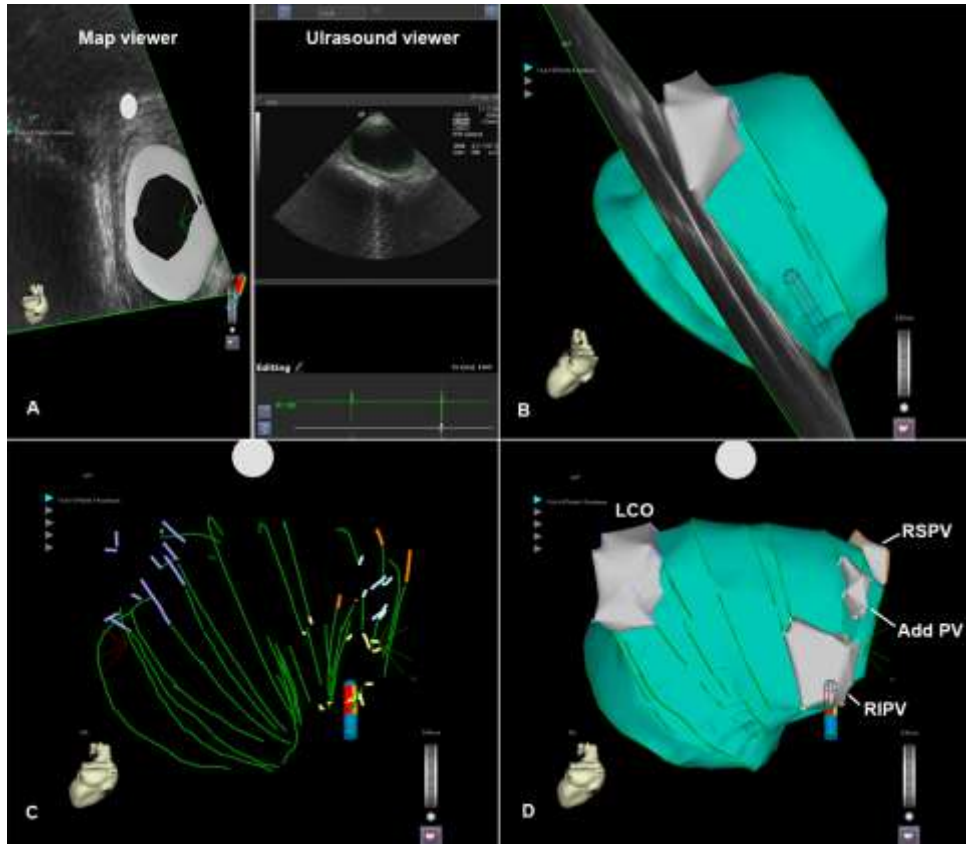


Figure 1. Three-dimensional (3D) mapping with intracardiac echocardiographic (ICE). Ultrasound images of the left atrium (LA) are acquired. The endocardial contour of the LA is traced on the ultrasound viewer of the mapping system. After assigning the contour to a map, it appears on the map viewer (A). By acquiring more contours and reconstructing them into a registered 3D shell (B), the shape of the LA and pulmonary veins (PVs) is depicted. Systematically, the LA and PVs are visualized (C) until a complete 3D map of the LA and PVs is acquired (D). Add PV = additional pulmonary vein, LCO = left common ostium, RIPV = right inferior pulmonary vein, RSPV = right superior pulmonary vein.

Intracardiac echocardiography was performed using a Sequoia ultrasound system (Siemens Medical Solutions USA, Mountain View, California)

which transferred real-time ICE data to the mapping system. On the mapping system, the endocardial contours were traced manually after which they were assigned to a map (Figure 1A). All contours within a map were used to generate a registered 3D shell (Figure 1B and 1C). For each map a separate shell was generated. Different maps were created for the LA and for each of the PVs (Figure 1D).

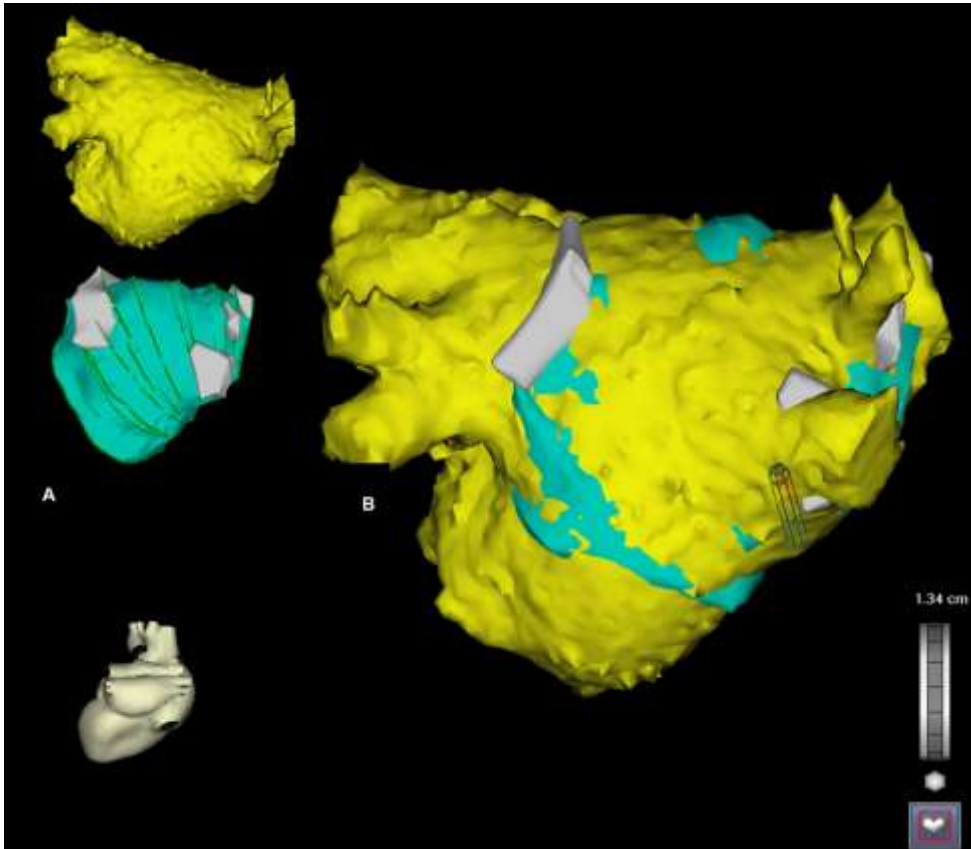


Figure 2. After three-dimensional (3D) mapping with intracardiac echocardiography, the 3D map and multi-slice computed tomography (MSCT) image are displayed next to each other (A). Then a manual registration process was performed. This resulted in the integration of the 3D map and the MSCT image in order to anatomically guide the ablation procedure (B).

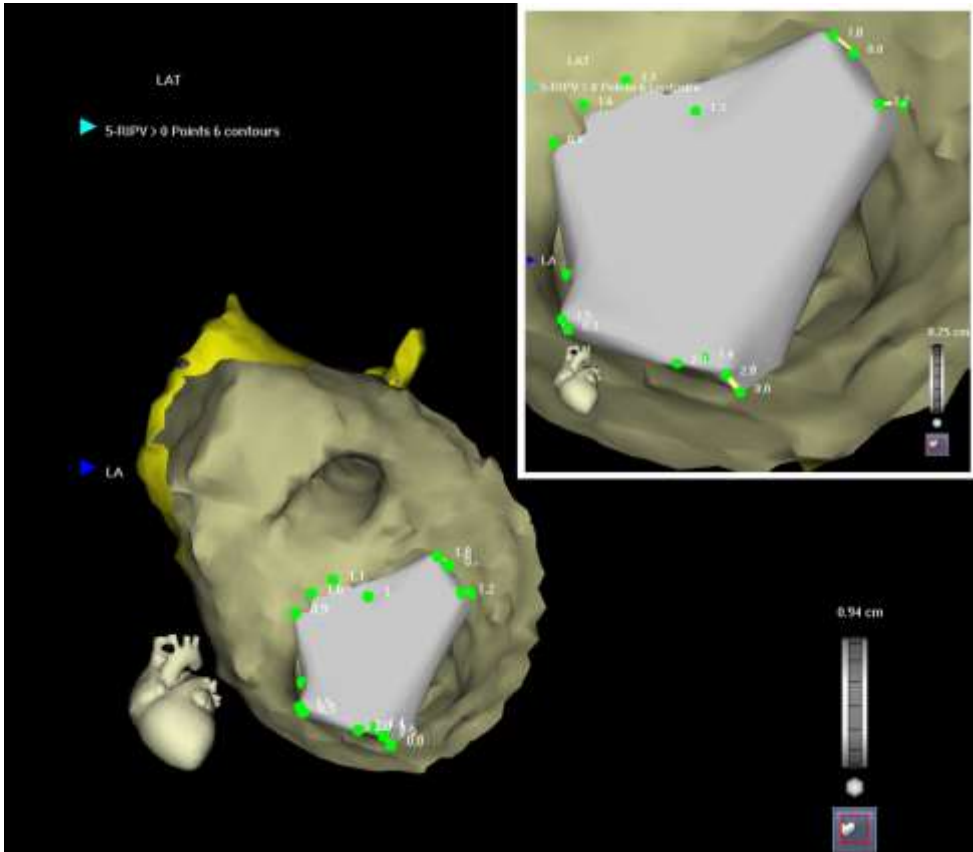


Figure 3. The quality of the registration process was reviewed at the level of the pulmonary vein ostium by measuring the distance between multi-slice computed tomography and three-dimensional map at 5 representative points.

Registration

After creating a map with ICE, a registration process was performed to integrate the MSCT surface image and the 3D map. First, the MSCT surface image was displayed next to the anatomical map (Figure 2A). A landmark was placed at a distinct anatomical structure on the anatomical map and at a corresponding point on the MSCT model. Then 'visual alignment' was performed by minimizing the distance between both landmarks. Next, the maps created during the mapping procedure were each assigned to the

corresponding MSCT surface image and a 'surface registration' was performed. During this process the ICE contours were represented as a line of adjacent mapping points. An internal algorithm was used to minimize the distance between these points and the MSCT surface image (Figure 2B).

The accuracy of the registration process was then reviewed. The mean value, standard deviation and range of the distance between the points along the ICE contours and the MSCT surface were provided by the algorithm. The accuracy of the registration process at the level of the PVs was evaluated by measuring the distance between the contours and MSCT surface at 5 representative points around each PV ostium (Figure 3).

Pulmonary vein anatomy and quantitative measurements

After an accurate registration had been acquired the PVs and their atrial insertion were evaluated on both MSCT and ICE. Pulmonary vein anatomy was classified according to the presence or absence of a common ostium/trunk and/or additional veins. As described previously, a common ostium was defined as a PV carina located outside the extrapolated endocardial border of the LA ⁴. A common trunk was defined as a clearly recognizable common part in which both superior and inferior PV drain before emptying into the LA ⁸. An additional vein was defined as a supranumerical vein entering the LA with a separate ostium. The same criteria for PV classification were used for MSCT and ICE evaluation.

Pulmonary vein diameters on MSCT were measured in anterior-posterior (AP) and superior-inferior (SI) direction inside the PV ostium, as previously described ⁴. Pulmonary vein diameters on ICE were measured at the widest point. Left atrial diameter was measured in AP direction on both MSCT and the 3D map created with ICE.

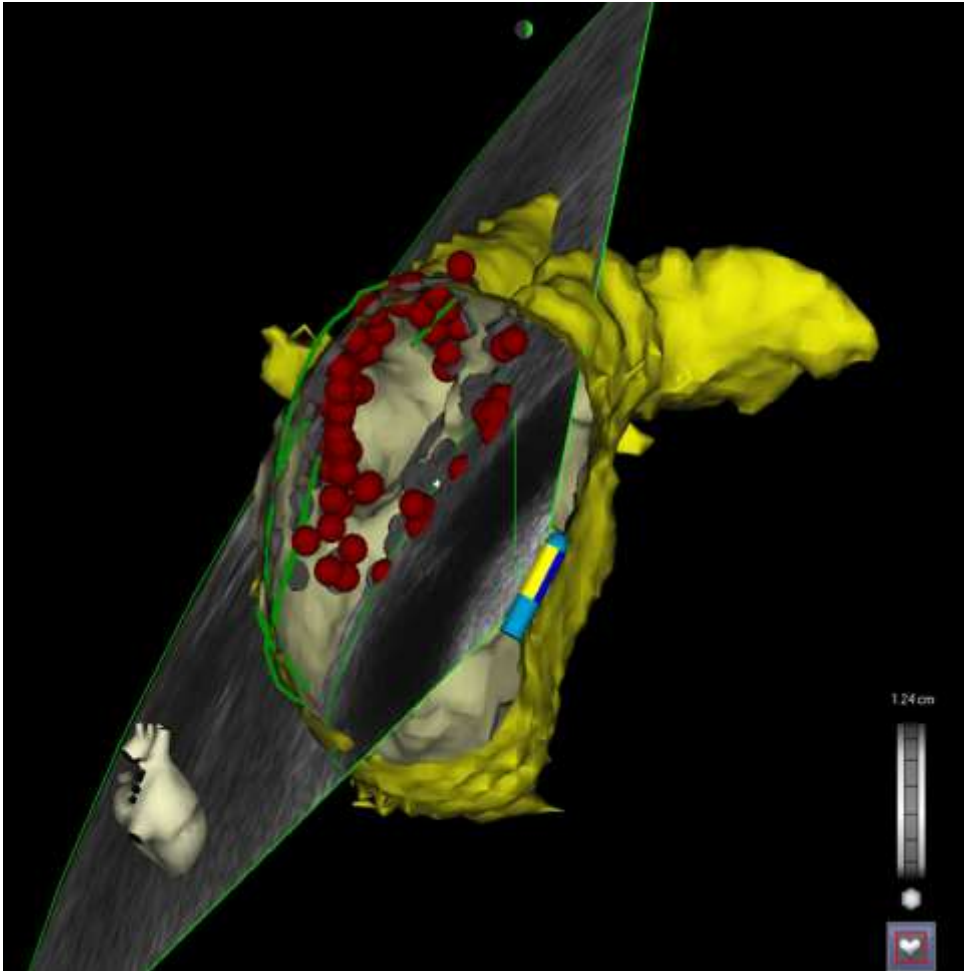


Figure 4. After registration the three-dimensional map created with intracardiac echocardiography and integrated multi-slice computed tomography image were used to facilitate the ablation procedure. Circumferential lesions were created outside the pulmonary vein ostia. Red tags represent the sites of radiofrequency current application.

Radiofrequency catheter ablation

Radiofrequency catheter ablation was performed by creating two circumferential lesions around the left and right PV antrum (Figure 4). Additional lesions consisting of a roofline, a mitral valve isthmus line or sites exhibiting fractionated activity were created if deemed necessary. After

excluding an intracardiac thrombus, and in the absence of a patent foramen ovale, a transseptal puncture was performed under ICE guidance. All patients received a bolus of intravenous heparin (5000 IU) with an additional bolus to maintain an activated clotting time between 300-400 s. The ablation procedure was guided by the 3D map created with ICE and integrated with the MSCT image. An open loop irrigated 4-mm tip quadripolar mapping/ablation catheter (7Fr Navistar™, Biosense Webster) was introduced in the LA and used to apply radiofrequency current outside the ostia of all PVs. At each point, radiofrequency current was applied at 30-35 W (maximum tip temperature 45 °C) until a voltage of <0.1 mV was achieved, with a maximum of 60 seconds per point.

Statistical analysis

Data are presented as mean \pm SD or as number (percentage). Statistical analysis was performed using SPSS 14.0 software (SPSS Inc., Chicago, Illinois). Statistical comparisons were performed **with two tailed Student's T-test**, paired or unpaired as appropriate. Kappa analysis was used to quantify the level of agreement in PV anatomy classification with MSCT and ICE. Bland-Altman analysis was used to quantify the level of agreement between measurements of PV diameter with ICE and MSCT. A P value <0.05 was considered statistically significant.

Results

Study population

Seventeen patients were studied (13 men, mean age 56 ± 8 years). Atrial fibrillation was paroxysmal in 11 patients and persistent in 6 according to the ACC/AHA/ESC Guidelines definition⁹. Mean duration of AF was 72 ± 58 months

and the mean number of anti-arrhythmic drugs used was 3.7 ± 1.3 per patient. Mean LA size measured by transthoracic echocardiography was 41.8 ± 5.3 mm; mean left ventricular ejection fraction was 58 ± 7 %. Four patients had undergone another radiofrequency catheter ablation procedure for AF previously.

Table 1. Result of the registration process per patient

Patient	Age (years)	Gender	No. of contours	Distance between contours and MSCT surface image (mm)		
				Mean	SD	Range
1	46	F	20	2.1	1.6	0.00-8.45
2	55	M	19	1.9	1.4	0.00-8.91
3	61	M	27	2.3	1.6	0.00-8.82
4	72	M	23	2.5	1.9	0.01-10.27
5	57	M	18	2.1	1.7	0.01-10.17
6	40	F	36	1.8	1.4	0.01-7.19
7	58	M	39	2.6	1.9	0.00-9.99
8	48	M	38	2.0	1.5	0.00-7.68
9	61	F	29	1.9	1.4	0.15-6.45
10	47	M	42	1.7	1.4	0.00-7.44
11	68	M	22	2.3	1.5	0.01-7.03
12	50	M	40	2.1	1.6	0.01-9.15
13	53	F	38	1.9	1.7	0.00-12.50
14	58	M	31	2.8	1.9	0.02-11.56
15	60	M	43	2.5	1.8	0.00-8.57
16	54	M	30	2.5	1.7	0.01-8.36
17	58	M	34	2.3	1.6	0.01-8.38
Mean	55.6		31.1	2.2	1.7	
SD	8.0		8.5	0.3	0.2	

MSCT = multi-slice computed tomography, No. = number, SD = standard deviation.

Mapping and registration accuracy

In order to acquire a good geometry of LA and PVs a mean of 31.1 ± 8.5 ICE contours were drawn per patient (range 18-43 contours). The mean time needed to make a 3D map with ICE was 76 ± 27 minutes (range 25-126 minutes). It was noted that the time needed to make a map significantly decreased from 97 ± 20 minutes during the first 4 procedures to 39 ± 10

minutes during the last 13 procedures ($p < 0.001$). After the registration process the mean distance between the drawn ICE contours and the MSCT surface image ranged from 1.7 to 2.8 mm (mean 2.2 ± 0.3 mm). The standard deviation of the ICE-MSCT difference ranged from 1.4 mm to 1.9 mm (mean 1.7 ± 0.2 mm). Individual results of the registration process are given in Table 1.

The accuracy of the registration process at the level of the PVs was evaluated by calculating the mean value of the distance between the contours and MSCT surface at 5 representative points around each PV ostium. The mean distance between the drawn contours and the MSCT surface image at the level of the PV ostia ranged from 0.7 to 4.4 mm (mean 1.7 ± 1.1 mm) and was smallest around the left inferior PV (mean 1.5 ± 1.1 mm) and largest around the left superior PV (mean 2.1 ± 1.3 mm) (Table 2).

Classification pulmonary vein anatomy

An equal number of 70 PVs were visualized with MSCT and ICE (4.12 ± 0.49 per patient). The most common PV variant consisted of 2 left sided PVs with separate ostia and 2 right sided PVs with separate ostia (7 patients, 41%). A common ostium of the left PVs was noted in 8 patients (47%) with MSCT and in 10 patients (59%) with ICE. A common trunk of the left superior and left inferior PV was recognized in 3 patients (18%) with both MSCT and ICE. An additional PV was identified in 5 patients (29%). All additional PVs were located at the right side of the LA. Using kappa analysis, an excellent agreement between MSCT and ICE for the classification of the left-sided PVs ($\text{kappa} = 0.77$) and the right-sided PVs ($\text{kappa} = 1.00$) was observed.

Table 2. Result of the registration process at pulmonary vein ostia

Pulmonary vein	Distance between contours and MSCT surface image (mm)		
	Mean	SD	Range
RSPV	1.7	1.0	0.8-3.2
RIPV	1.6	1.0	0.7-3.2
LSPV	2.1	1.3	0.8-4.4
LIPV	1.5	1.1	1.0-2.4
LCT	1.7	1.2	1.3-1.9
Both RPV	1.7	1.0	0.7-3.2
Both LPV	1.8	1.2	0.8-4.4
All PV	1.7	1.1	0.7-4.4

MSCT = multi-slice computed tomography, LCT = left common trunk, LIPV = left inferior pulmonary vein, LPV = left pulmonary veins, LSPV = left superior pulmonary vein, PV = pulmonary vein, RIPV = right pulmonary vein, RPV = right pulmonary veins, RSPV = right superior pulmonary vein, SD = standard deviation, SI = superior-inferior.

Quantitative measurements

Pulmonary vein diameters were measured in two directions on MSCT (AP and SI) and in the direction of the largest diameter possible on ICE, as previously described⁴. Superior-inferior diameters measured on MSCT were significantly larger for all PVs compared to the diameters measured on ICE (Table 3). The AP diameters of the right superior PV, left superior PV and additional veins measured on MSCT were not significantly different from the diameters measured on ICE. In contrast, the AP diameters of the right inferior PV on MSCT were significantly larger than the PV diameters on ICE (Table 3). Bland-Altman analysis demonstrated that there was a good overall agreement between ICE and MSCT for the assessment of the PV ostium diameter (Figure 5).

Left atrial diameter was measured in AP direction on both MSCT and ICE. Mean AP diameter of the LA on MSCT was 39.6 ± 7.2 mm compared to 35.9 ± 7.2 mm on ICE. The mean difference between AP diameter on MSCT and ICE was 3.7 ± 5.0 mm ($p < 0.01$) and ranged from 0.3 to 15.6 mm.

Table 3. Measurements of pulmonary vein ostium diameter MSCT versus ICE

	MSCT SI (mm)	MSCT AP (mm)	ICE (mm)	SI diameter MSCT vs ICE (p-value)	AP diameter MSCT vs ICE (p-value)
RSPV	24.0 ± 3.5	19.2 ± 3.3	18.3 ± 3.3	<0.01	NS
RIPV	20.8 ± 3.0	17.9 ± 3.3	15.3 ± 2.4	<0.01	<0.05
LSPV	21.6 ± 3.9	15.4 ± 3.0	15.2 ± 2.2	<0.01	NS
LIPV	19.0 ± 2.1	11.9 ± 2.3	14.6 ± 2.4	<0.01	<0.05
LCT	38.2 ± 3.8	22.4 ± 1.0	28.2 ± 0.4	<0.05	<0.05
ADD	9.6 ± 1.9	8.5 ± 2.4	8.5 ± 0.9	<0.05	NS
All PV	21.5 ± 5.7	16.2 ± 4.5	16.0 ± 4.3	<0.01	NS

ADD = additional pulmonary vein, AP = anterior-posterior, ICE = intracardiac echocardiography, LCT = left common trunk, LIPV = left inferior pulmonary vein, LSPV = left superior pulmonary vein, MSCT = multi-slice computed tomography, PV = pulmonary vein, RIPV = right pulmonary vein, RSPV = right superior pulmonary vein, SI = superior-inferior

Radiofrequency catheter ablation

Transseptal puncture was performed under ICE guidance in 13 patients. A patent foramen ovale existed in 4 patients. The mean ablation time was 80 ± 34 minutes and mean fluoroscopy time was 35 ± 6 minutes. Radiofrequency catheter ablation was targeted at the PVs in all patients. No differences between heart rhythm during MSCT acquisition and ablation procedure were observed. No complications occurred during and after the ablation procedure.

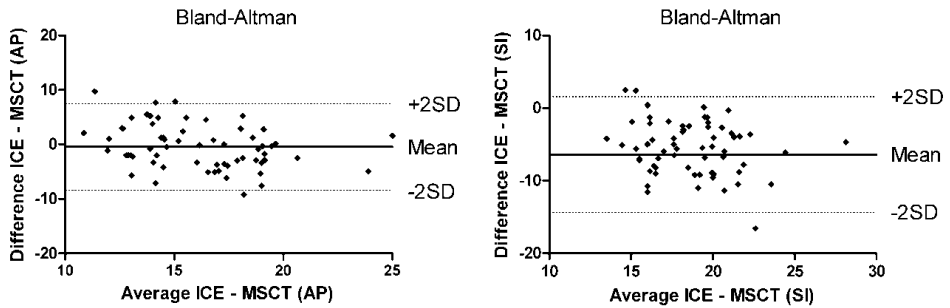


Figure 5. Bland-Altman analysis of measurements performed with multi-slice computed tomography and intracardiac echocardiography in anterior-posterior direction (left panel) and in superior-inferior direction.

Discussion

The present study is the first to report on the feasibility of creating a 3D map of the LA and PVs with ICE and integrating this map with MSCT in order to facilitate RFCA for AF. This study has three main findings: 1) It is feasible to create an anatomical map of the LA and PVs using ICE contours; 2) The anatomical map created by ICE can accurately be merged with a MSCT surface image and 3) Anatomical ICE mapping is a sensitive imaging modality to visualize PVs and classify LA and PV anatomy.

3D mapping with ICE and MSCT integration

In the present study a novel mapping system was used that enables detection of a specifically designed ICE catheter with an imbedded CARTO navigation sensor. This mapping system allows acquisition of ECG gated ICE images and reconstructs them into a registered 3D shell. With this new technology, it has become possible to acquire accurate real-time anatomical information of the LA and PVs without entering the left side of the heart. Khaykin et al first reported on the use of 3D mapping with ICE during the ablation of a right free wall accessory pathway ¹⁰. Okumura et al demonstrated the accuracy of navigation based on 3D mapping with ICE in animal experiments ¹¹. Both groups subsequently demonstrated the feasibility of creating a 3D map with ICE to guide RFCA for AF ¹¹⁻¹³. The present study supports these findings and additionally demonstrates the accuracy of creating a 3D map of the LA and PVs with ICE by comparing LA and PV geometry on the 3D ICE map with MSCT.

In addition, the current study is the first to demonstrate the feasibility of integrating a 3D map created with ICE and a MSCT image. Integration of MSCT images with conventional electroanatomical mapping is commonly used to guide RFCA for AF ¹⁴. In an animal study, Dong et al ¹⁵ demonstrated that the integration of MSCT and electroanatomical mapping allows accurate

placement of anatomically guided ablation lesions in all cardiac chambers. Furthermore, several studies demonstrated the feasibility of the integration of MSCT and electroanatomical mapping to guide RFCA for AF^{5,16-18}. Importantly, Kistler et al⁶ showed that the integration of a MSCT image to guide RFCA for AF is associated with reduced fluoroscopy time and an improved outcome of the procedure.

However, the time interval between the MSCT data acquisition and the ablation procedure is a limitation of MSCT image integration. This delay may result in differences in heart rhythm, heart rate and fluid status which may cause errors in the image integration process, thereby compromising the accuracy of lesion placement. By integrating real-time ICE, MSCT and electroanatomical mapping, it has become possible to combine real-time anatomical and electrophysiological information with highly detailed anatomical information, thereby potentially increasing the accuracy of the placement of ablation lesions. The present study demonstrates the accuracy of integrating a MSCT image with a 3D map created with ICE. This was illustrated by a mean distance of only 2.2 mm between the MSCT image and the ICE contours, which is comparable with the integration results between an electroanatomical map and MSCT^{5,16-18}. However, despite acquiring a good overall match between ICE and MSCT, the distance between the represented points along the ICE contours and MSCT ranged from 0.00 to 12.50 mm (Table 1). Similar ranges have been reported for the integration of electroanatomical maps and MSCT^{5,16}. This wide range may be related to differences in reconstructed LA and PV anatomy between MSCT and ICE in areas that are strongly influenced by cardiac and respiratory movement.

Pulmonary vein visualization

Left atrial and PV anatomy are highly variable ^{3,4,19}. Importantly, accurate visualization of the PV ostia during RFCA for AF is required to avoid ablation within the PVs ². In the present study, the PV ostia were visualized with ICE and MSCT. Both imaging modalities recorded an equal number of PVs, which suggests that 3D mapping with ICE has a high sensitivity for detecting PVs. Furthermore, there was good agreement between ICE and MSCT for classification of the PV anatomy.

In the present study, ICE slightly underestimated PV diameter, as compared with MSCT. This observation is in agreement with a study by Jongbloed et al ⁴ who found that ICE underestimated PV diameter for all PVs by 3.5 mm in SI direction and 0.2 mm in AP direction. An explanation for the underestimation of left sided PV diameters on ICE may be the fact that these PVs are visualized in longitudinal cross-sections thereby potentially missing the middle and widest part of the PVs. In contrast, the underestimation of the right sided PV diameters may be due to the fact that the exact PV-LA junction can be challenging to visualize in transversal cross-sections. However, since radiofrequency current is typically applied outside the PVs, this should have little implications for the safety of the ablation procedure.

The present study shows that 3D mapping with ICE provides an accurate visualization of PV ostia and PV anatomy with a high sensitivity for detecting additional PVs and gives a good estimation of PV dimensions, as compared with MSCT.

Clinical implications

The integration of MSCT with electroanatomical mapping allows accurate placement of ablation lesions ¹⁵ and has improved the outcome of anatomically guided RFCA targeting the PVs ⁶. However, it is reported that the accuracy of navigating with MSCT integration depends on the quality of the registration

process⁷. With the release of a new electroanatomical mapping system that allows integration of ICE it has become possible to acquire calibrated real-time 3D anatomical information without performing a manual registration process.

The ablation procedures in this study were guided by a 3D map made with ICE, integrated with a MSCT surface image. Importantly, this study demonstrates that 3D mapping with ICE alone provides accurate visualization of the LA geometry and PV ostia which is required to safely perform RFCA for AF targeting the PVs. Therefore it should be possible to perform an anatomically guided ablation procedure targeting the PVs on 3D mapping with ICE alone. This may result in a considerable reduction in radiation exposure for the patient. Further studies are therefore needed to fully explore the value of this promising new technique.

Limitations

This study represents an initial experience with 3D mapping using ICE to guide RFCA for AF. The time necessary to make a map with ICE was therefore relatively long. However, due to a clear learning curve, this time decreased in the later procedures. Therefore, it can be expected that the time needed to make a 3D ICE map can be shortened significantly.

In this study RFCA was guided by the 3D map made with ICE and integrated with the MSCT image. As a consequence no data has been acquired on guidance by 3D ICE mapping alone. Furthermore, at present no data is available on the outcome of the ablation procedures.

Intracardiac echocardiography allows real-time visualization of important cardiac structures. However, some areas of the LA may be challenging to visualize with ICE due to their parallel orientation to the ultrasound beam. Examples of these areas are the right sided PV-LA junction and the left side of the anterior wall. By positioning the ICE catheter inside the

right ventricle these structures can be visualized from another angle thereby providing more insight in LA and PV anatomy. Additionally, conventional electroanatomical mapping can also be used to acquire anatomical information in these and other areas.

Three-dimensional mapping with ICE is very sensitive to respiratory phase. Small differences in respiratory phase during image acquisition may result in contours situated outside the interpolated continuity of the other contours of the 3D map. However, by acquiring all ICE images during expiratory breath hold, consistent sets of contours could be acquired in all patients.

Three-dimensional mapping with ICE is a very promising but expensive technique. The ICE catheters used in this study are single-use only and a dedicated mapping system with image integration modules is needed to integrate ICE with the electroanatomical mapping and MSCT images. Furthermore this technology is only available on one electroanatomical mapping system (CARTO XP) and on limited echocardiographic machines (Sequoia ultrasound system and Cypress ultrasound system, Siemens Medical Solutions). Nonetheless, integration of ICE provides accurate anatomical information that could potentially replace MSCT integration in RFCA for AF. Replacing MSCT would render the use of ICE cost-efficient and would reduce radiation exposure to the patient. Furthermore, the ability to acquire registered real-time anatomical information of important structures with ICE has a significant additional value compared to MSCT integration.

Conclusions

Using a novel mapping system that allows integration of ICE and electroanatomical mapping it is feasible to create a real-time registered 3D

shell of LA and PV anatomy. Furthermore, the 3D map created with ICE can accurately be integrated with a MSCT surface image. This approach combines real-time anatomy with high detailed anatomy potentially providing highly accurate lesion placement during anatomical ablation procedures.

References

1. Haissaguerre M, Jais P, Shah DC, Takahashi A, Hocini M, Quiniou G, Garrigue S, Le MA, Le MP, Clementy J Spontaneous initiation of atrial fibrillation by ectopic beats originating in the pulmonary veins. *N Engl J Med* 1998;339:659-666.
2. Calkins H, Brugada J, Packer DL, Cappato R, Chen SA, Crijns HJ, Damiano RJ, Jr., Davies DW, Haines DE, Haissaguerre M, Ilescu S, Jackman W, Jais P, Kottkamp H, Kuck KH, Lindsay BD, Marchlinski FE, McCarthy PM, Mont JL, Morady F, Nademanee K, Natale A, Pappone C, Prystowsky E, Raviele A, Ruskin JN, Shemin RJ HRS/EHRA/ECAS expert Consensus Statement on catheter and surgical ablation of atrial fibrillation: recommendations for personnel, policy, procedures and follow-up. A report of the Heart Rhythm Society (HRS) Task Force on catheter and surgical ablation of atrial fibrillation. *Heart Rhythm* 2007;4:816-861.
3. Mansour M, Holmvang G, Sosnovik D, Migrino R, Abbara S, Ruskin J, Keane D Assessment of pulmonary vein anatomic variability by magnetic resonance imaging: implications for catheter ablation techniques for atrial fibrillation. *J Cardiovasc Electrophysiol* 2004;15:387-393.
4. Jongbloed MR, Bax JJ, Lamb HJ, Dirksen MS, Zeppenfeld K, van der Wall EE, de RA, Schalij MJ Multislice computed tomography versus intracardiac echocardiography to evaluate the pulmonary veins before radiofrequency catheter ablation of atrial fibrillation: a head-to-head comparison. *J Am Coll Cardiol* 2005;45:343-350.
5. Tops LF, Bax JJ, Zeppenfeld K, Jongbloed MR, Lamb HJ, van der Wall EE, Schalij MJ Fusion of multislice computed tomography imaging with three-dimensional electroanatomic mapping to guide radiofrequency catheter ablation procedures. *Heart Rhythm* 2005;2:1076-1081.
6. Kistler PM, Rajappan K, Jahngir M, Earley MJ, Harris S, Abrams D, Gupta D, Liew R, Ellis S, Sporton SC, Schilling RJ The impact of CT image integration into an electroanatomic mapping system on clinical outcomes of catheter ablation of atrial fibrillation. *J Cardiovasc Electrophysiol* 2006;17:1093-1101.
7. Fahmy TS, Mlcochova H, Wazni OM, Patel D, Cihak R, Kanj M, Beheiry S, Burkhardt JD, Dresing T, Hao S, Tchou P, Kautzner J, Schweikert RA, Arruda M, Saliba W, Natale A Intracardiac echo-guided image integration: optimizing strategies for registration. *J Cardiovasc Electrophysiol* 2007;18:276-282.
8. Marom EM, Herndon JE, Kim YH, McAdams HP Variations in pulmonary venous drainage to the left atrium: implications for radiofrequency ablation. *Radiology* 2004;230:824-829.
9. Fuster V, Ryden LE, Cannom DS, Crijns HJ, Curtis AB, Ellenbogen KA, Halperin JL, Le Heuzey JY, Kay GN, Lowe JE, Olsson SB, Prystowsky EN, Tamargo JL, Wann S, Smith SC, Jr., Jacobs AK, Adams CD, Anderson JL, Antman EM, Hunt SA, Nishimura R, Ornato JP, Page RL, Riegel B, Priori SG, Blanc JJ, Budaj A, Camm AJ, Dean V, Deckers JW, Despres C, Dickstein K, Lekakis J, McGregor K, Metra M, Morais J, Osterspey A, Zamorano JL ACC/AHA/ESC 2006 guidelines for the management of patients with atrial fibrillation--executive summary: a report of the American College of Cardiology/American Heart Association Task Force on Practice Guidelines and the European Society of Cardiology Committee for Practice Guidelines (Writing Committee to Revise the 2001 Guidelines for the Management of Patients With Atrial Fibrillation). *J Am Coll Cardiol* 2006;48:854-906.
10. Khaykin Y, Klemm O, Verma A First human experience with real-time integration of intracardiac echocardiography and 3D electroanatomical imaging to guide right free wall accessory pathway ablation. *Europace* 2008;10:116-117.

11. Okumura Y, Henz BD, Johnson SB, Bunch TJ, O'Brien CJ, Hodge DO, Altman A, Govari A, Packer DL Three-Dimensional Ultrasound for Image-Guided Mapping and Intervention: Methods, Quantitative Validation, and Clinical Feasibility of a Novel Multimodality Image Mapping System. *Circ Arrhythmia Electrophysiol* 2008;1:110-119.
12. Khaykin, Y., Klemm, O., Whaley, B, Seabrook, C, Beardsall, M, Wulffhart, Z et al. First human experience with real time integration of intracardiac echocardiography and 3D electroanatomical imaging to guide pulmonary vein antrum isolation. *J.Am.Coll.Cardiol.* 51(10), A1-A34. 11-3-2008.
13. Khaykin, Y, Skanes, A, Wulffhart, Z, Gula, L, Whaley, B, Oosthuizen, R et al. Intracardiac ECHO Integration With Three Dimensional Mapping: Role in AF Ablation. *JAFIB* . 2008.
14. Tops LF, van der Wall EE, Schalij MJ, Bax JJ Multi-modality imaging to assess left atrial size, anatomy and function. *Heart* 2007;93:1461-1470.
15. Dong J, Calkins H, Solomon SB, Lai S, Dalal D, Lardo AC, Brem E, Preiss A, Berger RD, Halperin H, Dickfeld T Integrated electroanatomic mapping with three-dimensional computed tomographic images for real-time guided ablations. *Circulation* 2006;113:186-194.
16. Kistler PM, Earley MJ, Harris S, Abrams D, Ellis S, Sporton SC, Schilling RJ Validation of three-dimensional cardiac image integration: use of integrated CT image into electroanatomic mapping system to perform catheter ablation of atrial fibrillation. *J Cardiovasc Electrophysiol* 2006;17:341-348.
17. Martinek M, Nesser HJ, Aichinger J, Boehm G, Purerfellner H Accuracy of integration of multislice computed tomography imaging into three-dimensional electroanatomic mapping for real-time guided radiofrequency ablation of left atrial fibrillation-influence of heart rhythm and radiofrequency lesions. *J Interv Card Electrophysiol* 2006;17:85-92.
18. Dong J, Dalal D, Scherr D, Cheema A, Nazarian S, Bilchick K, Almasry I, Cheng A, Henrikson CA, Spragg D, Marine JE, Berger RD, Calkins H Impact of heart rhythm status on registration accuracy of the left atrium for catheter ablation of atrial fibrillation. *J Cardiovasc Electrophysiol* 2007;18:1269-1276.
19. Wood MA, Wittkamp M, Henry D, Martin R, Nixon JV, Shepard RK, Ellenbogen KA A comparison of pulmonary vein ostial anatomy by computerized tomography, echocardiography, and venography in patients with atrial fibrillation having radiofrequency catheter ablation. *Am J Cardiol* 2004;93:49-53.

Chapter 10

Real-time integration of intracardiac echocardiography to facilitate atrial tachycardia ablation in a patient with a Senning baffle

Dennis W. den Uijl, Nico A. Blom, Adrianus P. Wijnmaalen, Jeroen J. Bax, Martin J. Schalij, Katja Zeppenfeld.

Circ Arrhythm Electrophysiol. 2009 Oct;2(5):e28-30



Introduction

This case-report concerns a 10-year-old boy who previously underwent a Senning operation for transposition of the great arteries with an intramural course of the coronary arteries. The patient suffered from recurrent episodes of atrial tachycardia (AT) with 1:1 atrioventricular conduction which caused, in combination with dysfunction of the systemic right ventricle, hemodynamic instability. Unresponsive to antiarrhythmic drug treatment, the patient was referred to our institution for an electrophysiological study and radiofrequency catheter ablation.

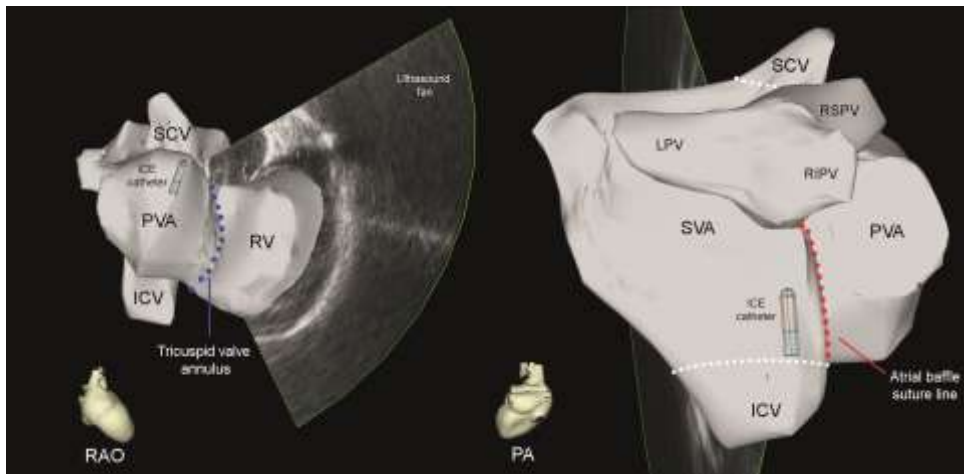


Figure 1. A three-dimensional shell of the cardiac anatomy created with intracardiac echocardiography (ICE). Positioning the ICE catheter inside the systemic venous atrium (SVA), anatomical and surgical lines of conduction block were identified such as caval veins, tricuspid valve annulus and atrial baffle suture line. ICV = inferior caval vein, LPV = left pulmonary veins, PA = posterior-anterior view, PVA = pulmonary venous atrium, RAO = right anterior oblique view, RIPV = right inferior pulmonary vein, RSPV = right superior pulmonary vein, RV = right ventricle, SCV = superior caval vein.

Electrophysiological examination and ablation

The procedure was performed under general anesthesia. Because the AT caused hemodynamic instability, the mapping procedure was aimed at

identification of the arrhythmogenic substrate and critical isthmus of a presumed macro-reentrant circuit with only brief episodes of induced tachycardia. First, a registered three-dimensional (3D) shell of the cardiac anatomy was created on an electroanatomical mapping system (Cartosound, Biosense Webster, Diamond Bar, California, USA) using intracardiac echocardiography (ICE). By positioning the ICE catheter inside the systemic venous atrium, the entire cardiac anatomy could be visualized including structures that form a potential area of conduction block such as the caval veins, the tricuspid valve annulus and surgical suture lines (e.g. atrial baffle suture line)(Figure 1). Second, bipolar voltage mapping of the systemic venous atrium was performed during sinus rhythm to further evaluate the arrhythmogenic substrate and to confirm areas of conduction block caused by surgical incisions (Figure 2). An area of low voltages (>0.5 mV) and persistent double potentials was found near the inter-atrial septum, confirming the location of the atrial baffle suture line. Based on these findings and the current literature on tachycardia ablation in Senning patients,¹ a selection of potential reentry circuit isthmus sites was made (Figure 2). Subsequently, the AT was induced and reentry was confirmed as the underlying mechanism by entrainment mapping at the selected sites. The responses to entrainment are given in figure 2. Pacing near the cavotricuspid isthmus (CTI) from inside the pulmonary venous atrium resulted in identical flutter-wave (F-wave) morphology in all 12 electrocardiogram leads and a post-pacing interval similar to the intraatrial reentrant tachycardia (IART) cycle length (Figure 2), indicating a CTI dependent flutter. Most likely, the reentrant circuit involved the posterior wall of the systemic venous atrium with the atrial baffle suture line acting as the posterior barrier, the anterior septal remnant and the CTI. A linear lesion was created between the tricuspid valve annulus and inferior caval vein (Figure 3). During ablation, the IART cycle length progressively prolonged until finally

the IART terminated. Importantly, in Senning patients the CTI is divided into a systemic venous part and a pulmonary venous part by the atrial baffle. To assure a complete line of block, applications were delivered on both sides of the CTI. At the end of the procedure the IART was no longer inducible. During the 5-month follow-up period no recurrences have been observed.

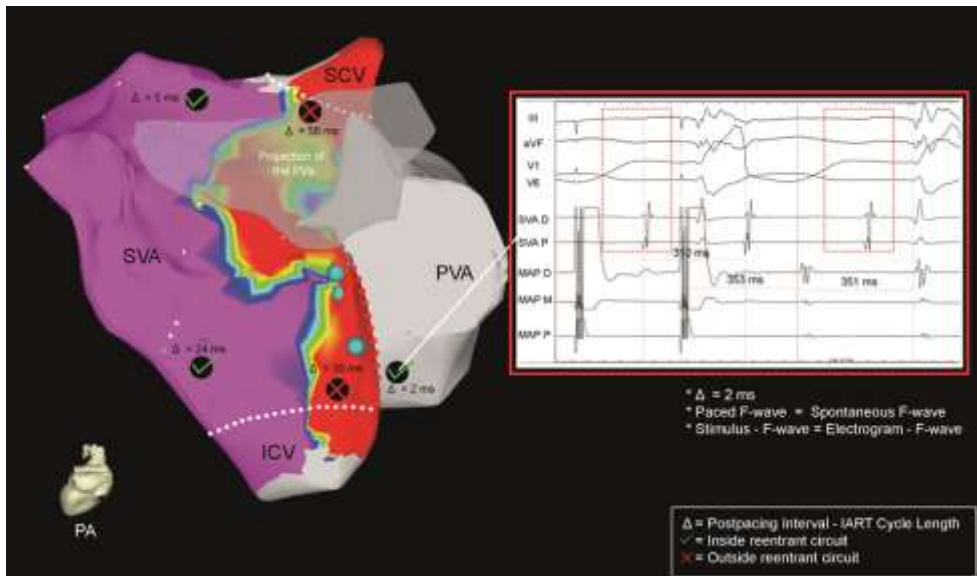


Figure 2. Bipolar voltage map of the systemic venous atrium (SVA) integrated with the three-dimensional shell of the cardiac anatomy created with intracardiac echocardiography in a posterior view. Bipolar voltages are color coded: low voltages (arbitrarily defined as <0.5 mV) are displayed in red, high voltages (≥ 0.5 mV) are displayed in pink. Green dots represent sites with double potentials. Black dots represent sites selected for entrainment pacing during intraatrial reentrant tachycardia (IART). For each selected site the difference between post-pacing interval and tachycardia cycle length (Δ) is given. Additionally, a tracing of the response to entrainment pacing at the cavotricuspid isthmus is given (white box). The tracing includes surface electrocardiogram leads III, aVF, V1, V6 and intracardiac recordings from the reference catheter inside the SVA and the mapping catheter (p = proximal, m = mid and d = distal). Pacing was performed from the distal electrodes of the mapping catheter (first two beats on each tracing). ICV = inferior caval vein, MAP = mapping catheter, PA = posterior-anterior view, PVS = pulmonary veins, SCV = superior caval vein.

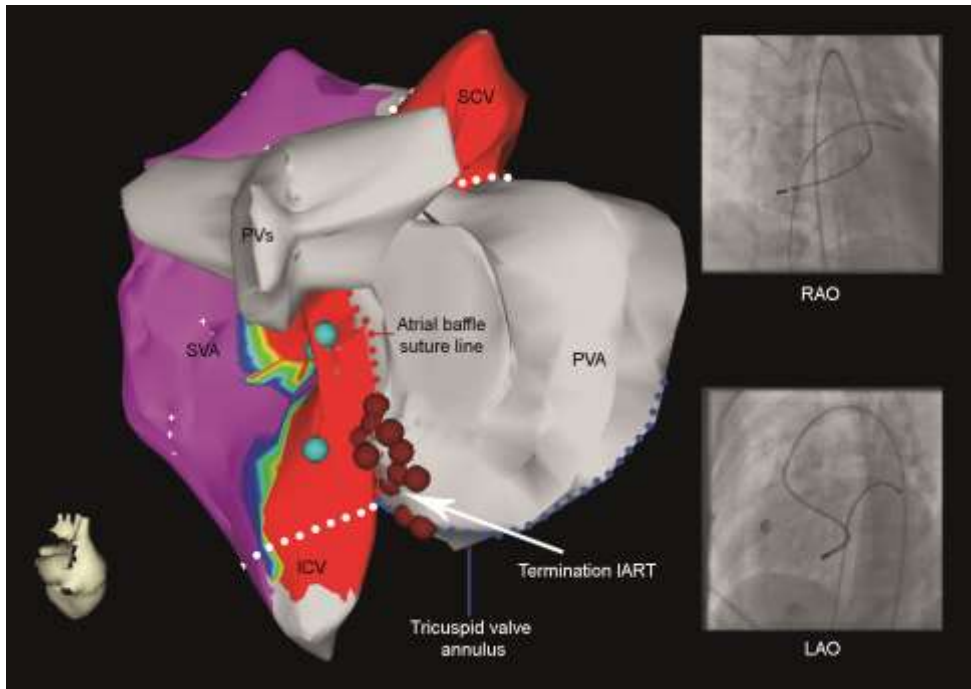


Figure 3. Map containing voltage data of the systemic venous atrium (SVA) and anatomical data acquired with intracardiac echocardiography (seen from a right posterior oblique view; color coding similar as in figure 2). The ablation catheter was positioned inside the pulmonary venous atrium using a retrograde approach. A linear radiofrequency (RF) lesion connecting the tricuspid valve annulus and inferior caval vein resulted in prolongation of the intraatrial reentrant tachycardia (IART) cycle length and eventually in IART termination (red dots represent RF ablation sites, white arrow indicates site of termination). Insets: catheter position during termination of the tachycardia on a fluoroscopic right anterior oblique (RAO) and left anterior oblique (LAO) view.

Discussion

Intra-atrial reentry is the most common mechanism for supraventricular tachycardia in patients with a Mustard or Senning baffle.^{1,2} Image integration (e.g. Multi-Slice Computed Tomography and electroanatomical mapping) can facilitate the ablation of these tachycardias by visualizing the complex cardiac anatomy and its relation to the position of the ablation catheter.³ However, the accuracy of image integration is limited by the quality of the registration process.⁴ Differences in heart rate, heart rhythm and fluid status can negatively

influence this process. In the present report, a new anatomical mapping technique is used to create a 3D anatomical map of the cardiac anatomy with ICE. This technique does not require a registration process and allows visualization of landmark structures with minimal radiation exposure. The anatomical information acquired with ICE in combination with rough voltage mapping enabled us to identify and confirm the critical isthmus by limited entrainment mapping at selected sites during only brief episodes of the tachycardia.

References

1. Kanter RJ, Papagiannis J, Carboni MP, Ungerleider RM, Sanders WE, Wharton JM Radiofrequency catheter ablation of supraventricular tachycardia substrates after mustard and senning operations for d-transposition of the great arteries. *J Am Coll Cardiol* 2000;35:428-441.
2. Zrenner B, Dong J, Schrieck J, Ndrepepa G, Meisner H, Kaemmerer H, Schomig A, Hess J, Schmitt C Delineation of intra-atrial reentrant tachycardia circuits after mustard operation for transposition of the great arteries using biatrial electroanatomic mapping and entrainment mapping. *J Cardiovasc Electrophysiol* 2003;14:1302-1310.
3. Aryana A, Liberthson RR, Heist EK, d'Avila A, Mandapati R, Cury RC, Ruskin JN, Mansour MC Images in cardiovascular medicine. Ablation of atrial flutter in a patient with mustard procedure using integration of real-time electroanatomical mapping with 3-dimensional computed tomographic imaging. *Circulation* 2007;116:e315-e316.
4. Fahmy TS, Mlcochova H, Wazni OM, Patel D, Cihak R, Kanj M, Beheiry S, Burkhardt JD, Dresing T, Hao S, Tchou P, Kautzner J, Schweikert RA, Arruda M, Saliba W, Natale A Intracardiac echo-guided image integration: optimizing strategies for registration. *J Cardiovasc Electrophysiol* 2007;18:276-282.

Chapter 11

Anatomical perspective on radiofrequency
ablation of AV nodal reentry tachycardia after

Mustard correction for transposition of the great
arteries

Monique R.M. Jongbloed, Tim P. Kelder, Dennis W. den Uijl, Margot M.
Bartelings, Sander G. Molhoek, Ramon Tukkie, Martin J. Schalij.

PACE 2012; 35:e287–e290



Abstract

A case of radiofrequency catheter ablation of atrioventricular (AV) nodal re-entry tachycardia, in a patient with transposition of the great arteries after venous rerouting according to Mustard, is described. An electroanatomical map of the His and AV nodal region was created from inside the systemic venous atrium. Retrograde mapping of the pulmonary venous atrium was performed and the arterial catheter retracted to a position in close proximity to the venous catheter inside the intra-atrial baffle. This position was chosen to deliver radiofrequency current.

Introduction

Transposition of the great arteries (TGA) is a congenital cardiac malformation characterized by concordant atrioventricular (AV) and discordant ventriculo-arterial connections that accounts for approximately 2.4% of all congenital heart diseases.¹ Currently, anatomical correction of TGA by performing an arterial switch procedure is the treatment of first choice. This operation is regularly performed since the 1980s, before which surgical treatment consisted of physiological correction with venous rerouting of blood according to Mustard or Senning (Figure 1).^{2,3} Thus, the majority of adults with TGA have undergone either a Mustard or Senning procedure. Common complications following Mustard and Senning procedures include conduction disorders and arrhythmias, often of atrial origin. The mechanism most commonly described is intra-atrial re-entry based on scar tissue,⁴ whereas AV nodal re-entry is far less common. In patients with normal cardiac anatomy, radiofrequency catheter ablation (RFCA) is highly effective.⁵ Literature on RFCA in patients after venous switch procedures is, however, limited.^{4,6-8}

In this paper, we describe a case of RFCA of AV nodal re-entry tachycardia (AVNRT) performed in a patient with TGA treated by venous rerouting according to Mustard, with focus on the anatomical situation following this operation and implications for the ablation procedure.

Case presentation

A 24-year-old man was referred for recurrent episodes of narrow complex tachycardia, despite the use of different antiarrhythmic drugs. The patient was born with TGA, for which a Mustard operation was performed 2 weeks after birth. Tachycardia events had a sudden onset and its clinical signs were palpitations and laryngeal discomfort. Chemical cardioversion using adenosine

was necessary to terminate events. On physical examination, blood pressure was 140/85 mmHg and heart rate 65 beats per minute (bpm). The electrocardiogram showed right ventricular (RV) hypertrophy, consistent with a systemic RV after the Mustard procedure. Laboratory tests were normal. Transthoracic echocardiography showed a dilated RV with reasonable function (tricuspid annular plane systolic excursion 14 mm) and minor AV leakage. Given the frequent symptomatic recurrences, it was decided to perform an electrophysiological examination and subsequent ablation.

Electrophysiological examination and ablation

The procedure was performed under local anaesthesia and guided by fluoroscopy and a three-dimensional (3D) non-fluoroscopic mapping system (**CARTO XP™, Biosense Webster, Diamond Bar, CA, USA**). A 7-F ablation catheter (Navistar, Biosense Webster) and two 6-F quadripolar electrophysiological catheters were introduced through the right femoral vein into the systemic venous atrium (His position, systemic venous atrium, and left ventricle, respectively). A second 7-F ablation catheter was later inserted through the right femoral artery and guided via the aorta, RV, and tricuspid valve to the pulmonary venous atrium, containing the AV node. A bolus of intravenous Heparin (7,500 IU) was administered.

At the beginning of the electrophysiological study, the patient was in sinus rhythm (cycle length [CL] 1,100 ms, AV 82 ms, His ventricular 40 ms). The antegrade Wenckebach point was at 300 ms and a significant A-His jump (53 ms) was observed. The retrograde Wenckebach point was at 340 ms and there was concentric decremental ventriculoatrial (VA) conduction, suggesting that retrograde conduction occurred through the AV node. During catheter manipulation, there were spontaneous episodes of tachycardia with a cycle length of 370–390 ms and a short VA interval of 58 ms. Atrial and ventricular

extrastimulations could not reset the tachycardia and it was consistently noted that the tachycardia started with a prolongation of the atrial-to-His interval, all of this being compatible with the diagnosis common-type AVNRT.⁷ Importantly, the tachycardia could reproducibly be induced by atrial electrical stimulation with a cycle length of 600/400 ms and two extrastimulations (Figure 1).

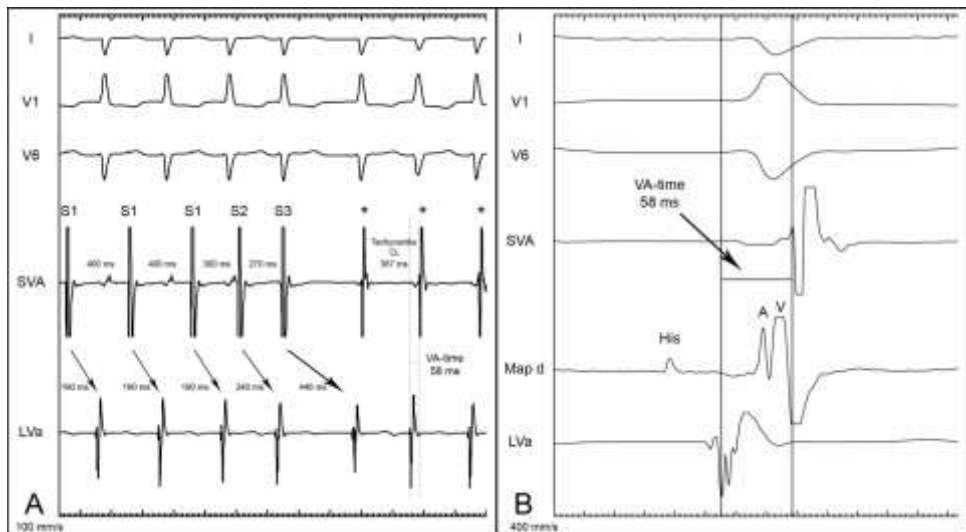


Figure 1. (panel A) Induction of the tachycardia by atrial programmed stimulation (100 mm/s). The tracing includes surface electrocardiogram leads I, V1, V6, and intracardiac recordings from electrophysiological catheters inside the systemic venous atrium (SVA) and left ventricle apex (LVa). In this tracing electrical stimulation with 400 ms (S1) and extrastimulation with 300 ms (S2) and 270 ms (S3) resulted in a critical prolongation of the atrioventricular (AV) time (190–240–446 ms) after which the tachycardia started (*). The tachycardia cycle length (CL) was 387 ms and the ventriculoatrial (VA) time was 58 ms. (panel B) Tracing of the tachycardia including a His registration (400 mm/s). The tracing includes surface electrocardiogram leads I, V1, V6, and intracardiac recordings from electrophysiological catheters inside the SVA, LVa, as well as from the mapping catheter, which was placed in His position. On the distal electrodes of the mapping catheter (Map d) a clear His potential can be seen followed by a superimposed atrial (A) and ventricular (V) signal.

Next, to obtain a 3D reconstruction of the complex atrial anatomy, an electroanatomical map of the His and AV nodal region was created from inside the systemic venous atrium using the CARTO system. Anatomical references (including His position and AV node) were marked on the map (Figure 2). Well-defined His signals as well as fragmented signals could be obtained from inside the intra-atrial baffle. However, since these signals were most likely derived from the AV node positioned in the posterior wall of the pulmonary venous atrium on the other side of the baffle, ablation at this site would mean that radiofrequency current had to be applied through the baffle. Although this was considered as an option, a direct approach via the pulmonary venous atrium was preferred to minimize the risk of injury to the baffle. Subsequently, retrograde mapping of the pulmonary venous atrium was performed by inserting the catheter through the femoral artery, passing the aorta, RV, and tricuspid valve into the pulmonary venous atrium. The arterial catheter was retracted to a position in close proximity to the venous catheter inside the intra-atrial baffle (Figure 2). This position was chosen to deliver radiofrequency current. Radiofrequency current was applied at 60 W with a maximum of 30 seconds on each ablation site. Location markers were placed at each ablation site on the electroanatomical map to obtain optimal insight in catheter positions in relation to the AV node and His bundle. During ablation of the slow pathway, an accelerated junctional rhythm consistently occurred. After ablation, AVNRT could no longer be induced with induction pacing even after intravenous administration of isoprenaline. The patient remained free of tachycardia during follow-up (3 months), without antiarrhythmic medication.

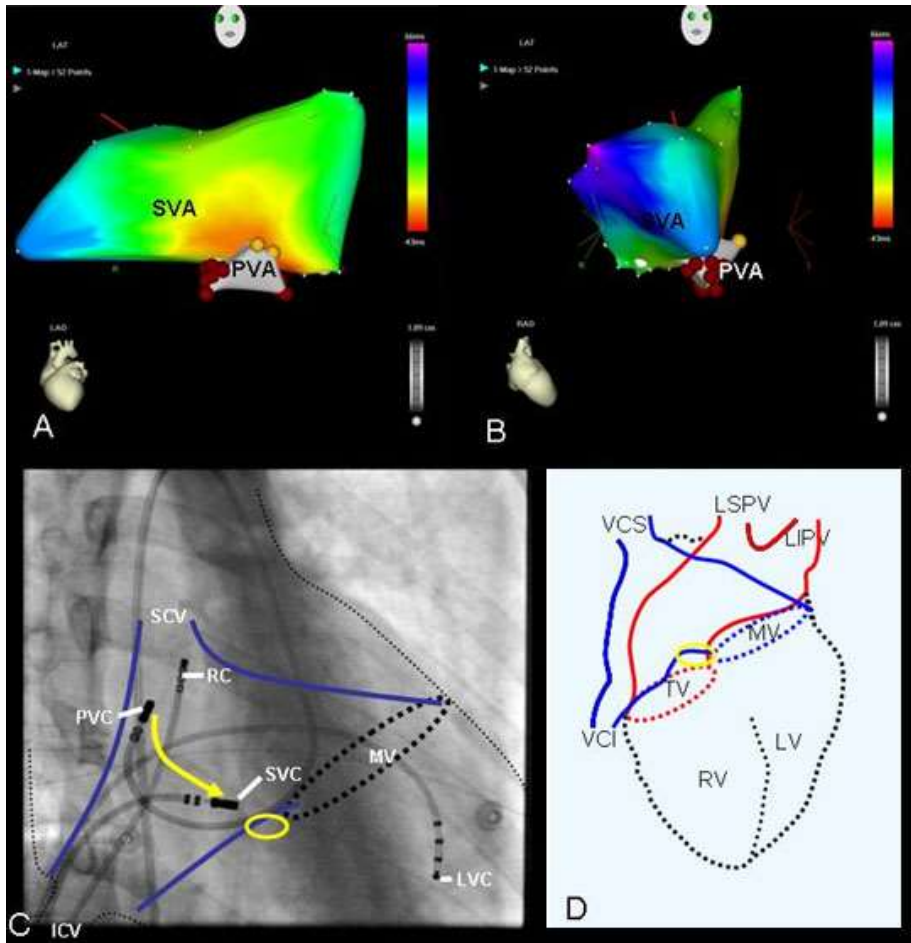


Figure 2. Three-dimensional electroanatomical map of the atrioventricular junction. Left anterior (A) and right anterior (B) oblique views. Anatomical maps were obtained from the systemic venous atrium (SVA) and pulmonary venous atrium (PVA). Red dots implicate ablation points in the area of the AV node, posterior in the PVA, inferior to the intraatrial baffle. Yellow dots indicate the His position. (C) Fluoroscopy. A reference catheter (RC) is located high in the SVA and a mapping catheter (SVC = systemic venous catheter) inferiorly in the intraatrial baffle pointing in the direction where the AV node is located just inferior to the baffle. The arterial catheter has been inserted in a retrograde fashion via the aorta, right ventricle, and tricuspid valve into the pulmonary venous atrium (PVC = pulmonary venous catheter) that contains the AV node. This catheter was retracted to a position in close proximity to the catheter in the SVA, close to the AV node, as indicated by the yellow arrow. At this location, radiofrequency current was applied. (D) Scheme of the anatomy. The AV node is indicated as a yellow oval. LIPV = left inferior pulmonary vein; LSPV = left superior pulmonary vein; LVC = left ventricular catheter; MV = mitral valve; TV = tricuspid valve; VCI = inferior caval vein; VCS = superior caval vein.

Discussion

This report describes RFCA of AVNRT in a patient after venous rerouting according to Mustard. In patients with normal cardiac anatomy, ablation of AVNRT is usually performed by a transvenous approach. In patients with TGA, the location of the AV node inside the right atrium is similar to patients with normal cardiac anatomy. However, after venous rerouting the caval veins drain into the systemic venous atrium/intra-atrial baffle, connected to the LV. As a consequence, the AV node is localized inside the pulmonary venous part of the atria and cannot be reached through a transvenous approach. Although a transbaffle approach to ablate AVNRT has been described,⁸ this approach constitutes the risk of damaging the intra-atrial baffle, thereby creating a shunt between the systemic venous and pulmonary venous atria with the risk of hemodynamic overload or paradox embolism. Cryoablation is an alternative; however, there are reports indicating that this approach may be more time consuming with higher recurrence rates.⁹ Still, its application might prove safer in terms of catheter stability in patients with complex anatomy. In the current situation, we preferred the arterial, retrograde approach. A disadvantage of this approach may be the difficult positioning of the catheters. Therefore, optimal insight and knowledge of the anatomy is mandatory. In the present report, we describe this procedure using intraoperative fluoroscopy and CARTO mapping.

A disadvantage of the retrograde arterial approach in ablation of AVNRT in Mustard patients is the relatively sharp angle that the ablation catheter must make in order to reach the location of the AV node. The venous catheter in the baffle toward the mitral valve (below which the AV node is located) can be used to guide the arterial catheter in the pulmonary venous atrium, as was described in our case. Also, the use of multidirectional steerable catheters may facilitate ablation using the arterial approach.

References

1. Warnes CA Transposition of the great arteries. *Circulation* 2006;114:2699-2709.
2. Mustard WT, Keith JD, Trusler GA, Fowler R, Kidd L The Surgical Management of Transposition of the Great Vessels. *J Thorac Cardiovasc Surg* 1964;48:953-958.
3. Senning A Surgical correction of transposition of the great vessels. *Surgery* 1959;45:966-980.
4. Khairy P, Van Hare GF Catheter ablation in transposition of the great arteries with Mustard or Senning baffles. *Heart Rhythm* 2009;6:283-289.
5. Akhtar M, Jazayeri MR, Sra J, Blanck Z, Deshpande S, Dhala A Atrioventricular nodal reentry. Clinical, electrophysiological, and therapeutic considerations. *Circulation* 1993;88:282-295.
6. Greene AE, Skinner JR, Dubin AM, Collins KK, Van Hare GF The electrophysiology of atrioventricular nodal reentry tachycardia following the Mustard or Senning procedure and its radiofrequency ablation. *Cardiol Young* 2005;15:611-616.
7. Kanter RJ, Papagiannis J, Carboni MP, Ungerleider RM, Sanders WE, Wharton JM Radiofrequency catheter ablation of supraventricular tachycardia substrates after mustard and senning operations for d-transposition of the great arteries. *J Am Coll Cardiol* 2000;35:428-441.
8. Khairy P, Fournier A, Mercier LA, Dubuc M Wolff-Parkinson-white syndrome in d-transposition of the great arteries and mustard baffle. *Heart Rhythm* 2006;3:853-856.
9. Zrenner B, Dong J, Schreieck J, Deisenhofer I, Estner H, Luani B, Karch M, Schmitt C Transvenous cryoablation versus radiofrequency ablation of the slow pathway for the treatment of atrioventricular nodal re-entrant tachycardia: a prospective randomized pilot study. *Eur Heart J* 2004;25:2226-2231.

Samenvatting en conclusie



Samenvatting en conclusie

De algemene introductie van deze thesis geeft een overzicht van het belang van pre-procedurele diagnostiek bij patiënten die in aanmerking komen voor radiofrequente catheter ablatie (RFCA) voor atriumfibrilleren (AF). Nieuwe echocardiografische technieken om atriale remodelering op te sporen worden besproken, alsmede de plaats van de cardiale computed tomography (CT) en natriuretische peptiden binnen de pre-procedurele evaluatie. Daarnaast wordt een overzicht gegeven van het gebruik van beeldvormende technieken tijdens RFCA van complexe atriale ritmestoornissen en worden de voor- en nadelen van de meest gebruikte modaliteiten besproken. Ten slotte wordt de integratie van verschillende beeldvormingsmodaliteiten besproken met als doel de individuele beperkingen van de verschillende technieken te compenseren.

Deel I: Pre-procedurele evaluatie voorafgaand aan radiofrequente catheter ablatie voor atriumfibrilleren

Het eerste deel van deze thesis richt zich op de rol van echocardiografie, cardiale CT en natriuretische peptiden om patiënten te identificeren met een hoge kans op sinus ritme na RFCA voor AF.

Hoofdstuk 1 betreft een editoriaal commentaar over de beperkingen van linker boezem grootte als voorspeller van recidief AF na RFCA. De grootte van de linker boezem wordt over het algemeen bepaald door de anterior-posterior diameter te meten gebruikmakend van twee-dimensionele echocardiografie. Echter de vergroting van de linker boezem kan asymmetrisch zijn en daarom zou een drie-dimensionele evaluatie wellicht een beter weergave geven van de werkelijke grootte. Een drie-dimensionele meting van de linker boezem grootte kan worden verkregen middels cardiale CT, drie-dimensionele echocardiografie en magnetische resonantie imaging.

In Hoofdstuk 2 wordt calibrated integrated backscatter gebruikt om echocardiografisch de mate van linker boezem fibrosering (verlittekening) in te schatten en dit te relateren aan de effectiviteit van RFCA voor AF. Calibrated integrated backscatter is een echocardiografische techniek waarmee weefselkarakterisering kan worden verricht op basis van de weerkaatsing van ultrasoon geluid. In een groep van 170 patiënten bleek een hoge mate van fibrosering van de linker boezem voorspellend te zijn voor een AF recidief na RFCA (OR 1.217 per dB, $p < 0.001$). Daarnaast bleek dat het gecombineerd inschatten van de hoeveelheid linker boezem fibrosering en linker boezem grootte een significante verbetering gaf van de precisie waarmee patiënten met een grote kans op een succesvolle ablatie konden worden geïdentificeerd.

Hoofdstuk 3 beschrijft de invloed van de totale atriale geleidingstijd op de effectiviteit van RFCA voor AF. De totale atriale geleidingstijd geeft een indruk van de mate waarin er zowel elektrische als structurele remodelering van de boezems heeft plaatsgevonden waardoor AF kan ontstaan en in stand wordt gehouden. De totale atriale geleidingstijd wordt gemeten middels tissue Doppler imaging door de tijd te meten tussen het begin van de p-golf in **afleiding II van het electrocardiogram en de piek van de A'-golf** op de tissue Doppler opname van de laterale wand van de linker boezem (PA-TDI tijd). De PA-TDI tijd bleek beter in staat om een recidief AF na RFCA te voorspellen dan conventionele maten zoals linker boezem grootte (receiver-operator characteristics analyses: area under the curve 0.765 vs. 0.561, respectievelijk).

In Hoofdstuk 4 wordt de invloed onderzocht van coronarialijden op de effectiviteit van RFCA voor AF. In een populatie van 125 patiënten werd de aanwezigheid en uitgebreidheid van coronarialijden bepaald door middel van een cardiale CT scan (coronair angiografie en/of calcium score) en dit werd gerelateerd aan het optreden van een recidief AF. De aanwezigheid en de

uitgebreidheid van coronarialijden had geen invloed op de effectiviteit van RFCA voor AF.

Naast informatie over de aanwezigheid en uitgebreidheid van coronarialijden biedt cardiale CT ook informatie over de anatomie van de pulmonaal venen en de linker boezem grootte. In Hoofdstuk 5 wordt de invloed van pulmonaal venen anatomie, pulmonaal venen dimensies en linker boezem dimensies op de effectiviteit van RFCA voor AF bestudeerd. Een atypische configuratie van de rechtzijdige pulmonaal venen, gedefinieerd als een extra uitmondende pulmonaal vene, was aanwezig bij 17% van de patiënten en was geassocieerd met een lager risico op een AF recidief. Er werd geen relatie gevonden tussen linkszijdige pulmonaal venen anatomie en de effectiviteit van RFCA voor AF. Pulmonaal venen dimensies waren eveneens niet voorspellend voor de effectiviteit van RFCA. Linker boezem grootte gemeten met CT bleek een grotere voorspellende waarde te hebben voor een AF recidief dan linker boezem grootte gemeten met twee-dimensionele echocardiografie.

In Hoofdstuk 6 wordt de waarde van natriuretische peptiden (NT-proANP en NT-proBNP) bestudeerd in de evaluatie van patiënten voorafgaand aan RFCA voor AF. In theorie kunnen natriuretische peptiden een aanwijzing geven over de aanwezigheid van een cardiaal lijden dat de effectiviteit van RFCA voor AF beperkt. Bij 87 patiënten met symptomatisch medicatie-resistent AF werden voor de procedure de bloedspiegels van NT-proANP en NT-proBNP bepaald. Alle bloedmonsters werden afgenomen tijdens sinus ritme om een potentieel vertroebelend effect van het AF op de natriuretische peptide spiegels te voorkomen. Na een follow-up van 12 maanden bleek het pre-procedurele NT-proBNP spiegel een onafhankelijke voorspeller van recidief AF na RFCA.

Het eerste deel van deze thesis suggereert dat uitgebreide evaluatie van het aritmogene substraat van de boezems, daarin meenemende de hoeveelheid fibrosering en de elektromechanische eigenschappen, een betere patiënt selectie mogelijk maakt dan aan de hand van linker boezem grootte alleen. Daarnaast suggereren de uitslagen dat het pre-procedureel meten van de natriuretische peptiden een sensitief middel biedt voor het bestaan van een aritmogeen substraat buiten de tijdens RFCA aangepakte pulmonaal venen regio.

Deel II: Beeldvormende technieken ter ondersteuning van radiofrequente catheter ablatie van complexe atriale ritmestoornissen

Het tweede deel van deze thesis beschrijft de rol van beeldvormende technieken en de integratie hiervan tijdens RFCA voor complexe atriale ritmestoornissen. Om dit soort procedures uit te kunnen voeren is een nauwkeurige beeldvorming van de intracardiale catheters in relatie tot de cardiale anatomie noodzakelijk. Daarnaast is, gezien de aanzienlijke stralen belasting voor zowel de patiënt als de operateur, de behoefte aan niet-ioniserende beeldvormende modaliteiten groot.

Hoofdstuk 7 beslaat een overzicht van de verschillende toepassingen van intracardiale echocardiografie tijdens interventie en elektrofysiologische procedures. Intracardiale echocardiografie wordt verricht met een speciale catheter, uitgerust met een ultrasone transducer op de punt, die in de rechter boezem of de rechter ventrikel wordt gepositioneerd. Intracardiale echocardiografie verstrekt real-time anatomische informatie zonder stralingsbelasting en kan gebruikt worden tijdens RFCA procedures. Echter, op dit moment is intracardiale echocardiografie een twee-dimensionele modaliteit en is het niet in staat de hoge mate van detaillering te leveren die cardiale CT wel heeft.

In Hoofdstuk 8 wordt de integratie tussen intracardiale echocardiografie, elektroanatomisch mappen en cardiale CT beschreven om RFCA voor AF mee te faciliteren. Hiervoor wordt een nieuw elektroanatomisch mapping system gebruikt dat in staat is om de positie te bepalen van een speciaal ontworpen echocardiografie catheter en daarmee het twee-dimensionele echo beeld in de drie-dimensionele mapping omgeving kan projecteren. Door het markeren van de endocardiale contouren van de linker boezem en pulmonaal venen op de verschillende echo beelden werd er een drie-dimensionele kaart gecreëerd van de linker boezem op het elektroanatomische mapping systeem. Daarna werd een CT scan van de linker boezem in het mapping systeem geladen en geïntegreerd met de verkregen drie-dimensionele kaart. In een groep van 17 patiënten bleek het mogelijk om een drie-dimensionele kaart te creëren van de linker boezem door middel van intracardiale echocardiografie met een gemiddelde van 31.1 ± 8.5 contouren. De integratie met cardiale CT resulteerde in een gemiddelde afstand tussen kaart en CT reconstructie van 2.2 ± 0.3 mm. Drie-dimensioneel mappen met intracardiale echocardiografie liet een hoge sensitiviteit zien om de pulmonaal venen te detecteren en visualiseren.

Hoofdstuk 9 bestaat uit een case-report over de integratie van intracardiale echocardiografie en elektroanatomisch mappen om de ablatie van een atriale tachycardie te faciliteren bij een jonge patiënt die in het verleden een Senning operatie heeft ondergaan vanwege een transpositie van de grote vaten. De ritmestoornis leidde tot hemodynamische instabiliteit waardoor de mogelijkheid tot activatie mapping tijdens tachycardie werd beperkt. Door de anatomische informatie verkregen met intracardiale echocardiografie in combinatie met het grof in kaart brengen van de atriale voltages bleek het mogelijk om de kritische isthmus te identificeren door

middel van entrainment mapping op een beperkt aantal geselecteerde posities en tijdens slechts korte episodes van tachycardie.

Hoofdstuk 10 beschrijft de casus van een 24-jarige man die in het verleden een Mustard operatie onderging vanwege een transpositie van de grote vaten. Hij werd verwezen vanwege recidiverende tachycardiën. Het elektrofysiologisch onderzoek toonde een AV-knoop re-entry tachycardie aan. Daaropvolgend werd elektroanatomische mapping verricht om de complexe cardiale anatomie in beeld te brengen en vervolgens succesvol RFCA te verrichten van het langzame pad. Afsluitend wordt een beschouwing gegeven van de veranderde anatomische situatie na een Mustard operatie.

Conclusies

De implementatie van nieuwe echocardiografische technieken om atriale remodelering te meten alsmede het gebruik van natriuretische peptiden in de beoordeling van patiënten voorafgaand aan RFCA voor AF, verbetert de identificatie van diegenen met een hoge kans om sinus ritme te verkrijgen na de procedure. De integratie van verschillende beeldvormende modaliteiten tijdens RFCA van complexe atriale ritmestoornissen stelt de operateur in staat om belangrijke cardiale structuren te herkennen, reduceert logischerwijs de stralingsbelasting en verbetert in potentie de uitkomst van deze procedures.

Summary and conclusion



Summary and conclusion

The general introduction outlines the role and importance of pre-procedural evaluation of patients undergoing RFCA for AF. Novel echocardiographic techniques to estimate atrial remodelling are discussed as well as the role of MSCT and natriuretic peptides during the pre-procedural evaluation. In addition, the use of imaging and image integration during RFCA for complex atrial arrhythmias is discussed. An overview of the advantages and limitations of the most common used imaging modalities is provided and the benefit of image integration to overcome these limitations is discussed.

Part I: Pre-procedural evaluation of patients undergoing radiofrequency catheter ablation for atrial fibrillation

The first part of this thesis discusses the role of echocardiography, MSCT and natriuretic peptides in the pre-procedural evaluation to identify patients with a high likelihood to maintain sinus rhythm after RFCA for AF.

Chapter 1 comprises an editorial comment about the limitations of left atrial size as a predictor of AF recurrence after RFCA. Left atrial size is commonly estimated by measuring the anterior-posterior left atrial diameter on two-dimensional echocardiography. However as left atrial enlargement may not be symmetrical, a 3-dimensional evaluation provides a more accurate estimate of true left atrial size. Three-dimensional measurement of left atrial size can be performed MSCT, 3-dimensional echocardiography and magnetic resonance imaging.

In Chapter 2, echocardiography derived calibrated integrated backscatter is used to estimate the extent of left atrial fibrosis and to relate this to the outcome of RFCA for AF. Calibrated integrated backscatter is an echocardiographic technique that allows tissue characterisation based on

ultrasound reflectivity. In a group of 170 patients undergoing RFCA for AF, a high extent of left atrial fibrosis was an independent predictor of AF recurrence (OR 1.217 per dB, $p < 0.001$). Moreover, the combined assessment of left atrial fibrosis and left atrial size significantly improved the accuracy to identify patients with a high likelihood to maintain sinus rhythm.

Chapter 3 describes the impact of total atrial conduction time on the efficacy of RFCA for AF. Total atrial conduction time reflects the extent of both electrical and structural remodelling of the atria and can be assessed using tissue Doppler imaging by measuring the time delay between the onset of the **P-wave in lead II of the surface ECG and the peak A'-wave** on the tissue Doppler tracing of the left atrial lateral wall (PA-TDI duration). The PA-TDI duration demonstrated a superior accuracy to predict AF recurrence after RFCA compared to left atrial size (receiver-operator characteristics analyses: area under the curve 0.765 vs. 0.561, respectively).

In Chapter 4, the impact of coronary artery disease on the efficacy of RFCA for AF is studied. In a population of 125 consecutive patients MDCT is used to determine the presence and extent of coronary artery disease (coronary angiography and/or coronary calcium score) prior to RFCA for AF. The presence and extent of coronary artery disease had no negative impact on the efficacy of RFCA for AF.

In addition to information about the presence of coronary artery disease, multi-slice computed tomography provides information about the pulmonary veins and left atrial dimensions. Chapter 5 studies the impact of pulmonary vein anatomy and dimensions, as well as left atrial dimensions, on the efficacy of RFCA for AF. Atypical anatomy of the right-sided pulmonary veins, defined as an additional right pulmonary vein, was present in 17% of patients and was associated with a lower risk for AF recurrence after RFCA. Left sided pulmonary vein anatomy as well as pulmonary vein dimensions were not

predictive for AF recurrence after RFCA. Left atrial size measured by MSCT demonstrated a superior accuracy to predict AF recurrence compared to left atrial size on two-dimensional echocardiography.

Finally, Chapter 6 describes the role of natriuretic peptides (NT-proANP and NT-proBNP) in the pre-procedural evaluation of patients undergoing RFCA for AF. Theoretically, natriuretic peptides can provide information about the presence and severity of a previously undetected cardiac condition limiting the efficacy of RFCA for AF. In 87 patients with symptomatic drug-refractory AF, pre-procedural serum levels of natriuretic peptide levels were determined. Importantly, all samples were collected during sinus rhythm to avoid the potentially obscuring effect of AF on the natriuretic peptide levels. After a follow-up of 12 months, pre-procedural NT-proBNP was an independent predictor of AF recurrence after RFCA.

The first part of this thesis suggests that comprehensive evaluation of left atrial substrate, taking into consideration the extent of atrial fibrosis and electromechanical properties, may provide a better identification of patients who will benefit from RFCA for AF than measurement of left atrial dimensions. Furthermore, measurement of natriuretic peptides levels may provide a more sensitive marker for the presence of non-pulmonary vein related arrhythmogenic substrate to develop AF.

Part II: Imaging to facilitate radiofrequency catheter ablation of complex atrial arrhythmias

The second part of this thesis describes the role of imaging and image integration to facilitate RFCA of complex atrial arrhythmias. To perform these procedures, accurate visualization of the intracardiac catheters in relation to the cardiac anatomy is crucial. Furthermore, as these procedures are associated

with a high radiation exposure to both patient and operator, the need for non-fluoroscopic imaging modalities has increased.

Chapter 7 comprises an overview of the use of intracardiac echocardiography during interventional and electrophysiological procedures. Intracardiac echocardiography is performed using a catheter with an ultrasound transducer at its tip which is typically positioned inside the right atrium or right ventricle. Intracardiac echocardiography provides real-time information about the cardiac anatomy without radiation exposure and can be used to guide RFCA procedures. However, currently intracardiac echocardiography is a 2-dimensional imaging modality and does not provide the highly detailed anatomical information that multi-slice computed tomography does.

In Chapter 8 the integration of intracardiac echocardiography, electroanatomical mapping and MSCT to guide RFCA for AF is described. A novel electroanatomical mapping system was used that allows tracking of a specifically designed ultrasound catheter thereby allowing to project the 2-dimensional ultrasound image into its 3-dimensional mapping environment. By tracing the endocardial contours of the left atrium and pulmonary veins on these ultrasound images a 3-dimensional map was created on the electroanatomical mapping system. Finally, a pre-procedurally acquire MSCT image of the left atrium was uploaded to the mapping system and integrated with the 3-dimensional map. In a group of 17 patients, 3-dimensional mapping of the left atrium using intracardiac echocardiography was feasible with a mean of 31.1 ± 8.5 contours. Integration with multi-slice computed tomography resulted in a mean distance of 2.2 ± 0.3 mm between the map and the multi-slice computed tomography image. Three-dimensional mapping using intracardiac echocardiography demonstrated a high sensitivity to detect and visualize the pulmonary veins.

Chapter 9 comprises a case-report about the integration of intracardiac echocardiography and electroanatomical mapping to facilitate ablation of an atrial tachycardia in a young patient who previously underwent a Senning operation for transposition of the great arteries. The arrhythmia caused hemodynamic instability thereby limiting activation mapping of the presumed macro-reentrant circuit during on-going tachycardia. However, the anatomic information acquired with intracardiac anatomy in combination with rough voltage mapping enabled the identification and confirmation of the critical isthmus by limited entrainment mapping at selected sites during only brief episodes of tachycardia.

Finally, Chapter 10 describes the case of a 24-year-old male who previously underwent a Mustard operation for transposition of the great arteries and suffered from recurrent episodes of tachycardia. The electrophysiological examination revealed an atrioventricular nodal re-entry tachycardia. Subsequently, electroanatomical mapping was performed to visualize the complex cardiac anatomy and successfully guide RFCA of the slow-pathway. In addition, an anatomical perspective is provided about the cardiac anatomy following a Mustard operation.

Conclusions

Implementation of novel echocardiographic techniques to measure atrial remodelling as well as natriuretic peptide levels in the assessment of patient undergoing RFCA for AF improves the identification of those with a high likelihood to maintain sinus rhythm after the procedure. Moreover, integration of multiple imaging modalities during RFCA of complex atrial arrhythmias allows for an improved identification of important cardiac structures, reduced radiation exposure and potentially an improved outcome.

List of publications

A handwritten signature in black ink, consisting of several stylized, connected letters and flourishes, located at the bottom right of the page.

List of publications

den Uijl DW, Tops LF, Tolosana JM, Schuijf JD, Trines SA, Zeppenfeld K, Bax JJ, Schalij MJ. Real-time integration of intracardiac echocardiography and multislice computed tomography to guide radiofrequency catheter ablation for atrial fibrillation. *Heart Rhythm*. 2008 Oct;5(10):1403-10.

Tops LF, Schalij MJ, den Uijl DW, Abraham TP, Calkins H, Bax JJ. Image integration in catheter ablation of atrial fibrillation. *Europace*. 2008 Nov;10 Suppl 3:iii48-56.

Tops LF, den Uijl DW, Delgado V, Marsan NA, Zeppenfeld K, Holman E, van der Wall EE, Schalij MJ, Bax JJ. Long-term improvement in left ventricular strain after successful catheter ablation for atrial fibrillation in patients with preserved left ventricular systolic function. *Circ Arrhythm Electrophysiol*. 2009 Jun;2(3):249-57.

den Uijl DW, Bax JJ. Left atrial size as a predictor of successful radiofrequency catheter ablation for atrial fibrillation. *Europace*. 2009 Oct;11(10):1255-6.

den Uijl DW, Blom NA, Wijnmaalen AP, Bax JJ, Schalij MJ, Zeppenfeld K. Real-time integration of intracardiac echocardiography to facilitate atrial tachycardia ablation in a patient with a Senning baffle. *Circ Arrhythm Electrophysiol*. 2009 Oct;2(5):e28-30.

den Uijl DW, Tops LF, van de Veire NR, Bax JJ. Intracardiac Echocardiography. *Cardiovascular Catheterization and Intervention: A Textbook of Coronary*,

Peripheral, and Structural Heart Disease, Chapter 40. Informa Healthcare USA, New York.

Bertini M, Delgado V, den Uijl DW, Nucifora G, Ng AC, van Bommel RJ, Borleffs CJ, Boriani G, Schalij MJ, Bax JJ. Prediction of cardiac resynchronization therapy response: value of calibrated integrated backscatter imaging. *Circ Cardiovasc Imaging.* 2010 Jan;3(1):86-93.

Tops LF, Delgado V, Bertini M, Marsan NA, den Uijl DW, Trines SA, Zeppenfeld K, Holman E, Schalij MJ, Bax JJ. Left atrial strain predicts reverse remodeling after catheter ablation for atrial fibrillation. *J Am Coll Cardiol.* 2011 Jan 18;57(3):324-31.

den Uijl DW, Delgado V, Tops LF, Ng AC, Boersma E, Trines SA, Zeppenfeld K, Schalij MJ, van der Laarse A, Bax JJ. Natriuretic peptide levels predict recurrence of atrial fibrillation after radiofrequency catheter ablation. *Am Heart J.* 2011 Jan;161(1):197-203.

den Uijl DW, Tops LF, Delgado V, Schuijf JD, Kroft LJ, de Roos A, Boersma E, Trines SA, Zeppenfeld K, Schalij MJ, Bax JJ. Effect of pulmonary vein anatomy and left atrial dimensions on outcome of circumferential radiofrequency catheter ablation for atrial fibrillation. *Am J Cardiol.* 2011 Jan 15;107(2):243-9.

van Huls van Taxis CF, Wijnmaalen AP, den Uijl DW, Gawrysiak M, Putter H, Schalij MJ, Zeppenfeld K. Reversed polarity of bipolar electrograms for predicting a successful ablation site in focal idiopathic right ventricular outflow tract arrhythmias. *Heart Rhythm.* 2011 May;8(5):665-71.

den Uijl DW, Delgado V, Bertini M, Tops LF, Trines SA, van de Veire NR, Zeppenfeld K, Schalij MJ, Bax JJ. Impact of left atrial fibrosis and left atrial size on the outcome of catheter ablation for atrial fibrillation. *Heart*. 2011 Nov;97(22):1847-51.

den Uijl DW, Gawrysiak M, Tops LF, Trines SA, Zeppenfeld K, Schalij MJ, Bax JJ, Delgado V. Prognostic value of total atrial conduction time estimated with tissue Doppler imaging to predict the recurrence of atrial fibrillation after radiofrequency catheter ablation. *Europace*. 2011 Nov;13(11):1533-40.

Jongbloed MR, Kelder TP, den Uijl DW, Bartelings MM, Molhoek SG, Tukkie R, Schalij MJ. Anatomical perspective on radiofrequency ablation of AV nodal reentry tachycardia after Mustard correction for transposition of the great arteries. *Pacing Clin Electrophysiol*. 2012 Oct;35(10):e287-90.

den Uijl DW, Boogers MJ, Compier M, Trines SA, Scholte AJ, Zeppenfeld K, Schalij MJ, Bax JJ, Delgado V. Impact of coronary atherosclerosis on the efficacy of radiofrequency catheter ablation for atrial fibrillation. *Eur Heart J Cardiovasc Imaging*. 2013 Mar;14(3):247-52.

Acknowledgements

A handwritten signature in black ink, consisting of several connected, stylized characters that are difficult to decipher.

Acknowledgements

Dit proefschrift is het eindproduct van mijn promotieonderzoek op de afdeling cardiologie van het Leids Universitair Medisch Centrum. Graag bedank ik een ieder die het mogelijk heeft gemaakt om dit onderzoek uit te voeren.

Daarnaast zijn er een aantal personen die ik in het bijzonder wil bedanken.

Allereerst Ellen, Jael, Carine en Sander. Op 'onze' kamer was er naast hard werken altijd ruimte voor een goed gesprek en een lekker kopje koffie. Het was mij een genoegen!

Het staf- en planningssecretariaat cardiologie: Bea, Carine, Christine, Cora, Marina, Monique en Talitha. Het onderzoek dat wij doen is alleen mogelijk door jullie strakke planning en ondersteuning.

Grote dank ben ik verschuldigd aan alle medewerkers van de cathkamer: Alice, Annemiek, Agatha, Ardien, Claudia, Edith, Els, Gerlinde, Hilse, Ineke, Jolanda, Joost, Loes, Loes, Louise, Mariska, Marjon, Nanda, Norma, Ramona, Truike en Yvonne. Voor de vele uren die werden doorgebracht achter de CARTO met op de achtergrond het hypnotiserende geluid van de RF generator: Burn baby burn!!!

Mijn tuingenoten (het zijn er bijna te veel om op te noemen...): Agnieszka, Arnold, Claudia, Daniël, Dominique, Douwe, Eline, Fleur, Gaetano, Gabya, Georgette, Gijs, Hadrian, Hans, Helène, Ivo, Jaap, Jan, Jan-Willem, Jeffrey, Joanne, Joëlla, Joep, Kees, Laurens, Louisa, Maaïke, Mark, Marlieke, Matteo, Michiel, Miriam, Mihaly, Nina, Noor, Roderick, Roxana, Rutger, Sebastiaan, Sjoerd, Sum-Che, Thomasz en Ulash. Ik ben blij dat ik dit pad samen met jullie heb kunnen bewandelen.

De elektrofysiologie fellows: Adolpho, Bart, José, Peter, Marta, Marcin, Michiel, Sander en Tim. Bedankt voor de gezellige tijd in het EP-lab. Hopelijk kruisen onze paden zich nogmaals in de toekomst.

Beste Monique, Marianne, Serge en Katja. De bevoegenheid waarmee jullie je beroep uitoefenen is inspirerend. Ik hoop ooit jullie voorbeeld te kunnen volgen.

Dear Victoria, your support and patience during this thesis have been enormous. I am thankful that you will be my co-promotor.

Beste André en Stefan, jullie zijn twee van mijn oudste vrienden, ik ben blij dat jullie mijn paranimfen zijn.

Lieve Thierry en Eelke, lieve schoonouders, de laatste loodjes wegen het zwaarst. Bedankt voor jullie steun tijdens het afronden van mijn promotie.

Lieve Bob en Rinza, lieve ouders, jullie hebben mij altijd de gelegenheid gegeven om te worden wie ik zelf wilde zijn. Deze is voor jullie.

Lieve Caroline, de grootste ontdekking van mijn promotietijd ben jij. Met veel vreugde, geluk en liefde kijk ik naar ons leven samen en naar de toekomst die voor ons ligt.

Curriculum Vitae



Curriculum Vitae

De auteur van dit proefschrift is geboren op 31 oktober 1980, te Schiedam. In 1999 behaalde hij het eindexamen VWO (cum laude) aan de Scholengemeenschap Spieringshoek te Schiedam. Een jaar later begon hij aan de studie Geneeskunde aan de Erasmus Universiteit te Rotterdam waar hij in 2007 het artsexamen behaalde. Tijdens de opleiding Geneeskunde voerde hij wetenschappelijk onderzoek uit naar de relatie tussen de activiteit van het autonome zenuwstelsel en het ontwikkelen van psychiatrische problematiek bij jonge kinderen aan de afdeling Kinderpsychiatrie van het Sophia Kinderziekenhuis te Rotterdam (begeleiding Dr. R.F. Ferdinand). Na het behalen van het artsexamen verrichtte hij promotieonderzoek aan de afdeling cardiologie van het Leids Universitair Medisch Centrum onder begeleiding van Prof. dr. J.J. Bax en Prof. dr. M.J. Schalij. De resultaten van dit onderzoek staan beschreven in dit proefschrift. In 2011 startte hij met de vooropleiding Interne Geneeskunde in het Rijnland Ziekenhuis te Leiderdorp onder begeleiding van Dr. M.J.F.M. Janssen. In 2013 begon hij de opleiding Cardiologie in het Rijnland Ziekenhuis te Leiderdorp onder begeleiding van Dr. C.J.H.J. Kirchhof. Momenteel heeft hij zijn opleiding Cardiologie vervolgd in het Leids Universitair Medisch Centrum te Leiden onder begeleiding van Prof. dr. M.J. Schalij.